Complement activation on surfaces carrying hydroxyl or amino groups

Mitsuaki TODA

2010

Dedicated to
my family
Tsuneyo Toda,
Noriaki Toda,
and my father in the heaven
Sei-ichi Toda

Contents

Abbreviations

Immunnology & serum compoments

AP	Alternative pathway
CP	Classical pathway
LP	Lectin pathway
C1	Complement component 1
C1q	Complement component 1 fragment q
C3	Complement component 3
C3a	Complement component 3 fragment a
C3b	Complement component 3 fragment b
CH_{50}	Total hemolytic component
HSA	Human serum albumin
Ig	Immunoglobulin
IgG	Immunoglobulin G
IgM	Immunoglobulin M
NHS	Normal human serum
SC5b-9	Soluble phase-terminal complement complex
TCC	Terminal complement complex (also called C5b-9)

Compounds & components

EDTA	Ethylenediamine-*N*,*N*,*N*′,*N*′-tetraacetic acid

EGTA	*O,O'*-bis(2-aminoethyl)ethyleneglycol-*N,N,N',N'*-tetraacetic acid
MCT	Mercury cadmium telluride
mPEG	Methoxy-capped polyethylene glycol
PEI	Polyethyleneimine
PVA	Poly(vinyl alcohol)
SAM	Self-assembled monolayer
TFAA	Trifluoroacetic acid anhydride
VB	Veronal buffer

Analysis & units

DA	Degrees of angle
ELISA	Enzyme-linked immunosorbent assay
ESCA	Electron spectroscopy for chemical analysis
FCM	Flow cytometry
FTIR	Fourier-transform infrared spectroscopy
Mn	Number-average molecular weight
Mw	Weight-average molecular weight
RAS	Reflection adsorption spectroscopy
SDS-PAGE	Sodium dodecyl sulfate – polyacrylamide gel electrophoresis
SEM	Scanning electron microscopy
SPR	Surface plasmon resonance
XPS	X-ray photoelectron spectroscopy

Statistics

ANOVA	A one way analysis of variance test
SEM	Standard error of the mean

General Introduction

The author would like to ask the reader's forgiveness for opening this thesis with a personal story instead of a scholarly discussion with references and acknowledgment of those who have come before him. The author believes that his personal story is the origin of motivation of the author and its revelation is necessary to set the stage for the remainder of this thesis.

During senior year of the author as an undergraduate, the father of the author passed away as a result of cancer. Only four months had elapsed from the time his father was diagnosed with carcinoma to the death of his father. With the brevity of this interval, the author had no ability to help his father, his family, or himself; there was no time for preparation, and all the author could do was accept the unacceptable reality.

The lives have limits. It's an unavoidable truth that no modern scientific knowledge or technology can overcome at this time. Death serves as an agent of change, clearing the path of the old to make way for the new[1], and it may not be ethical or even possible for humans to maneuver around death using human-made means. Yet, don't we the human beings permit to apply modern technologies to recover from crises that once ended in death, especially death occurring before one's natural lifespan has been completed?

Ordinary people may be inclined to accept such early deaths as simply individ-

ual fate or to say that it is not in the hands of humans to operate against such fate because it is ultimately unavoidable. The author believes, however, that we the people who produce any technology should continue to strive to do their utmost with technology to ameliorate suffering of human beings even if it may be impossible to achieve complete recovery and should fulfill our obligation to contribute in this way to the overall welfare of the human beings. The helplessness of the author during the brief period of his father's terminal illness has led him to pursue development of technologies that can help people recover from or delay the outcome of such diseases. It is because of this personal background that the author became a researcher in biomedical engineering.

The development of technologies based on research results in biomedical engineering[2,3] has brought us enormous privileges in recent decades. The invention of novel medical devices has led to the development of many new treatments[4–11] and to cures and effective treatments for critical injuries and illness[12–14]. These medical devices, however, still have weaknesses and limitations[15,16].

Almost all materials used in such devices are artificial and therefore are recognized as foreign objects by the recipient's body. Several biological responses are induced to protect the body from foreign objects such as these biomedical materials[17–21]. In addition, medical devices have been used not only at the acute phase in emergency conditions but also in the chronic phase of illnesses, which has required long-term suppression of these defenses in the patient[22–24]. This long-term use can lead to numerous problems, such as loss of device function or even fatal side effects[15].

Therefore, an important challenge remains for understanding and developing methods of controlling these interactions between the artificial materials and the organismal defense, especially at the interface with the bioengineered materials[3].

The complement system is an enzyme cascade that consists of approximately 30 fluid-phase and cell-membrane bound proteins and that plays an important role in the body's defense systems against pathogenic xenobiotics[25–27]. It is activated through three separate pathways: the classical pathway (CP), the lectin pathway (LP), and the alternative pathway (AP). Interaction of complement protein C1q with immune-complexes initiates the CP[28,29]; the LP is triggered by the binding of mannose-binding lectin to carbohydrate chains on foreign microorganisms[30–32]; and the AP is activated by nonspecific deposition of complement protein C3 on the surfaces of foreign substances[33–36].

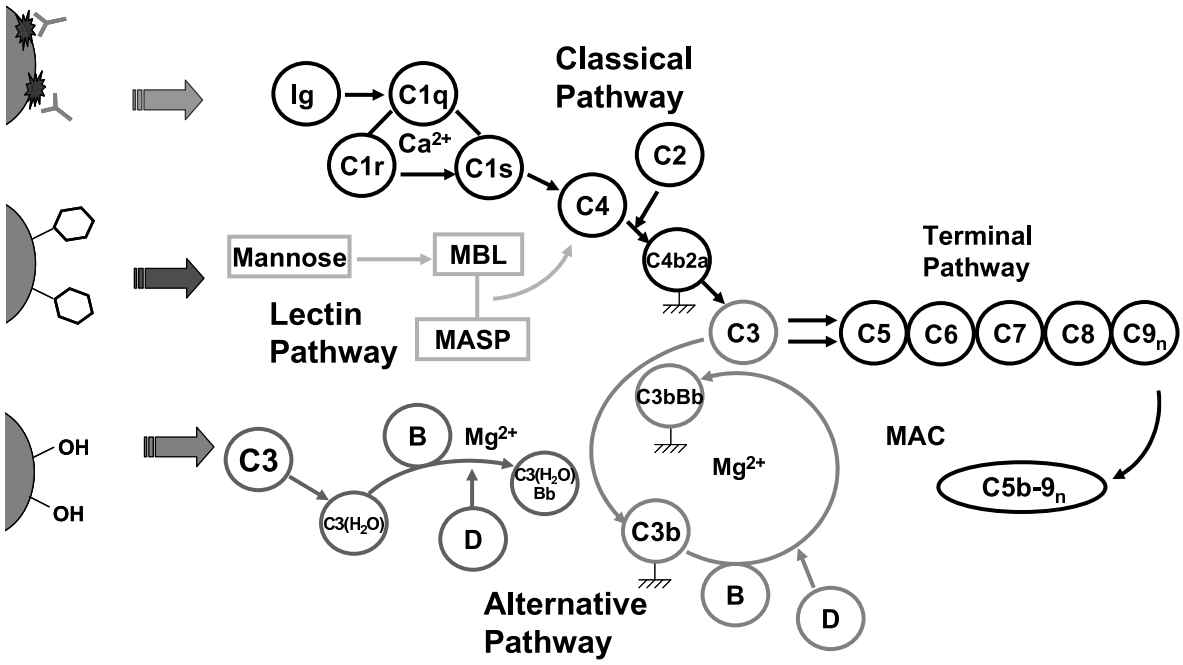

Scheme 1 Schematic illustration of the complement activation pathways.

Extensive studies have focused on complement activation against artificial bioma-

terials used for the preparation of implants and extracorporeal artificial organs[37–41], but these interactions involving the features of the material surfaces and the complement system are not completely understood. More fundamental knowledge about these interactions can lead to strategies for improving and modifying the surface of biomaterials and contribute to the development of novel medical devices with reduced side effects. Application of such knowledge can be expected to yield methods for controlling unspecific adsorption of various proteins onto the surfaces of biomaterials, improving the signal/noise ratio of the biosensors, and analyzing and distinguishing specific substances using controlled immobilization of the factors that recognize those substances.

This thesis provides fundamental information about interactions between biomaterials and living bodies, especially about the effect of surface properties with various characteristics on interactions with the complement system. This system may be involved in the harmful side effects of medical devices and in the cell behavior involved in displaying specific surface antigens.

Chapter 1 describes a study of interactions between the complement system and amino groups presented on model surfaces. Hydroxyl groups (OH) present on the surface of artificial biomaterials strongly activate the complement system via the AP. Amino groups (NH_2), the other representative nucleophilic group, also seem to be potential activators of the complement system through the AP[36]; however, few studies have examined the potential of artificial materials carrying amino groups to activate the complement system, and the detailed mechanism remains unclear.

In this chapter, a self-assembled monolayer (SAM) of 11-amino-1-undecanethiol

(NH_2-SAM) and a polyethyleneimine (PEI)-coated surface were used as model surfaces to study amino group activation of the complement pathway. The amounts of adsorbed proteins on the specimen surfaces were determined using the surface plasmon resonance (SPR) method. Adsorbed proteins were also analyzed with SDS-PAGE, and the amounts of cleavage components of the complement system were measured using ELISA. The results showed that a large amount of protein was adsorbed from serum solutions onto the two types of amino surfaces and that amounts of C3b deposition were much less than those observed on OH-SAM. The amounts of C3a released on the amino surfaces were the same as that for CH_3-SAM, but significantly less than that of OH-SAM. These findings suggest that the nucleophilic amino groups on NH_2-SAM and PEI-coated surfaces do not directly activate the AP but that the protein adsorbed layers formed on amino surfaces activate it to an extent much smaller than on OH-SAM.

Chapter 2 deals with a study of the effects of hydrophobicity and electrostatic charge on complement activation at the terminal amino group with mixed SAMs. Nucleophilic groups on blood-contacting biomaterials, such as OH groups on a dialysis membrane made of regenerated cellulose[42,43], can strongly activate the complement system. OH-SAM also acts as a strong activator of the complement system, as shown in a previous study[44]. Previous research[45] has also indicated that when using a series of mixed SAMs of various ratios of OH- and methyl (CH_3)-terminated alkanethiols, there was a threshold for the content of OH-terminated alkanethiols for activating the complement system. The degree of complement activation strengthened in proportion to that content.

In Chapter 1, the complement system was simply activated on surfaces carrying amino groups. In this chapter, the activation of the complement system was analyzed using series of mixed SAMs containing NH_2-terminated and CH_3-terminated or carboxyl (COOH)-terminated alkanethiols on several model surfaces that carried amino groups and had different surface hydrophobicities and electrostatic charge. The results showed that NH_2/CH_3-mixed SAMs were not potent activators of the complement system regardless of NH_2/CH_3 ratios in mixed SAMs. Many serum proteins, such as albumin, were adsorbed onto those SAMs, and the formed protein layer inhibited access of C3b to amino groups. On the other hand, plenty of C3b and/or C3bBb was deposited in a 1:1 mixture of NH_2/COOH-mixed SAM surface, and SC5b-9 was found in serum exposed to this surface, indicating activation of the complement system. These results suggest that C3b can easily access nucleophilic NH_2 groups because of the decreased electrostatic interaction between negatively charged proteins and the NH_2-SAM surface.

Chapter 3 describes an examination of the differences in complement activation caused by the soluble phase and immobilized phase of poly(vinyl alcohol) (PVA) and dextran. Complement activation by polymeric materials has been extensively studied in relation to hemodialysis membranes made of cellulose or its derivatives that activate the complement system[42,46]. Other studies indicate that polymeric membranes carrying surface OH groups or nucleophilic groups strongly activate the complement system through the alternative pathway[44,45,47–49]. Crosslinked dextran (Sephadex®) also activates the complement system[50]. In contrast to these observations, solutions of dextran, which have a medicinal application as a blood

substitute and a plasma expander, did not strongly activate the complement system at the dextran concentrations used in clinical settings[51]. Some questions have arisen from these seemingly contradictory findings, asking whether the state of the polymer, either immobilized on a surface or free in solution, affects complement activation.

In Chapter 3, dextran and PVA were used as model polymers carrying OH groups, and the deposition of serum proteins and complement fragment C3b onto polymer-immobilized surfaces was examined using an SPR apparatus. With ELISA, the release of complement fragments was compared after exposure of serum samples to either a polymer-immobilized surface or to a solution of polymer dissolved in neutral buffer. The results showed that the complement system was strongly activated on dextran- and PVA-immobilized surfaces but not in dissolved dextran or PVA in serum, even if amounts of the soluble polymers added to serum were 4–2000 times greater than those on the polymer-immobilized surfaces. Therefore, the physical states of the polymers, i.e., either immobilized on the surface or dissolved in serum, appear to greatly modulate complement activation.

Chapter 4 deals with an investigation of the relationship between complement activation and the surface properties and structure of PVA. Activation of the serum complement system was examined and described on SAMs of alkanethiols carrying OH groups[44,45], or OH-terminated oligo(ethylene glycol)[49]. In Chapter 3, it was found that dextran and PVA immobilized on surfaces strongly activated the complement system, but either of these polymers dissolved in serum could not. In the series of experiments, it was also found that the complement activation ability of

PVA, but not dextran, immobilized on surfaces highly depends on their preparation methods. In Chapter 4, the effect of water content in PVA layer on complement activation was examined. PVA immobilized surfaces were prepared by spin-coating of a PVA solution on a SAM carrying aldehyde and PVA layers with various thicknesses were prepared by changing concentrations of PVA solutions used for spin-coating. The PVA layers prepared were further annealed at 150 ℃ to increase crystallinity, accompanied by a decrease of water content[52–55]. Amounts of serum proteins and complement fragment C3b deposited onto PVA surfaces were determined by using a SPR apparatus and amounts of complement fragments SC5b-9 released were also determined after exposure of serum samples to PVA surfaces using ELISA. The results in Chapter 4 demonstrated that the thickness of the PVA layer immobilized on a substrate greatly modulated complement activation behavior, although all PVA layers regardless of their thickness reduced the non-specific adsorption of serum proteins. In addition, the PVA surface was converted by annealing to the complement-activating surface. Therefore, these findings suggested that the water content, conformation, and surface structure greatly affect complement activation.

In Chapter 5, the association between complement activation and the degradation of methoxy-capped polyethylene glycol (mPEG) was studied. In recent years, surface modification with polyethylene glycol (PEG) has been employed in the development of biomaterials to reduce unfavorable reactions. Unanticipated body reactions, however, have been reported, with activation of the complement system suggested as having involvement in these responses[56–60]. Hypersensitivity caused by PEG-modified liposomes[61–64] and rapid clearance of PEG-

modified liposomes from blood[65] have been reported. Activation of the complement system has been suggested as being associated with these reactions[66]. For the work described in this chapter, a PEG-modified surface on a gold surface using a SAM of α-mercaptoethyl-ω-methoxy-polyoxyethylene (HS-mPEG) was prepared, and detailed surface analyses of PEG-modified surfaces was carried out using the reflection-adsorption method (FTIR-RAS) and X-ray photoelectron spectrometry (XPS). Activation of the complement system was examined using undiluted human serum to obtain more detailed insight into the mechanisms of complement system activation by the PEG-modified surfaces. The results of the surface analyses suggested that removal of low molecular weight substances produced by degradation of PEG chains occurred on the mPEG surfaces stored in a desiccator under room light (R-mPEG) or irradiated with UV light for 60 min (UV-mPEG) but not on the surface maintained in a -20 ℃ freezer for 12 days (F-mPEG). Strong activation of the complement system was observed when undiluted normal serum was applied to R-mPEG and UV-mPEG surfaces. On the other hand, if serum with EDTA was applied on the degraded mPEG surfaces, there was no observed activation of the complement system or adsorption of serum proteins. These results indicated that the resistance to protein adsorption remained but that the ability to prevent the complement activation was lost on those degraded mPEG surfaces. PEG-modified artificial materials, proteins, and liposomes, therefore, should be carefully stored.

In summary, this thesis addresses the effect of surface properties on biological reactions. Especially investigated was the activation of the serum complement system occurring with various kinds of terminal functional groups presented on the

surface. Precise examinations of interactions between the surface properties and biological responses including cell behavior were achieved using several well-defined surfaces provided by alkanethiols.

The author of this thesis strongly believes that the findings reported in this thesis provide basic information for continuing research on the interactions at the interface of materials and the living body, hold promise for application in the development of novel medical devices, and lead to technologies that give hope to people suffering injury and illness. The author also wishes and resolves to provide these technologies in this world.

References

1. Stanford News Service: Text of Steve Jobs' Commencement address [Internet]. Stanford(CA):Stanford University; 2005 Jun 14 [cited 2010 Jan 12]. Available from: http://news.stanford.edu/news/2005/june15/jobs-061505.html
2. Ikada Y. Basic Technologies Developed for Tissue Engineering. In: Tissue Engineering: Fundamentals and Applications. Amsterdam, The Netherlands : Elsevier; 2006. pp. 235–421
3. Cooke F W, Lemons J E, Ratner B D. Propterties of Materials. In: Ratner B D, Hoffman A S, Schoen F J, Lemons J E, editors. Biomaterials science : an introduction to materials in medicine;. California, USA : Academic Press Inc; 1996. pp. 11–35
4. Dudrick S J, Wilmore D W, Vars H M, Rhoads J E. Long term total parenteral nutrition with growth, development, and positive nitrogen balance. Surgery 1968;64(1):134–142
5. Walter C W. Invention and development of the blood bag. Vox Sang 1984;47(4):318–324
6. Kolff W J. Artificial kidney; treatment of acute and chronic uremia. Cleve Clin Q 1950;17(4):216–228
7. Voorhees A B J, Jaretzki A III, Blakemore A H. The use of tubes constructed from vinyon "N" cloth in bridging arterial defects. Ann Surg 1952;135(3):332–336
8. Soyer T, Lempinen M, Cooper P, Norton L, Eiseman B. A new venous pros-

thesis. Surgery 1972;72(6):864–872

9. Guglielmi G, Viñuela F, Sepetka I, Macellari V. Electrothrombosis of saccular aneurysms via endovascular approach. Part 1: Electrochemical basis, technique, and experimental results. J Neurosurg 1991;75(1):1–7
10. Guglielmi G, Viñuela F, Dion J, Duckwiler G. Electrothrombosis of saccular aneurysms via endovascular approach. Part 2: Preliminary clinical experience. J Neurosurg 1991;75(1):8–14
11. Burke J F, Didisheim P, Goupil D, Heller J, Kane J B, Katz L, Kim S W, Lemons J E, Refojo M F, Robblee L S, Smith D C, Sweeney J D, Tompkins R G, Watson J T, Yager P, Yarmush M L. Application of Materials in Medicine and Dentistry. In: Ratner B D, Hoffman A S, Schoen F J, Lemons J E, editors. Biomaterials science : an introduction to materials in medicine. California, USA : Academic Press Inc; 1996. pp. 283–388
12. Durston W. Mechanical Ventilation. In: Roberts J R, Hedges J R, editors. Clinical procedures in emergency medicine. Philadelphia, USA : W B Saunders Company; 1985. pp. 46–80
13. Gazak S. Direct Current Electrical Cardioversion. In: Roberts J R, Hedges J R, editors. Clinical procedures in emergency medicine. Philadelphia, USA : W B Saunders Company; 1985. pp. 151–159
14. Bergman G E. Transfusion Therapy. In: Roberts J R, Hedges J R, editors. Clinical procedures in emergency medicine. Philadelphia, USA : W B Saunders Company; 1985. pp. 372–389
15. Ikada Y. Challenges in Tissue Engineering. In: Tissue Engineering: Funda-

mentals and Applications. Amsterdam, The Netherlands : Elsevier; 2006. pp. 423–462

16. Ratner B D. Biomaterials Science: An Interdisciplinary Endeavor. In: Ratner B D, Hoffman A S, Schoen F J, Lemons J E, editors. Biomaterials science : an introduction to materials in medicine. California, USA : Academic Press Inc; 1996. pp. 1–8
17. Anderson J M, Miller K M. Biomaterial biocompatibility and the macrophage. Biomaterials 1984;5(1):5–10
18. Remes A, Williams D F. Immune response in biocompatibility. Biomaterials 1992;13(11):731–743
19. Gorbet M B, Sefton M V. Biomaterial-associated thrombosis: roles of coagulation factors, complement, platelets and leukocytes. Biomaterials 2004;25(26):5681–5703
20. Anderson J M, Gristina A G, Janson S R, Harker L A, Johnson R J, Merritt K, Naylor P T, Schoen F J. Host Reactions to Biomaterials and Their Evaluation. In: Ratner B D, Hoffman A S, Schoen F J, Lemons J E, editors. Biomaterials science : an introduction to materials in medicine. California, USA : Academic Press Inc; 1996. pp. 165–214
21. Nilsson B, Ekdahl K N, Mollnes T E, Lambris J D. The role of complement in biomaterial-induced inflammation. Mol Immunol 2007;44(1–3):82–94
22. Ridley H. Intra-ocular acrylic lenses; a recent development in the surgery of cataract. Br J Ophthalmol 1952;36(3):113–122
23. Ridley H. Intra-ocular acrylic lenses after cataract extraction. Lancet

1952;1(6699):118–121

24. Charnley J. Arthroplasty of the hip. A new operation. Lancet 1961;1(7187):1129–1132
25. Walport M J. Complement. First of two parts. N Engl J Med 2001;344(14):1058–1066
26. Walport M J. Complement. Second of two parts. N Engl J Med 2001;344(15):1140–1144
27. Goldfarb R D, Parrillo J E. Complement. Crit Care Med 2005;33(12 Suppl):S482-S484
28. Sim R B, Reid K B. C1: molecular interactions with activating systems. Immunol Today 1991;12(9):307–311
29. Reid K B M. Classical Pathway of Activation. In: Rother K, Till G O, Hänsch G M, editors. The Complement System, Second Revised Edition. Berlin: Springer-Verlag; 1998. pp. 68–86
30. Ikeda K, Sannoh T, Kawasaki N, Kawasaki T, Yamashina I. Serum Lectin with Known Structure Activates Complement though the Classical Pathway. J Biol Chem 1987;262(16):7451–7454
31. Fujita T, Matsushita M, Endo Y. The lectin-complement pathway–its role in innate immunity and evolution. Immunol Rev 2004;198(1):185–202
32. Reid K B M. Lectin Pathway of Non-self Recognition. In: Rother K, Till G O, Hänsch G M, editors. The Complement System, Second Revised Edition. Berlin: Springer-Verlag; 1998. pp. 86–92
33. Fearon D T, Austen K F. Activation of the Alternative Complement Pathway

with Rabbit Erythrocytes by Circumvention of the Regulatory Action of Endogenous Control Proteins. J Exp Med 1977;146(1):22–33

34. Pangburn M K, Muller-Eberhard H J. Complement C3 convertase: cell surface restriction of beta1H control and generation of restriction on neuraminidase-treated cells. Proc Natl Acad Sci U S A 1978;75(5):2416–2420
35. Law S-K A, Levine R P. Interaction between the third complement protein and cell surface macromolecules. Proc Natl Acad Sci U S A 1977;74(7):2701–2705
36. Pangburn M K. Alternative Pathway: Activation and Regulation. In: Rother K, Till G O, Hänsch G M, editors. The Complement System, Second Revised Edition. Berlin: Springer-Verlag; 1998. pp. 93–115
37. Craddock P R, Fehr J, Dalmasso A P, Brighan K L, Jacob H S. Hemodialysis leukopenia. Pulmonary vascular leukostasis resulting from complement activation by dialyzer cellophane membranes. J Clin Invest 1977;59(5):879–888
38. Craddock P R, Fehr J, Brigham K L, Kronenberg R S, Jacob H S. Complement and leukocyte-mediated pulmonary dysfunction in hemodialysis. N Engl J Med 1977;296(14):769–774
39. Chenoweth D E, Cooper S W, Hugli T E, Stewart R W, Blackstone E H, Kirklin J W. Complement activation during cardiopulmonary bypass: evidence for generation of C3a and C5a anaphylatoxins. N Engl J Med 1981;304(9):497–503
40. Maillet F, Petitou M, Choay J, Kazatchkine M D. Structure-function relationships in the inhibitory effect of heparin on complement activation: independency of the anti-coagulant and anti-complementary sites on the heparin

molecule. Mol Immunol 1988;25(9):917–923

41. Gu Y J, Van Oeveren W. Activation of plasma components by leukocyte removal filters. ASAIO J 1994;40(3):M598-M601
42. Wegmuller E, Montandon A, Nydegger U, Descoeudres C. Biocompatibility of different hemodialysis membranes: activation of complement and leukopenia. Int J Artif Organs 1986;9(2):85–92
43. Chenoweth D E. Complement activation during hemodialysis: clinical observations, proposed mechanisms, and theoretical implications. Artif Organs 1984;8(3):281–290
44. Hirata I, Morimoto Y, Murakami Y, Iwata H, Kitano E, Kitamura H, Ikada Y. Study of complement activation on well-defined surfaces using surface plasmon resonance. Colloids Surf B Biointerfaces 2000;18(3–4):285–292
45. Hirata I, Hioki Y, Toda M, Kitazawa T, Murakami Y, Kitano E, Kitamura H, Ikada Y, Iwata H. Deposition of complement protein C3b on mixed self-assembled monolayers carrying surface hydroxyl and methyl groups studied by surface plasmon resonance. J Biomed Mater Res A 2003;66(3):669–676
46. Pangburn M K, Schreiber R D, Muller-Eberhard H J. Formation of the initial C3 convertase of the alternative complement pathway. Acquisition of C3b-like activities by spontaneous hydrolysis of the putative thioester in native C3. J Exp Med 1981;154(3):856–867
47. Gorbet M B, Sefton M V. Complement inhibition reduces material-induced leukocyte activation with PEG modified polystyrene beads (Tentagel) but not polystyrene beads. J Biomed Mater Res A 2005;74(4):511–522

48. Jang H S, Ryu K E, Ahn W S, Chun H J, Dal Park H, Park K D, Kim Y H. Complement activation by sulfonated poly(ethylene glycol)-acrylate copolymers through alternative pathway. Colloids Surf B Biointerfaces 2006;50(2):141–146
49. Arima Y, Toda M, Iwata H. Complement activation on surfaces modified with ethylene glycol units. Biomaterials 2008;29(5):551–560
50. Carreno M-P, Labarre D, Jozefowicz M, Kazatchkine M D. The ability of sephadex to activate human complement is suppressed in specifically substituted functional sephadex derivatives. Mol Immunol 1988;25(2):165–171
51. Videm V, Mollens T E. Human Complement Activation by Polygeline and Dextran 70. Scand J Immunol 1994;39(3):314–320
52. Ikada Y, Iwata H, Horii F, Matsunaga T, Taniguchi M, Suzuki M, Taki W, Yamagata S, Yonekawa Y, Handa H. Blood compatibility of hydrophilic polymers. J Biomed Mater Res 1981;15(5):697–718
53. Fujimoto K, Minato M, Ikada Y. Poly(vinyl alcohol) Hydrogels Prepared under Different Annealing Conditions and Their Interactions with Blood Components. ACS Symposium Series 1994;540:228–242
54. Kulik E, Ikada Y. In vitro platelet adhesion to nonionic and ionic hydrogels with different water contents. J Biomed Mater Res 1996;30(3):295–304
55. Peppas N A. Infrared spectroscopy of semicrystalline poly(vinyl alcohol) networks. Makromol Chem 1977;178(2):595–601
56. Harris J M. Poly(ethylene Glycol) Chemistry: Biotechnical and Biomedical Applications. New York: Plenum Press; 1992.
57. Kingshott P, Griesser H J. Surfaces that resist bioadhesion. Curr Opin Solid

State Mater Sci 1999;4(4):403–412

58. Nucci M L, Shorr R, Abuchowski A. The therapeutic value of poly(ethylene glycol)-modified proteins. Adv Drug Deliv Rev 1991;6(2):133–151
59. Harris J M, Chess R B. Effect of pegylation on pharmaceuticals. Nat Rev Drug Discov 2003;2(3):214–221
60. Duncan R. The dawning era of polymer therapeutics. Nat Rev Drug Discov 2003;2(5):347–360
61. Uziely B, Jeffers S, Isacson R, Kutsch K, Wei-Tsao D, Yehoshua Z, Libson E, Muggia FM, Gabizon A. Liposomal doxorubicin: Antitumor activity and unique toxicities during two complementary phase I studies. J Clin Oncol 1995;13(7):1777–1785
62. de Marie S. Liposomal and lipid-based formulations of amphotericin B. Leukemia 1996;10(SUPPL. 2):93–96
63. Alberts D S, Garcia D J. Safety aspects of pegylated liposomal doxorubicin in patients with cancer. Drugs 1997;54(SUPPL. 4):30–35
64. Skubitz K M, Skubitz A P N. Mechanism of transient dyspnea induced by pegylated-liposomal doxorubicin (Doxil(TM)). AntiCancer Drugs 1998;9(1):45–50
65. Laverman P, Brouwers A H, Dams E T M, Oyen W J G, Storm G, Van Rooijen N, Corstens F H M, Boerman O C. Preclinical and clinical evidence for disappearance of long-circulating characteristics of polyethylene glycol liposomes at low lipid dose. J Pharmacol Exp Ther 2000;293(3):996–1001
66. Moghimi S M, Szebeni J. Stealth liposomes and long circulating nanoparti-

cles: critical issues in pharmacokinetics, opsonization and protein-binding properties. Prog Lipid Res 2003;42(6):463–78

Chapter 1

Complement activation on surfaces carrying amino groups

1.1 Introduction

The complement system is an enzyme cascade system that consists of approximately 30 fluid-phase and cell-membrane bound proteins, and plays an important role in the body's defense systems against pathogenic xenobiotics[1,2]. It is activated through three separate pathways: the classical pathway (CP), the lectin pathway (LP), and the alternative pathway (AP). The CP is initiated by interaction of complement protein C1q with immune-complexes[3,4], the LP is triggered by the binding of mannose-binding lectin to carbohydrate chains on foreign microorganisms[5-7], and the AP is activated by nonspecific deposition of complement protein C3 on the surfaces of foreign substances[8-11]. Extensive studies have been made on complement activation on artificial biomaterials used for the preparation of implants and extracorporeal artificial organs[12-17], and the current model is this occurs through the AP. AP activation is initiated in the fluid phase with spontaneous and continuous generation of enzymes that cleave C3 to C3a and C3b. C3b is conformationally changed, exposing a highly reactive thioester group which attacks nucleophilic groups, such as hydroxyl groups, on biomaterials to form a covalent linkage and subsequently

complex with factors B and D. For example, a dialysis membrane made of regenerated cellulose with surface hydroxyl groups[14,18]. And a self-assembled monolayer of 11-mercaptoundecanol (OH-SAM) also acted as a strong activator of the complement system, as shown in previous studies[19,20]. The other proposed mechanisms is that the CP is initiated by protein layers formed on artificial materials and the formed C3 convertase trigger the AP amplification loop. For example, polystyrene without nucleophilic groups is reported as an activator of the complement system[21].

Amino groups, the other representative nucleophilic group, seem to be potential activators of the complement system through the alternative pathway[11], and could form amide bonds with C3b, and C3 convertase with Bb. Consistent with this, low molecular weight amines react with the thioester group of C3[22-24] and C3b[24]. Few studies thus far[25,26] have identified a function of amino groups in alternative pathway activation. Here, a self-assembled monolayer of 11-amino-1-undecanethiol (NH_2-SAM) and a polyethyleneimine (PEI) coated surface on an 11-mercaptoundecanoic acid SAM (COOH-SAM) were used as model surfaces to study amino group activation of the complement pathway.

1.2 Materials and methods

1.2.1 Preparation of serum and veronal buffer

All subjects enrolled in this research have responded to an informed consent, which has been approved and accepted by the ethics review board of Institute for Frontier Medical Sciences, Kyoto University. Blood was donated from 8 healthy volunteers who had a meal at least 4 h before their donation. To separate serum, each 10 cm^3 of

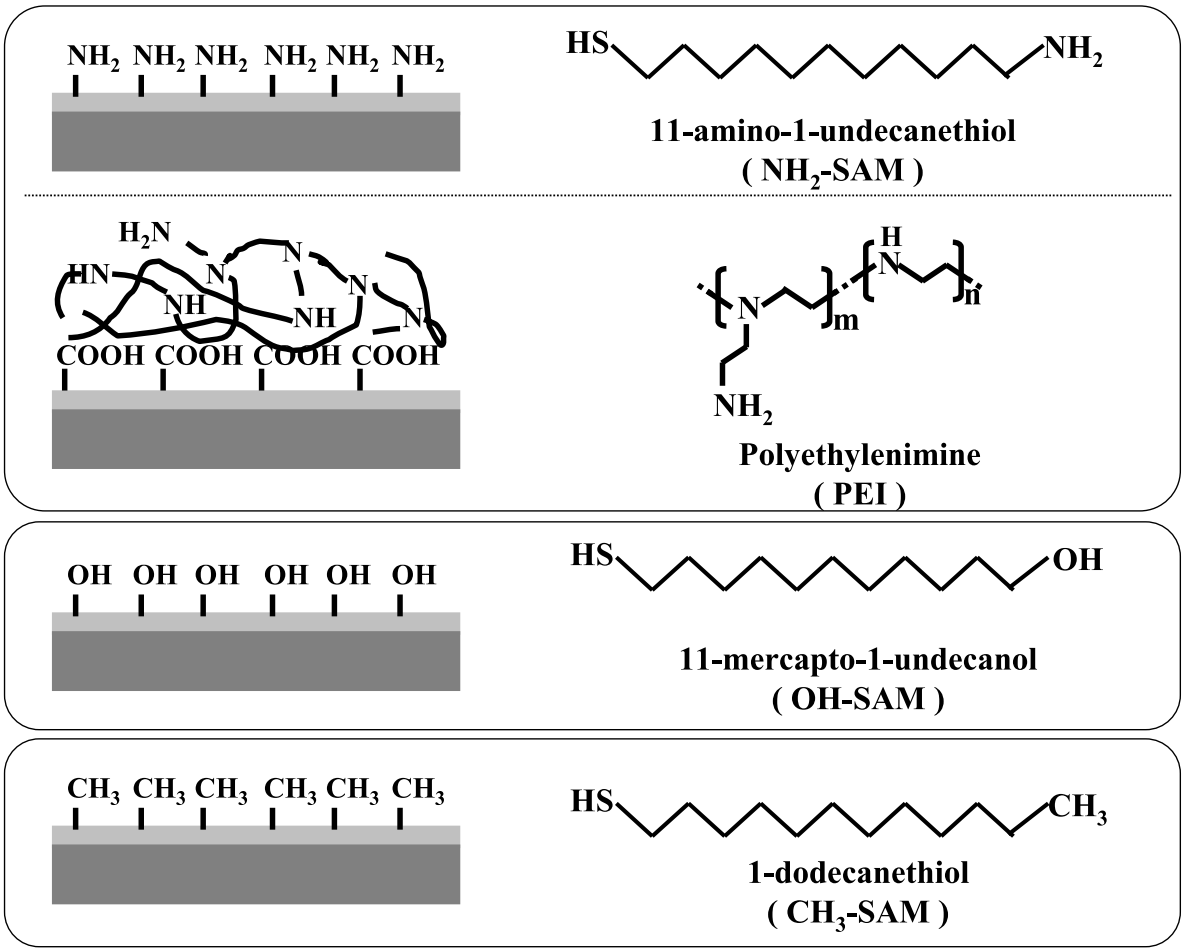

Scheme 1.1 NH_2-SAM and PEI coated surfaces

the blood was divided equally into sterile glass tubes, kept at ambient temperature for 30 min, and then centrifuged at 1100 × g at 4 ℃ for 30 min. Supernatant was pooled, mixed, and stored in 2 cm^3 vials at −80 ℃ until use. Veronal buffer (VB) was prepared referring to a protocol of CH_{50} measurement[27].

1.2.2 Preparation of surface carrying different functional groups

Glass plates (type BK7, refractive index: 1.515, size: 25 × 25 × 1 mm, Arteglass Associates Co., Kyoto, Japan) were immersed for 5 min in a piranha solution (7:3 mixture of concentrated sulfuric acid and 30% hydrogen peroxide, Wako Pure Chemical In-

dustries, Ltd., Osaka, Japan), washed three times with deionized water, sequentially rinsed three times with Milli-Q water (Milli-Q Synthesis, Millipore Co., MA, USA) and once with 2-propanol (Nacalai Tesque, Inc., Kyoto, Japan), and finally stored in 2-propanol until use. These glass plates were dried under a stream of dried nitrogen gas (Kyoto Teisan K.K., Kyoto, Japan) and mounted on the rotating stage of a thermal evaporation coating apparatus (V-KS200, Osaka Vacuum, Ltd., Osaka, Japan). A chromium layer (1 nm), and then a gold layer (49 nm) was deposited.

The gold-coated glass plate was immersed in a 1 $\mathrm{mmol\,dm^{-3}}$ ethanol (Nacalai Tesque, Inc., Kyoto, Japan) solutions of 11-amino-1-undecanethiol hydrochloride (Dojindo Laboratories, Kumamoto, Japan), 11-mercaptoundecanoic acid (Sigma-Aldrich Co., St. Louis, MO, USA), 11-mercaptoundecanol (Sigma-Aldrich), and 1-dodecanethiol (Sigma-Aldrich) for the formation of a NH_2-SAM, COOH-SAM, OH-SAM and CH_3-SAM, respectively at room temperature for at least 24 h. The glass plate with a monolayer was sequentially washed with ethanol, Milli-Q water and 2-propanol each three times and then dried under a stream of dried nitrogen gas.

Glass plates carrying a COOH-SAM were exposed to a 2% PEI (Sigma-Aldrich, Mn = 60,000, Mw = 750,000, branched) in VB for 5 min, and washed three times with VB solution. In surface plasmon resonance (SPR) experiments, a COOH-SAM plate was set in a sample holder of the SPR apparatus, and a 2% PEI solution was applied to the surface for 5 min, and washed with a VB solution for at least 5 min to remove the weakly-bound PEI.

1.2.3 Surface analyses of glass plates carrying amino groups

XPS Spectra of surfaces were collected by an ESCA-850V (Shimadzu Co., Kyoto, Japan): A magnesium target was used and the electric current through the filament was 30 mA at 8 kV, and the base pressure of the analysis chamber was less than 1×10^{-5} Pa. All spectra shown in the figures were corrected referring to the peak of Au $4f_{7/2}$ to 83.8 eV.

Infrared adsorption spectra of sample surfaces were collected by the reflection-adsorption method (FTIR-RAS) using a Spectrum One (Perkin-Elmer, USA) spectrometer equipped with a Refractor^{TM} (Harrick Sci. Co., NY, USA) and a mercury-cadmium telluride (MCT) detector cooled by liquid nitrogen (Taiyo Toyo Sanso Co., Ltd, Osaka, Japan). Gold-coated glass plates with a gold layer at 199 nm of thickness were used for FTIR-RAS analysis. Spectra were obtained using the *p*-polarized infrared light at an incident angle of 75° in the chamber purged with dry nitrogen gas for 128 scans at 4 cm^{-1} resolution from 4000 to 750 cm^{-1}.

Surface amino groups were modified through with trifluoroacetic acid anhydride[28]. 1 cm^3 of trifluoroacetic acid anhydride (TFAA, Nacalai Tesque, Inc., Kyoto, Japan) and 1 cm^3 of pyridine (Wako Pure Chemical Industries, Ltd., Osaka, Japan) were added to 15 cm^3 of benzene (Wako Pure Chemical Industries, Ltd., Osaka, Japan) and mixed well in a chemical hood. Gold-coated glass plates with a NH_2-SAM or PEI were soaked in this solution for 90 min. Plates were rinsed with benzene three times, soaked into benzene for a half hour, rinsed with diethylether (Wako Pure Chemical Industries Ltd., Osaka, Japan) three times, and left in diethylether overnight. Samples were rinsed with 2-propanol and dried

under a stream of dried nitrogen gas. Those surfaces were subjected to XPS and FTIR-RAS analyses.

1.2.4 Protein deposition observed by surface plasmon resonance (SPR)

Polyclonal rabbit anti-human C3b (RAHu/C3b, Nordic Immunology, The Netherlands), polyclonal sheep anti-human C1q (PC020, The Binding Site Ltd., Birmingham, UK), polyclonal rabbit anti-HSA (55029, ICN Pharmaceuticals, Inc., USA), and polyclonal goat anti-IgG (109-005-088, Jackson ImmunoResearch Laboratories, Inc., PA, USA) were diluted to 1% with VB. The SPR apparatus employed in this study was a home made apparatus[19,20]. Unless otherwise stated, 10% normal human serum (NHS) diluted with VB was circulated at 3.0 cm^3/min. The change of the resonance angle was monitored as a function of the time for 90 min. During each of the antisera/antibodies was applied, change of the resonance angle was estimated to see antibody immobilization. The change of the resonance angle was also examined when 1% solutions of these antisera/antibodies diluted by VB were exposed to human serum albumin pre-adsorbed surfaces to see non-specific adsorption. No clear increase in the resonance angle was observed for these antisera/antibodies.

Protein deposition on surfaces from human serum albumin (Fraction V, Sigma-Aldrich Co., St. Louis, MO, USA) and human IgG (Sigma-Aldrich Co., St. Louis, MO, USA) solutions was also determined in the similar way. Protein layer thickness was calculated from the shift in the resonance angle using Fresnel fits for the system BK7/Cr/Au/SAM/protein/water[29,30], where the refractive indices of SAM and protein were assumed to be 1.45. The thickness supposing that the density of the protein layer was assumed to be 1. From these, the amounts of proteins adsorbed

on the surfaces could be estimated from the following relation[19,20],

1.0 degree SPR angle shift (DA) $\rightarrow$ 0.5 μg of protein on 1 cm^2 of the surface (1.1)

1.2.5 Release of complement fragment C3a-desArg

500 μl of 10% serum diluted with VB was incubated on a SAM surface (4.0 cm^2) for 90 min at 37 ℃, a supernatant was collected, and EDTA was added at a final concentration of 10 mmol dm^{-3}. A commercial enzyme-linked immunosorbent assay (ELISA) kit (BD OptEIA Human C3a ELISA, BD Biosciences Pharmingen, CA, USA) was used to determine the amount of generated C3a-degArg fragment in the collected specimens. Control experiments were run on CH_3-SAM in parallel, and the concentration of the C3a-desArg fragment released on each surface was expressed after subtraction from the concentration obtained from the control surface, CH_3-SAM, to eliminate the effect of the fluid phase activation of C3.

1.2.6 Protein elution from sample surfaces, SDS-PAGE and immunoblot

A sample surface was rinsed with VB, and exposed to 10% NHS in VB for 90 min at ambient room temperature, and then washed with VB 4 times. Sodium dodecyl sulfate-polyacrylamide gel electrophoresis (SDS-PAGE) sample buffer with 2% SDS and 2% 2-mercaptoethanol[31] were applied to the surface and left for 30 min at 37 ℃. The supernatant was collected, and then analyzed by the SDS-PAGE on a $4-20$% gradient minigel (Ready Gel J, Bio-Rad Laboratories Japan, Japan) under reducing conditions. After electrophoresis, proteins were transferred to a nylon membrane (Hybond N+, Amersham pharmacia biotech UK Limited, UK) using Towbin's buffer with TransBlot SD (Bio-Rad Laboratories). The membrane

was incubated at ambient temperature for 1 h with blocking buffer (5% skim milk, 0.1% Tween 20, Tris-buffered saline), overnight with rabbit anti human C3b antiserum (1:500, Nordic Immunology) diluted with dilution buffer (1% skim milk, 0.1% Tween 20, Tris-buffered saline), and for 2 h with HRP-conjugated goat anti rabbit IgG (1:1000, Jackson ImmunoResearch Laboratories) diluted with dilution buffer. The membrane was washed 2 times with 0.1% Tween 20/Tris-buffered saline and two times with Tris-buffered saline. Probed proteins were visualized by enzyme immuno-staining using Immunostain HRP-1000 (Konica Minolta MG, Tokyo, Japan).

1.2.7 Statistical analysis

Data from the experiments are expressed as the mean values ± standard errors of the means (SEM). A one way analysis of variance test (ANOVA) was used to identify statistical significance of the data. ANOVA was followed by post hoc pair wise *t*-test adjusted by Holm method using R ver. 2.5.1[32].

1.3 Results

1.3.1 Surface analysis

Two surfaces were used to study amino group activation of the AP. NH_2-SAM is a well-defined and stable surface carrying primary amino groups, and the PEI coated surface carries primary, secondary and tertiary amino groups, which are less constrained than those on NH_2-SAM (Scheme 1.1). XPS spectra are shown in Fig. 1.1. The N*1s* signal from the NH_2-SAM can be seen at around 400 eV, but its intensity is weak. Atomic ratio of N and C calculated from XPS spectrum was

1 : 10.3. It is close to the theoretical value (1 : 11) from the molecular structure of 11-amino-1-undecanethiol. To confirm the surface amino groups, the NH_2-SAM surface was treated with TFAA[28] to convert surface amino groups to trifluoroacetyl groups. As shown in Fig. 1.1(a), a strong F *1s* signal is observed at 690 eV, and weak C *1s* signals are seen at 289 eV and 293 eV corresponding to a carbonyl and a CF_3 group, respectively. The N *1s* signal from the PEI coated surface could be much more clearly seen than that from NH_2-SAM, as well as the F *1s* signal and C *1s* signals of TFAA-treated PEI, indicating that the PEI coated surface carries a larger number of amino groups than the NH_2-SAM. Thus the amino groups of the NH_2-SAM and the PEI coated surfaces are presented as nucleophilic, TFAA-reactive groups.

Fig. 1.2 shows IR spectra of the surfaces obtained by the FTIR-RAS method. Detection of amino groups was difficult for the NH_2-SAM surface, and for the PEI coated surface, a peak, assigned to carbonyl of the COOH-SAM, was observed at 1739 cm^{-1} and 1716 cm^{-1}. After TFAA treatment, however, peaks assigned to amide I (1693 cm^{-1}), amide II (1558 cm^{-1}), and stretch vibration of C–F bond (1215 cm^{-1}) were clearly observed for both surfaces.

1.3.2 C3b and C1q deposition on surfaces

SPR sensorgrams for the serial treatment of the NH_2-SAM and the PEI-coated surfaces are shown in Fig. 1.3. The SPR angle increased sharply and then slowly over time when the NH_2-SAM was exposed to 10% NHS. After 90 min, the surface was washed and the SPR angle shift was around 1,700 mDA. The serum protein adsorbed surface was then exposed to an anti-human C3b antiserum solution, and

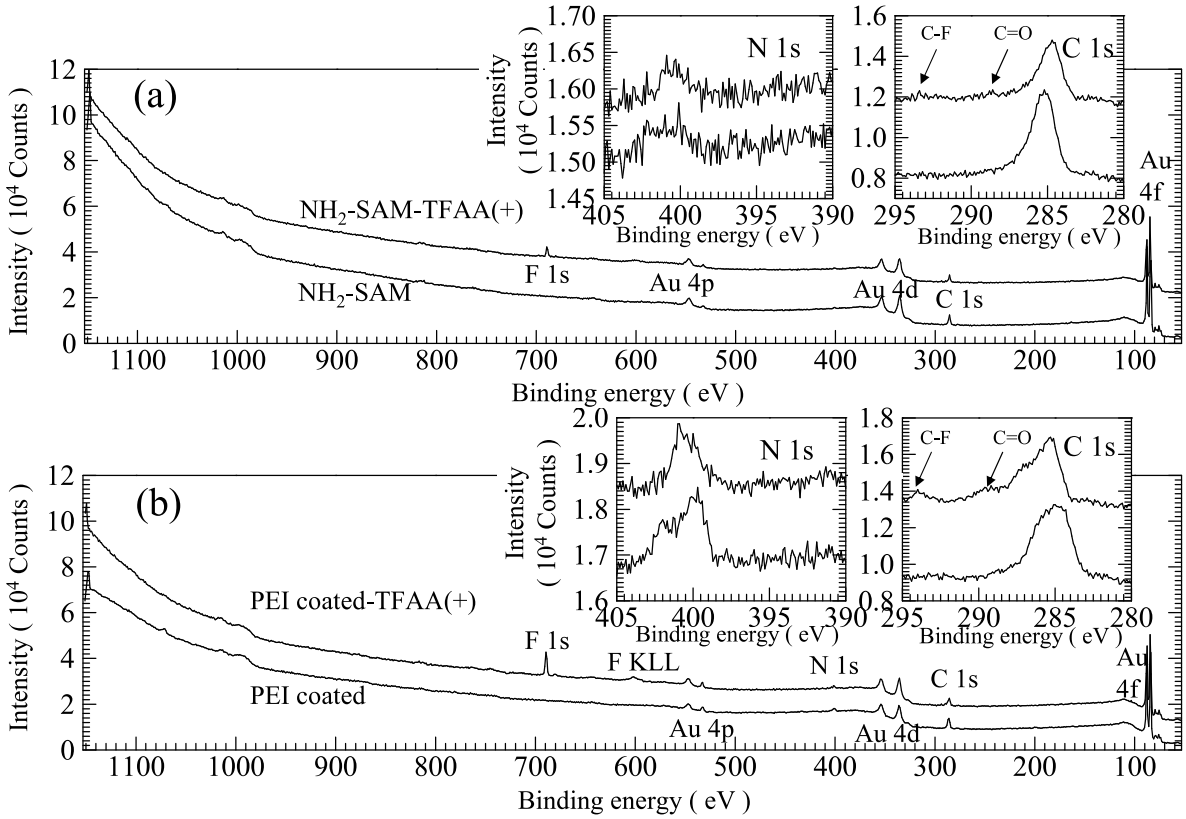

Fig. 1.1 XPS spectra of NH_2-SAM and PEI-coated surfaces before and after treatment with trifluoroacetic anhydride. (a): NH_2-SAM, (b): PEI coated surface

the SPR angle shift due to immobilization of anti-C3b antibody was small, less than 200 mDA. The SPR angle shift for the PEI coated surface was slightly larger, approximately 1,800 mDA, before and after 10% NHS exposure, and immobilization of anti-human C3b antibody was more obvious in the PEI coated surface. The spike observed upon NHS exposure is due possibly to conformation changes of the adsorbed PEI on the surface caused by interaction with serum proteins. Similar examinations were performed with 10% NHS supplemented 10 mmol dm^{-3} EDTA. Increases of the SPR angle shift were suppressed due to inhibition of the complement system by EDTA.

In the experiments shown in Fig. 1.3, 10% NHS was used as complement source.

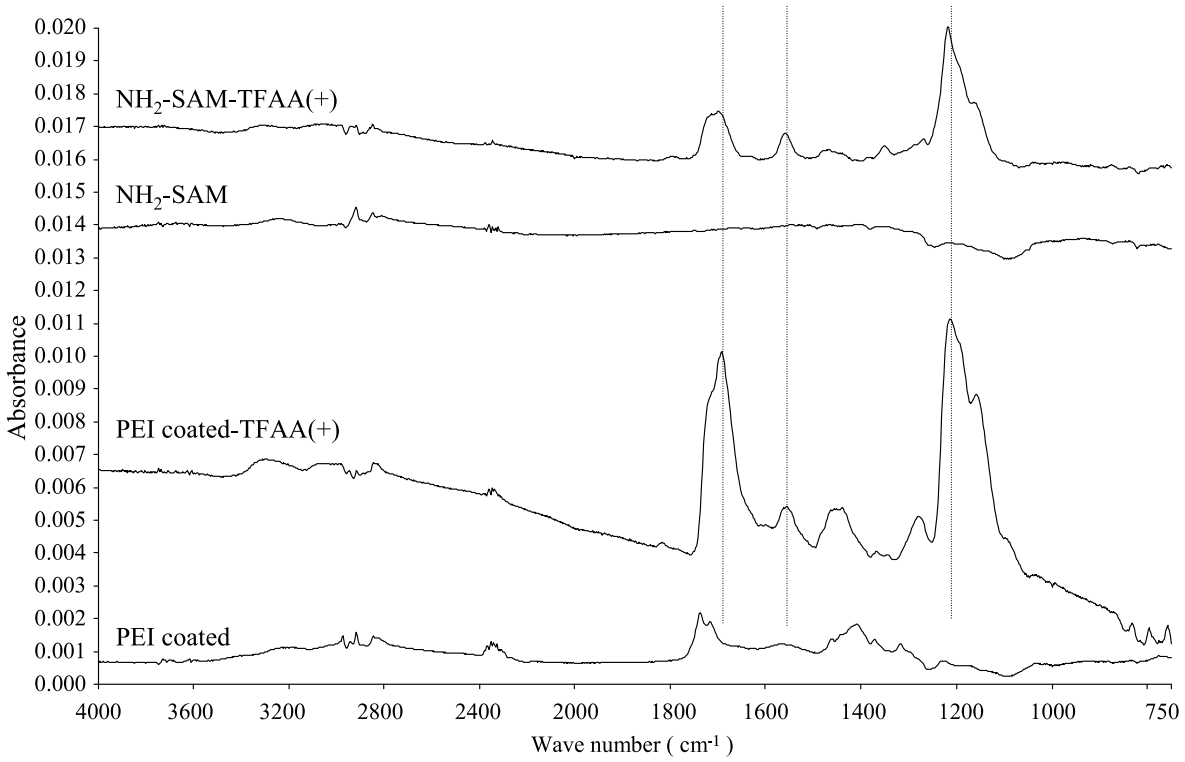

Fig. 1.2 FTIR-RAS spectra of NH_2-SAM and PEI-coated surfaces. NH_2-SAM and NH_2-SAM -TFAA(+): before and after treatment with trifluoroacetic anhydride, respectively. PEI coated and PEI coated-TFAA(+): before and after treatment with trifluoroacetic anhydride, respectively.

This is a non-physiological concentration of complement protein which is not found in vivo. It has been reported that dilution of serum might attenuates the alternative pathway of complement[33,34]. Undiluted NHS was used to see the effect of serum dilution on the complement activation on SAM surfaces carrying different functional groups. Undiluted serum was introduced into the flow cell at 8.0 μl/min., the change of the resonance angle was monitored as a function of the time for 90 min and then the surface was further exposed to anti-C3b antibody. The amounts of adsorbed serum proteins and deposition of anti-C3b antibody on surfaces were summarized in Fig. 1.4. It includes results obtained using 10% NHS for easy comparison. The amounts of adsorbed serum proteins and deposition of anti-C3b an-

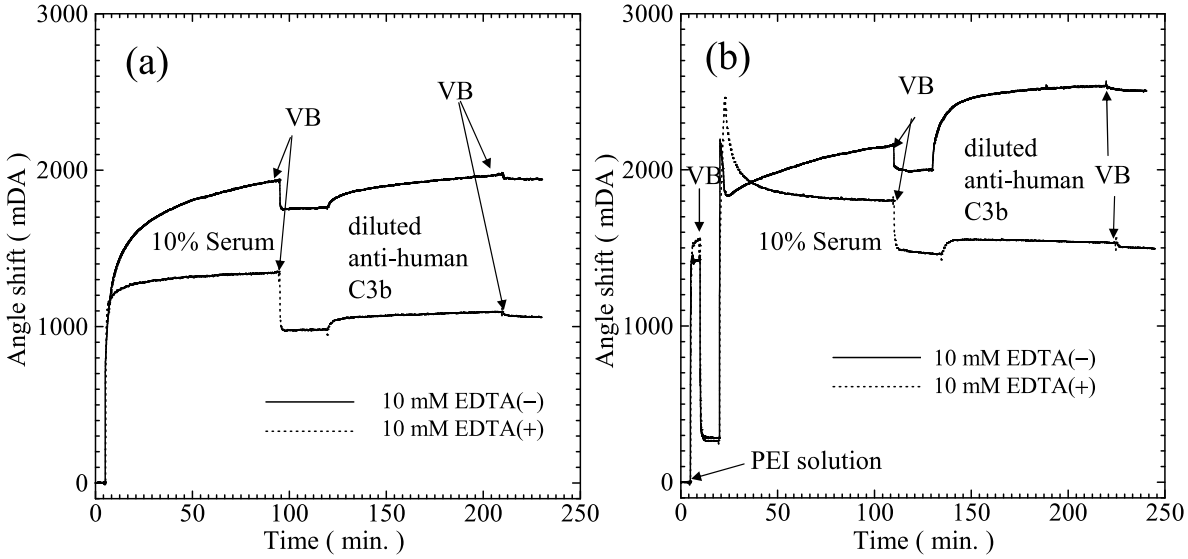

Fig. 1.3 Surface plasmon resonance sensorgrams of protein adsorption onto NH_2-SAM and PEI-coated surfaces from 10% human normal serum, and detection of C3b deposition on those surfaces using rabbit anti-human C3b serum. (a): NH_2-SAM surface, (b): PEI-coated surface. VB: Veronal buffer. Effect of complement activation on protein adsorption can be clearly seen using 10% human normal sera with/without addition of 10 mmol dm^{-3} EDTA, because EDTA effectively inhibits complement activation.

tibody on OH-SAM were higher than those on the other surfaces, indicating the OH-SAM is the strongest activator of the alternative pathway in the four surfaces examined. Plenty amounts of serum proteins were adsorbed on the NH_2-SAM and PEI surface, but amounts of anti-C3b antibody deposition were not large on either surface. All of these tendencies are same as those found when 10% NHS was used. In the following experiments, 10% NHS was used.

Protein compositions in the adsorbed protein layers formed on these amino surfaces as well as on OH-SAM and CH_3-SAM were further examined using specific antibodies to C1q, immunoglobulin G and serum albumin (Fig. 1.5). Amounts of NHS proteins adsorbed onto the 10% NHS-exposed NH_2-SAM and the PEI-coated surfaces were 720 $\pm$ 35 ng/cm^2 and 790 $\pm$ 51 ng/cm^2, respectively, and amounts

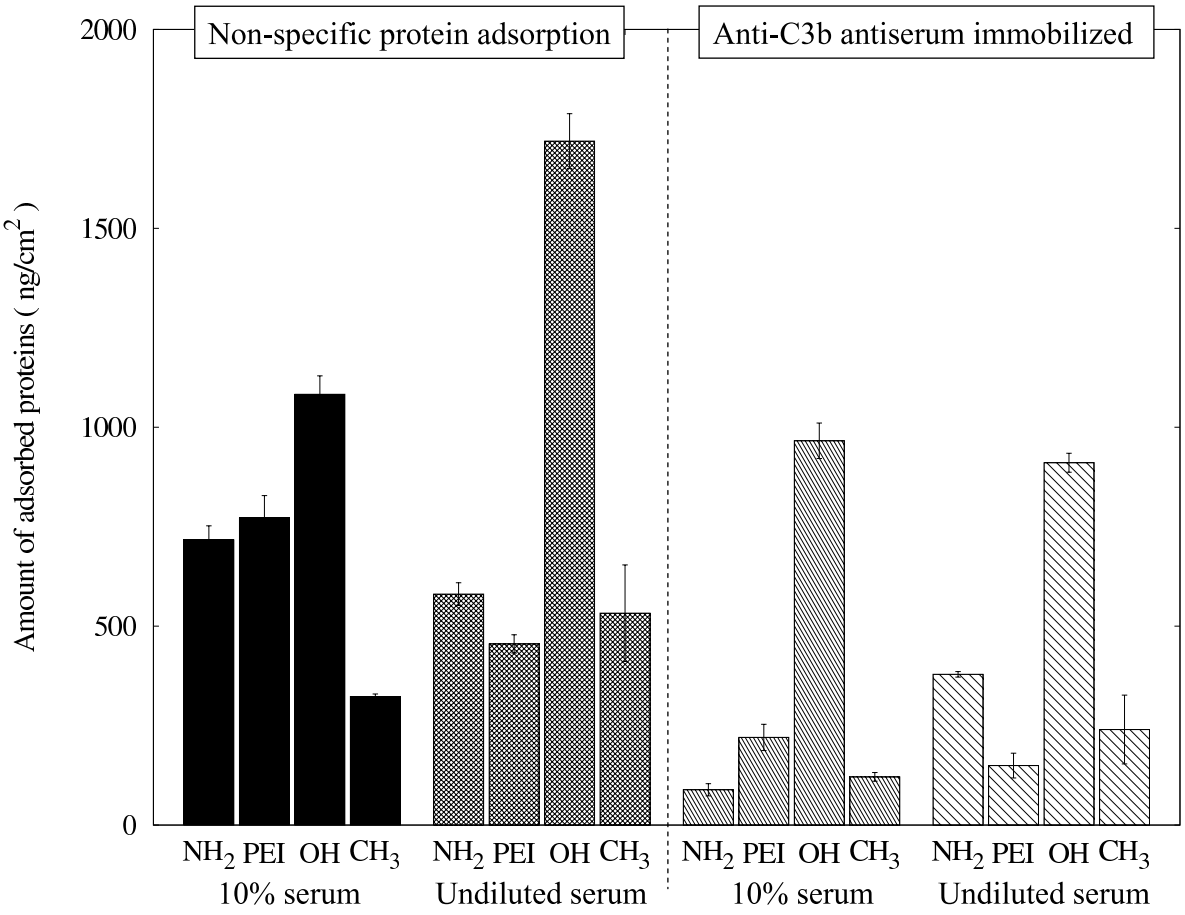

Fig. 1.4 Effects of serum dilution on amounts of proteins adsorbed onto NH_2-SAM, PEI-coated, OH-SAM and CH_3-SAM surfaces from undiluted normal human serum, and deposition of C3b. Experiments were repeated 3 times using same pooled serum from 8 healthy donors. Data from the experiments are expressed as the mean values $\pm$ SEM (n = 3).

of anti-C3b antibody immobilized on NHS protein adsorbed layers were 90 $\pm$ 15 ng/cm^2 (NH_2-SAM) and 220 $\pm$ 30 ng/cm^2 (PEI). Amount of anti-C3b antibody immobilization on OH-SAM was dramatically higher, at 970 $\pm$ 45 ng/cm^2. No evident immobilization of anti-C1q antibody, specific for the classical pathway, was detected on the adsorbed protein layers on either the NH_2-SAM or the PEI-coated surface. Immobilized concentrations of anti-HSA were analyzed and it was observed that adsorption varied highly depending on the surface. Serum albumin adsorbed on NH_2-SAM and CH_3-SAM to a greater extent than on PEI coated surface and OH-

SAM.

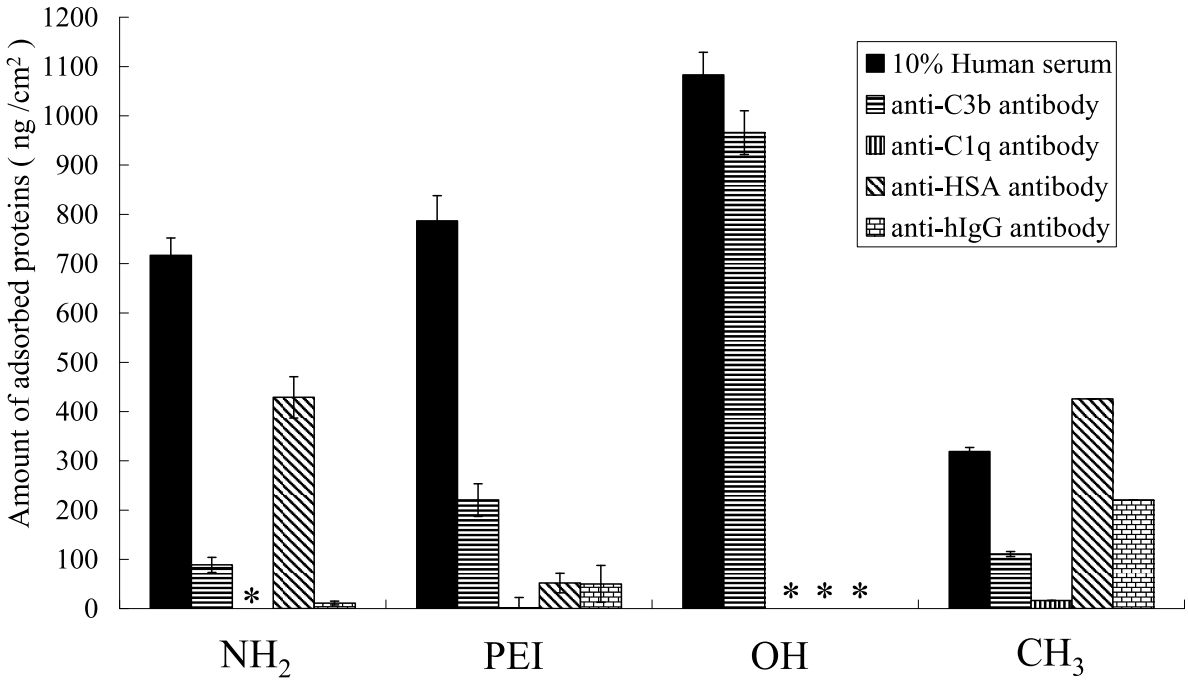

Fig. 1.5 Amounts of proteins adsorbed onto NH_2-SAM, PEI-coated, OH-SAM and CH_3-SAM surfaces from 10% normal human serum, and analyses of C3b, C1q, albumin and immunoglobulin in the protein adsorbed layers using respective anti-sera/antibodies. Experiments were repeated 4 times using same pooled serum from 8 healthy donors. Data from the experiments are expressed as the mean values ± SEM (n = 4). *: obtained amounts were very small.

1.3.3 Effect of pre-adsorption of albumin and IgG on complement activation

As shown in Fig. 1.5, a large amount of albumin adsorbed to NH_2-SAM exposed to 10% NHS. To determine the effects of pre-adsorption of albumin on complement activation, an NH_2-SAM surface was first exposed to 0.1% albumin solution and then exposed to 10% NHS (Fig. 1.6). Immobilization of anti-human C3b antibody on NH_2-SAM surface pre-adsorbed with albumin remained similar to the surface exposed only to 10% NHS. In contrast, when IgG pre-adsorbed NH_2-SAM was exposed first to 10% NHS and then to anti-human C3b antibody solution, large amounts of serum proteins and anti-human C3b antibody were immobilized. Simi-

lar examinations were performed on PEI coated surfaces. Pre-adsorption of albumin inhibited C3b deposition, as observed on the NH_2-SAM surface. On the other hand, the PEI coated surface with a pre-adsorbed IgG layer showed different behaviors to the pre-adsorbed IgG NH_2-SAM where amounts of IgG and either serum proteins or anti-human C3b antibody adsorbed were much less than those on the NH_2-SAM surface.

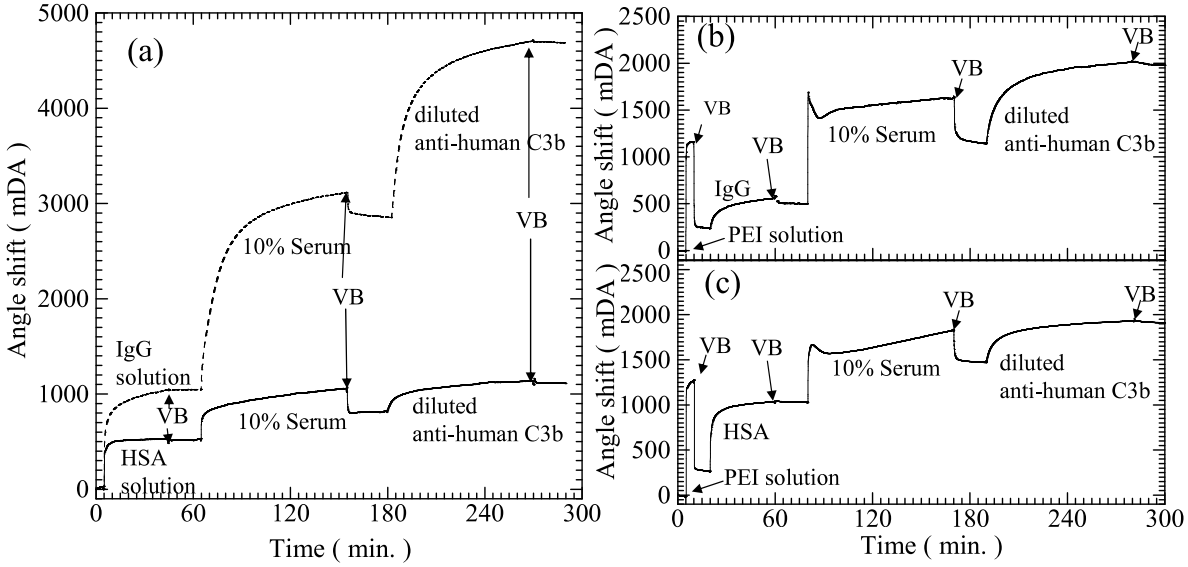

Fig. 1.6 Effects of albumin or immunoglobulin pre-adsorption on complement activation. Surfaces carrying amino groups, NH_2-SAM and PEI-coated surface, were pretreated with albumin or IgG solution and exposed to 10% human normal serum. C3b deposition on the surfaces was detected using rabbit anti-human C3b serum. (a): NH_2-SAM surface, (b), (c): PEI-coated surface. VB: Veronal buffer.

1.3.4 Release of complement fragment C3a

C3 is cleaved during activation of the complement system through all three pathways. The C3 convertases cleave the α-chain, generating C3a and C3b. The larger C3b carrying the thioester bond is immobilized on the nucleophile-carrying target surface, and the smaller 9 kDa anaphylatoxin C3a is released to the fluid phase. Thus the presence of C3a in the fluid phase indicates activation of the complement

system. C3a levels in 10% NHS-exposed surfaces were determined, and concentration of C3a released was normalized after subtracting the C3a concentration obtained on the control surface, CH_3-SAM, to account for spontaneous cleavage of C3 (Fig. 1.7). Amounts of C3a released in NH_2-SAM and PEI coated surface were significantly smaller than that on OH-SAM ($p < 0.001$). Together, the less effective C3b deposition and low levels of C3a release suggest that these amino group-carrying surfaces are less effective activators for the alternative pathway than OH-SAM.

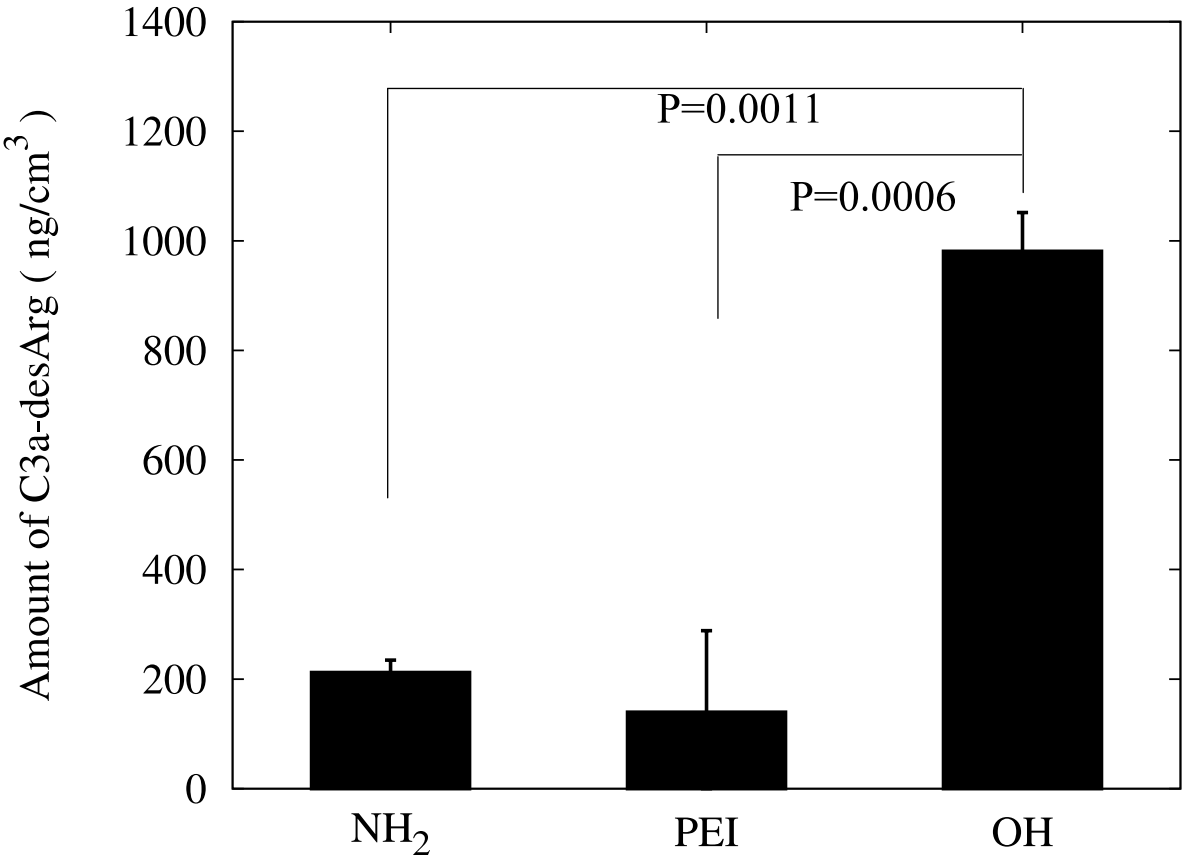

Fig. 1.7 Release of C3a-desArg in diluted serum exposed to NH_2-SAM, PEI-coated surface or OH-SAM. CH_3-SAM is used as a controlled surface. Experiments were repeated 4 times for each surface using same pooled serum from 8 healthy donors. C3a-desArg amount on each surface is presented after subtracting C3a-desArg amount on CH_3-SAM (2.5 $\pm$ 0.4 (SEM) $\mu g/cm^3$). Amount of C3a in naive10% NHS and fully activated by incubation with zymosan were 0.25 $\pm$ 0.02 $\mu g/cm^3$ (n = 4) and 5.4 $\mu g/cm^3$ (n = 2), respectively. Error bars are represent $\pm$ SEM (n = 4).

1.3.5 Analysis of C3b fragments on the surface

Proteins adsorbed on the various surfaces were eluted under reducing conditions to detect the presence of C3b fragments. Fig. 1.8 shows FTIR-RAS spectra of protein-adsorbed surfaces before and after SDS treatment. Peaks assigned to amide I and amide II were clearly observed at 1663 and 1547 cm^{-1}, respectively, for NH_2-SAM and PEI coated surfaces exposed to 10% serum. After SDS treatment, intensities of these two peaks were reduced to about 25% of their original values and new peaks appeared around 1400–1000 cm^{-1}, which are assigned to stretching vibration of sulfonyl groups of SDS molecules interacting with these surfaces. Strongly bound protein would be also left behind and this might be the protein of most interest. A portion of the proteins remaining on the surfaces could be fragments of C3dg (Fig. 1.9(a)) and C4, which might be covalently immobilized to the surfaces through amide bonds.

The eluents were further analyzed for C3b by western blot analysis. Distinct bands of approximately 75 kDa and 40 kDa were observed in the OH-SAM eluent, which were suspected to be the β-chain of C3b and a fragment of α-chain of iC3b (Fig. 1.9(b)). C3b is susceptible to proteolysis by a serine proteinase factor I, which cleaves the β-chain of C3b into a COOH-terminal 43-kDa polypeptide and a NH_2-terminal 68-kDa polypeptide[35]. Both the β-chain and the smaller 43-kDa polypeptide are bonded to the larger 68-kDa polypeptide by disulfide bonds (see Fig. 1.9(a)). When the surface was treated with a 2% SDS and 5% 2-mercaptoethanol mixed solution, the β-chain and the smaller 43-kDa polypeptide was expected to be released from the surface due to reduction of the disulfide bonds. The larger 68-kDa

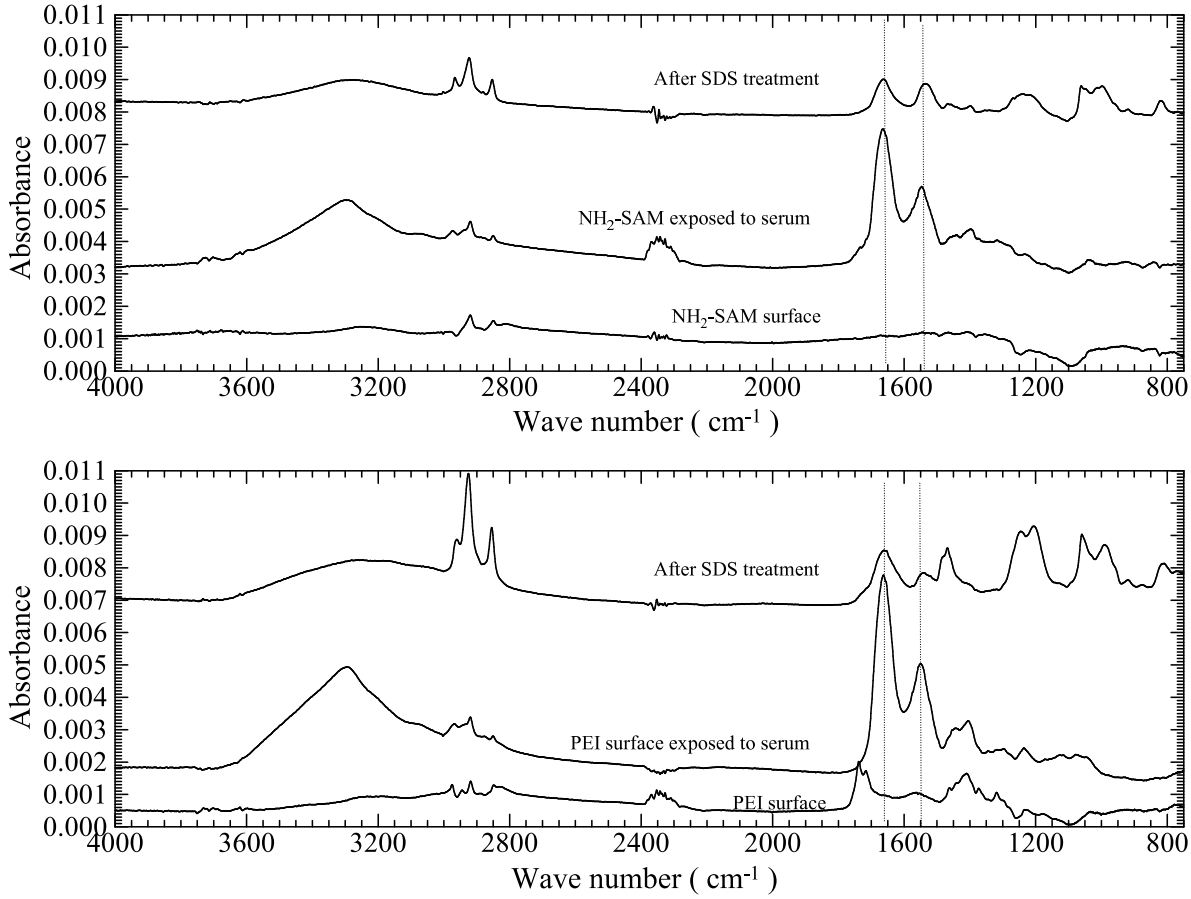

Fig. 1.8 FTIR-RAS spectra of protein-adsorbed surfaces before and after SDS treatment. Removal of proteins from NH_2-SAM (upper panel) and PEI-coated (lower panel) surfaces exposed to 10% normal human serum using 2% SDS solution containing 5% 2-mercaptoetanol.

polypeptide, however, could not be released from the surface, as it is immobilized through an ester bond on OH-SAM. Together these results indicate that OH-SAM activates the complement system, thus immobilizing C3b. Faint bands of approximately 120-kDa and 75-kDa were observed for the eluent from PEI coated surfaces, which may correspond to α- and β-chains (115 and 74 kDa, respectively). Small amount of adsorbed but not covalently bounded C3b was released from the PEI coated surfaces. No bands, however, were observed in the eluent from NH_2-SAM. Cheung et al reported that a large amount of C3a fragment (10 kDa) adsorbed onto a

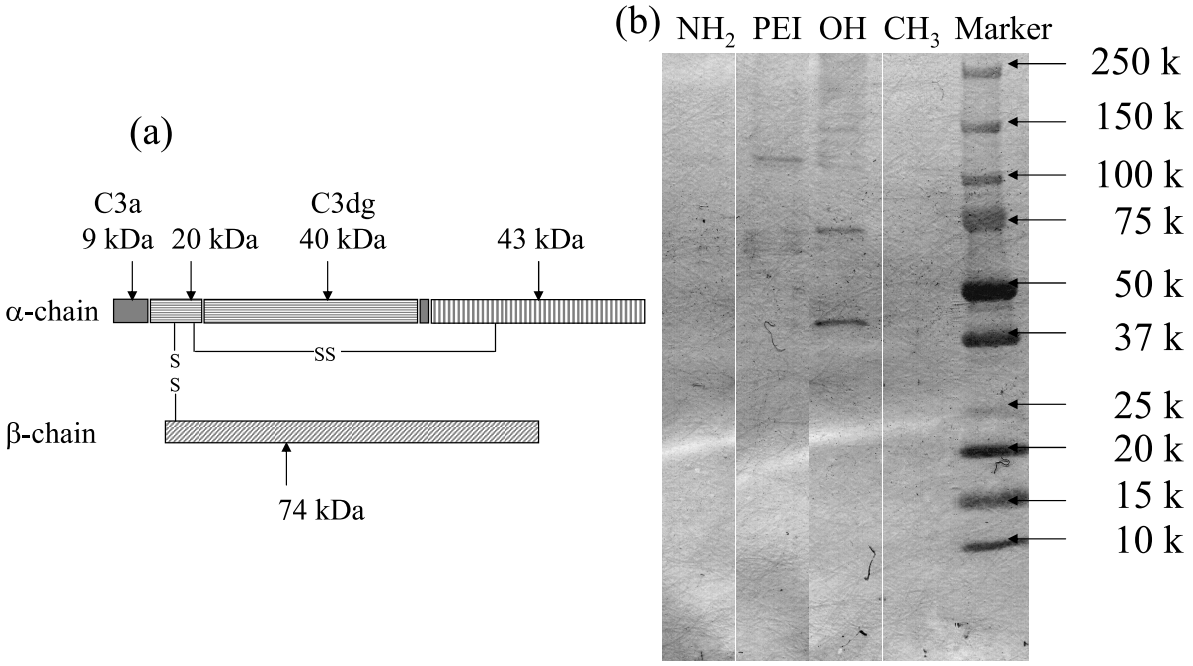

Fig. 1.9 Western blot analyses of C3 fragments, presented in (a) as schematic, in proteins extracted from NH_2-SAM and PEI-coated surfaces exposed to 10% human normal serum (b).

polyacrylonitrile surface[36]. However, no distinct band around 10 kDa was observed in an Ag-stained SDS-PAGE gel of eluents from the NH_2-SAM and the PEI-coated surface (data not shown).

1.4 Discussion

Amino groups, the representative nucleophilic groups, are considered to be potent activators of the complement system via the alternative pathway[11]. Reactivity of the amino groups in NH_2-SAM and PEI as functional nucleophilic groups was clearly demonstrated through the reaction with TFAA as seen in Fig. 1.1. Self assembled monolayers of alkanethiols with a long alkyl chain are stable in serum[37], and microcapsules made of polyion complexes between PEI and polyanions have been reported to be stable in ascites[38,39]. These two surfaces with nucleophilic amino

groups demonstrated stability in serum could serve as good model surfaces to study interaction between the complement system and the surface carrying amino groups.

Model surfaces prepared in this chapter were exposed to 10% human serum, and activation of the serum complement system was studied through deposition of C3b on the surfaces and release C3a-desArg in the serum. It has been reported that the concentration of serum strongly affects activation behavior of the complement system[33,34], and undiluted serum should be used to assess the complement activation on the surface[40]. The amounts of adsorbed serum proteins and deposition of anti-C3b antibody on surfaces were also assessed in the experimental set-up mentioned in this chapter using undiluted serum. (Fig. 1.4) Amounts of anti-C3b antibody deposited on surfaces were different between in serum and in dilute 10% serum, but those are OH-SAM $>$ CH_3-SAM = NH_2-SAM $>$ PEI in undiluted serum and OH-SAM $>$ CH_3-SAM $>$ NH_2-SAM $>$ PEI coated surface in 10% serum in those order. In undiluted NHS, deposition of anti-C3b antibody on PEI surface was smaller than that in 10% NHS. The significance of this observation in relation to complement activation in dilute serum is not clear yet. This result suggests that NH_2-SAM and PEI coated surfaces are much weaker activator of the complement system than OH-SAM even if those are under undiluted serum condition.

Several groups have studied complement-activating effects of amino groups, including those introduced onto polystyrene surface with RF plasma[25], which introduces not only amino groups, but also hydroxyl and carboxyl groups on the surface[28]. Thus, the potential contribution of hydroxyl groups in activating the complement system makes it difficult to assess amino group effectiveness in activation

in this system. PEI is a cationic polymer that strongly interacts with anionic polynucleotide, DNA[41], through the ionic binding, and thus has been used in gene delivery to cells in vitro and in vivo[42]. Plank studied interaction of various polycations, included PEI, with the complement system in conjunction with gene therapy[26]. The degree of complement activation by DNA complexes is strongly dependent on the ratio of polycation and DNA for all of polylysine, PEI and dendrimer, where activation gradually decreases as the cationic charge ratio is decreased. This suggests that free amino groups are necessary to activate the complement system. In the experiments in this chapter, PEI formed complexes with carboxylic acid groups of COOH-SAM. In addition, under physiological conditions, a primary amino group is positively charged, thus the surface carrying amino groups interact with negatively charged serum proteins. Albumin, abundant in serum, is physiologically negatively charged, and thus is expected to be strongly adsorbed to surface amino groups due to the electrostatic interaction. In this study, it was found that large amounts of serum albumin deposited on the NH_2-SAM surface, and large amounts of serum proteins, but not albumin, on the PEI coated surface. Reduction of number of free amino groups due to the complex formation appeared to decrease the potential of the PEI coated surface to activate the complement system. This reduction can explain the lower amount of anti-C3b binding to the protein layer formed on PEI coated surface after undiluted NHS.

In a pioneer work[43], Cornelius and Brash analyzed the protein layers formed during contact of plasma with hemodialysis membranes made of cellulose derivatives, polymethymethacrylate and polyacrylonitrile. Heparinized human plasma

was circulated through the dialysers for four hours. The proteins adsorbed to the membrane were eluted with 2% SDS. SDS-PAGE and western blots for C3 and its fragments were performed on the dialyser eluates. They found a decrease in intensity of the 110 kD band, and the appearance of a strong band at about 40 kD in the eluates from all the membranes. From these they concluded that the complement system appears to have been activated on the membrane carrying hydroxyl groups. In the cases in this chapter, the 40 kD band was found in an eluate from OH-SAM as shown in Fig. 1.9, but not eluates from NH_2-SAM and PEI coated surface. There was still the 110 kD band in the eluates from PEI coated surface. The complement system was activated on OH-SAM, but not on surfaces carrying amino groups.

No evident immobilization of anti-C1q antibody was detected on the adsorbed protein layers on either the NH_2-SAM or the PEI-coated surface, suggesting that these surfaces fail to activate the classical pathway (Fig. 1.5). More careful and well organized studies, however, are needed to conclude it, because many factors, serum concentration, incubation times with serum and shear, exert effects on C1q immobilization on surfaces, and it has been reported that C1q is only transiently detected at typical classical activation interfaces[34]. Several groups suggest that the mechanism of the activation through the alternative pathway is more complex than C3b thioester group attacking surface nucleophilic groups[44–46], and have proposed more relevant models[21,33,40,47]. When artificial materials are exposed to fluids such as plasma and serum, proteins adsorbed on the surface. The thioester group of C3b formed in the fluid phase attacks the nucleophilic groups of the protein layer adsorbed on artificial materials[11] to form C3 convertase with Bb, and/or IgG in

the protein layer activates the classical pathway and thus triggers the amplification loop of the alternative pathway[46,48,49]. CH_3-SAM was used as controlled surface to observe background levels of complement system activation. As mentioned in the caption of Fig. 1.7, a large amount of C3a was released in the serum, and small but considerable amount of anti-C3b antibody was deposited on the CH_3-SAM. This suggests that spontaneous proteins adsorption have some roles during complement activation. Amounts of C3a released on the NH_2-SAM and PEI coated surface were larger than that on CH_3-SAM, and considerable amounts of C3b deposition were seen on those surfaces, indicating that the protein adsorbed layers on NH_2-SAM and PEI coated surfaces activate the complement system, but to an extent much smaller than that on OH-SAM.

1.5 Conclusion

Interactions of two kinds of surfaces carrying amino groups, NH_2-SAM and PEI coated surfaces, with the complement system were studied. Amounts of C3b deposition on these surfaces and of C3a release in the serum were much less than that of OH-SAM, indicating that NH_2-SAM and PEI surfaces with nucleophilic amino groups are not effective activators of the complement system through the alternative pathway. Under physiological pH conditions, positively charged amino groups attract various negatively charged serum proteins, which adsorb on the surfaces via an electrostatic interaction. Surface coverage with the adsorbed protein layer interrupts access of C3b to the surface amino groups, thus, C3 convertase could not be formed through surface-bound C3b with Bb.

References

1. Walport M J. Complement. First of two parts. N Engl J Med 2001;344(14):1058–1066
2. Goldfarb R D, Parrillo J E. Complement. Crit Care Med 2005;33(12 Suppl):S482-S484
3. Sim R B, Reid K B. C1: molecular interactions with activating systems. Immunol Today 1991;12(9):307–311
4. Reid K B M. Classical Pathway of Activation. In: Rother K, Till G O, Hänsch G M, editors. The Complement System, Second Revised Edition. Berlin: Springer-Verlag; 1998. pp. 68–86
5. Ikeda K, Sannoh T, Kawasaki N, Kawasaki T, Yamashina I. Serum Lectin with Known Structure Activates Complement though the Classical Pathway. J Biol Chem 1987;262(16):7451–7454
6. Fujita T, Matsushita M, Endo Y. The lectin-complement pathway–its role in innate immunity and evolution. Immunol Rev 2004;198(1):185–202
7. Reid K B M. Lectin Pathway of Non-self Recognition. In: Rother K, Till G O, Hänsch G M, editors. The Complement System, Second Revised Edition. Berlin: Springer-Verlag; 1998. pp. 86–92
8. Fearon D T, Austen K F. Activation of the Alternative Complement Pathway with Rabbit Erythrocytes by Circumvention of the Regulatory Action of Endogenous Control Proteins. J Exp Med 1977;146(1):22–33
9. Pangburn M K, Muller-Eberhard H J. Complement C3 convertase: cell surface

restriction of β1H control and generation of restriction on neuraminidase-treated cells. Proc Natl Acad Sci U S A 1978;75(5):2416–2420

10. Law S-K A, Levine R P. Interaction between the third complement protein and cell surface macromolecules. Proc Natl Acad Sci U S A 1977;74(7):2701–2705
11. Pangburn M K. Alternative Pathway: Activation and Regulation. In: Rother K, Till G O, Hänsch G M, editors. The Complement System, Second Revised Edition. Berlin: Springer-Verlag; 1998. pp. 93–115
12. Craddock P R, Fehr J, Dalmasso A P, Brighan K L, Jacob H S. Hemodialysis leukopenia. Pulmonary vascular leukostasis resulting from complement activation by dialyzer cellophane membranes. J Clin Invest 1977;59(5):879–888
13. Craddock P R, Fehr J, Brigham K L, Kronenberg R S, Jacob H S. Complement and leukocyte-mediated pulmonary dysfunction in hemodialysis. N Engl J Med 1977;296(14):769–774
14. Chenoweth D E. Complement activation during hemodialysis: clinical observations, proposed mechanisms, and theoretical implications. Artif Organs 1984;8(3):281–290
15. Chenoweth D E, Cooper S W, Hugli T E, Stewart R W, Blackstone E H, Kirklin J W. Complement activation during cardiopulmonary bypass: evidence for generation of C3a and C5a anaphylatoxins. N Engl J Med 1981;304(9):497–503
16. Maillet F, Petitou M, Choay J, Kazatchkine M D. Structure-function relationships in the inhibitory effect of heparin on complement activation: independency of the anti-coagulant and anti-complementary sites on the heparin

molecule. Mol Immunol 1988;25(9):917–923

17. Gu Y J, Van Oeveren W. Activation of plasma components by leukocyte removal filters. ASAIO J 1994;40(3):M598-M601
18. Wegmuller E, Montandon A, Nydegger U, Descoeudres C. Biocompatibility of different hemodialysis membranes: activation of complement and leukopenia. Int J Artif Organs 1986;9(2):85–92
19. Hirata I, Morimoto Y, Murakami Y, Iwata H, Kitano E, Kitamura H, Ikada Y. Study of complement activation on well-defined surfaces using surface plasmon resonance. Colloids Surf B Biointerfaces 2000;18(3–4):285–292
20. Hirata I, Hioki Y, Toda M, Kitazawa T, Murakami Y, Kitano E, Kitamura H, Ikada Y, Iwata H. Deposition of complement protein C3b on mixed self-assembled monolayers carrying surface hydroxyl and methyl groups studied by surface plasmon resonance. J Biomed Mater Res A 2003;66(3):669–676
21. Sellborn A, Andersson M, Hedlund J, Andersson J, Berglin M, Elwing H. Immune complement activation on polystyrene and silicon dioxide surfaces Impact of reversible IgG adsorption. Mol Immunol 2005;42(5):569–574
22. Pangburn M K, Muller-Eberhard H J. Relation of putative thioester bond in C3 to activation of the alternative pathway and the binding of C3b to biological targets of complement. J Exp Med 1980;152(4):1102–1114
23. Law S-K A. The covalent binding reaction of C3 and C4. Ann N Y Acad Sci 1983;421:246–258
24. Sim R B, Sim E. Autolytic fragmentation of complement components C3 and C4 and its relationship to covalent binding activity. Ann N Y Acad Sci

1983;421:259–276

25. Ekdahl K N, Nilsson B, Golander C G, Elwing H, Lassen B, Nilsson U R. Complement Activation on Radio Frequency Plasma Modified Polystyrene Surfaces. J Colloid Interface Sci 1993;158(1):121–128
26. Plank C, Mechtler K, Szoka F C J, Wagner E. Activation of the complement system by synthetic DNA complexes: a potential barrier for intravenous gene delivery. Hum Gene Ther 1996;7(12):1437–1446
27. Whaley K, North J. Haemolytic assays for whole complement activity and individual components. In: Sim R B, Dodds A W, editors. Complement. Walton Street, Oxford : Oxford University Press; 1997. pp. 19–47
28. Everhart D S, Reilley C N. Chemical Derivatization in Electron Spectroscopy for Chemical Analysis of Surface Functional Groups Introduced on Low-Density Polyethylene Film. Anal Chem 1981;53(4):665–676
29. Azzam R M A, Bashara N M. Reflection and Transmission of Polarized Light by Stratified Planar Strucures. In: Ellipsometry and Polarized Light. Amsterdam : Elsevier; 1987. pp. 269–363
30. Knoll W. Polymer thin films and interfaces characterized with evanescent light. Makromol Chem 1991;192(12):2827–2856
31. Laemmli U K. Cleavage of Structural Proteins during the Assembly of the Head of Bacteriophage T4. Nature 1970;227(5259):680–685
32. R Development Core Team. R: A Language and Environment for Statistical Computing. Vienna, Austria : R Foundation for Statistical Computing; 2007. ISBN 3–900051–07–0, URL: http://www.R-project.org/

33. Andersson J, Ekdahl K N, Lambris J D, Nilsson B. Binding of C3 fragments on top of adsorbed plasma proteins during complement activation on a model biomaterial surface. Biomaterials 2005;26(13):1477–1485

34. Tengvall P, Askendal A, Lundström I. Temporal studies on the deposition of complement on human colostrum IgA and serum IgG immobilized on methylated silicon. J Biomed Mater Res 1997;35(1):81–92

35. Davis A E III, Harrison R A. Structural characterization of factor I mediated cleavage of the third component of complement. Biochemistry 1982;21(23):5745–5749

36. Cheung A K, Parker C J, Wilcox L A, Janatova J. Activation of complement by hemodialysis membranes: polyacrylonitrile binds more C3a than cuprophan. Kidney Int 1990;37(4):1055–1059

37. Flynn N T, Tran T N T, Cima M J, Langer R. Long-Term Stability of Self-Assembled Monolayers in Biological Media. Langmuir 2003;19(26):10909–10915

38. Gaumann A, Laudes M, Jacob B, Pommersheim R, Laue C, Vogt W, Schrezenmeir J. Effect of media composition on long-term in vitro stability of barium alginate and polyacrylic acid multilayer microcapsules. Biomaterials 2000;21(18):1911–1917

39. Schneider S, Feilen P J, Slotty V, Kampfner D, Preuss S, Berger S, Beyer J, Pommersheim R. Multilayer capsules: a promising microencapsulation system for transplantation of pancreatic islets. Biomaterials 2001;22(14):1961–1970

40. Nilsson B, Ekdahl K N, Mollnes T E, Lambris J D. The role of complement in

biomaterial-induced inflammation. Mol Immunol 2007;44(1–3):82–94

41. Atkinson A, Jack G W. Precipitation of nucleic acids with polyethyleneimine and the chromatography of nucleic acids and proteins on immobilised polyethyleneimine. Biochim Biophys Acta 1973;308(7):41–52
42. Boussif O, Lezoualc'h F, Zanta M A, Mergny M D, Scherman D, Demeneix B, Behr J-P. A versatile vector for gene and oligonucleotide transfer into cells in culture and in vivo: polyethylenimine. Proc Natl Acad Sci U S A 1995;92(16):7297–7301
43. Cornelius R M, Brash J L. Identification of proteins absorbed to hemodialyser membranes from heparinized plasma. J Biomater Sci Polym Ed 1993;4(3):291–304
44. Cheung A K, Parker C J, Wilcox L, Janatova J. Activation of the alternative pathway of complement by cellulosic hemodialysis membranes. Kidney Int 1989;36(2):257–265
45. Françoise Gachon A M, Mallet J, Tridon A, Deteix P. Analysis of proteins eluted from hemodialysis membranes. J Biomater Sci Polym Ed 1991;2(4):263–276
46. Lhotta K, Wurzner R, Kronenberg F, Oppermann M, Konig P. Rapid activation of the complement system by cuprophane depends on complement component C4. Kidney Int 1998;53(4):1044–1051
47. Wetterö J, Askendal A, Bengtsson T, Tengvall P. On the binding of complement to solid artificial surfaces in vitro. Biomaterials 2002;23(4):981–991
48. Nilsson U R. Deposition of C3b/iC3b leads to the concealment of antigens,

immunoglobulins and bound C1q in complement-activating immune complexes. Mol Immunol 2001;38(2–3):151–160

49. Tengvall P, Askendal A, Lundström I. Studies on protein adsorption and activation of complement on hydrated aluminium surfaces in vitro. Biomaterials 1998;19(10):935–940

Chapter 2

Effects of hydrophobicity and electrostatic charge on the complement activation by amino group

2.1 Introduction

When medical devices are implanted, various responses occur at the interface between living tissue and the artificial materials such as adsorption of proteins, activation of the complement and the coagulation systems, platelet activation and cell adhesion. The interaction of plasma proteins with artificial materials is the first reaction in a series of events leading to thrombosis and inflammatory responses toward medical devices in contact with blood. These interactions should be controlled for the successful development of these devices. Thus, extensive studies have been performed to understand the interactions of body fluids, especially blood, with material surfaces.

The complement system is a cascade of enzymes consisting of approximately 30 fluid-phase and cell-membrane bound proteins, and plays an important role in the body's defense systems against pathogenic xenobiotics[1,2]. It is activated through three separate pathways: the classical pathway (CP), the lectin pathway (LP), and the alternative pathway (AP). The development of the hemodialyzer has allowed

the study of the activation of the complement system on artificial materials. It has been made clear that nucleophilic groups, such as hydroxyl groups on a dialysis membrane composed of regenerated cellulose[3,4], strongly activate the complement system. In previous studies, it was reported that a self-assembled monolayer of 11-mercaptoundecanol (OH-SAM) also acted as a strong activator of the complement system[5,6]. The amino group, another representative nucleophilic group, is expected to be a potential activator of the complement system through the alternative pathway, but few studies have demonstrated this result[7]. Some investigations in Chapter 1 found that a self-assembled monolayer of 11-amino-1-undecanethiol (NH_2-SAM) carrying amino groups at a high density could not effectively activate the complement system. It was also observed in Chapter 1 that a large amount of serum proteins deposited on the NH_2-SAM, which led us to speculate that amino groups on the SAM surface were masked by the adsorbed protein layer, and thus the amino groups could not activate the complement systems effectively. However, many aspects of this system remain to be elucidated.

In the present work, the effects of surface densities of amino groups, hydrophobicity of surfaces, and electrostatic charges upon activation of the complement system on SAMs modified with amino groups were examined. Two series of mixed SAMs, amino/methyl or amino/carboxy terminated alkanethiols, with different densities of surface amino groups were employed as model surfaces and the occurrence of complement activation on those surfaces was evaluated.

2.2 Materials and methods

2.2.1 Reagents and antibodies

1-Dodecanethiol ($C11CH_3$, Wako pure chemical industries, Ltd., Osaka, Japan), 11-mercaptoundecanoic acid (C10COOH, Sigma-Aldrich Co., St. Louis, MO, USA) and 11-amino-1-undecanethiol hydrochloride ($C11NH_2$, Dojindo Laboratories, Kumamoto, Japan), barbital sodium, calcium chloride, magnesium chloride, ethanol (all purchased from Nacalai Tesque, Inc., Kyoto, Japan) and ethylenediamine-*N,N,N',N'*-tetraacetic acid (EDTA; Dojindo Laboratories, Kumamoto, Japan) were of reagent grade and were used as obtained. Solutions of rabbit anti-human C3b (RAHu/C3b, Nordic Immunology, The Netherlands), sheep anti-human C1q (PC020, The Binding Site Ltd., Birmingham, UK), rabbit anti-HSA (55029, ICN Pharmaceuticals, Inc., USA), and goat anti-IgG (109-005-088, Jackson ImmunoResearch Laboratories, Inc., PA, USA) were prepared and stored in accordance with supplier instructions.

2.2.2 Preparation of serum and buffers

All donors of blood enrolled in this research provided informed consent. The process was approved and accepted by the ethics review board of the Institute for Frontier Medical Sciences, Kyoto University. Blood was donated from 8 healthy volunteers who had consumed a meal at least 4 h before the donation. The preparation method for the serum has been described elsewhere[6]. Briefly, the collected blood was kept at ambient temperature for 30 min to induce blood coagulation, and centrifuged at 1100 $\times$ g for 30 min at 4 ℃. The supernatant serum was then pooled

in a bottle and mixed well, and divided into polypropylene vials in an ice bath, and stored at −80 ℃ until use. Water was purified with a MilliQ system (Millipore Co.). Veronal buffer (VB), composed of 5 mmol dm^{-3} sodium barbital, 142 mmol dm^{-3} NaCl, 3.7 mmol dm^{-3} HCl, 0.15 mmol dm^{-3} $CaCl_2$, and 1.0 mmol dm^{-3} $MgCl_2$ (pH 7.4), was prepared according to the protocol for CH_{50} measurement[8]. For experiments under the inhibition of complement activation, EDTA was added to VB (without $CaCl_2$ and $MgCl_2$) to a final concentration of 10 mmol dm^{-3} (EDTA-VB).

2.2.3 Preparation of self-assembled monolayer (SAM) surfaces carrying different functional groups

Glass plates were coated with gold as previously reported[6]. Ethanol was deoxygenized with nitrogen gas before use. The series of reaction solutions with different molar ratios of two thiols ($C11NH_2$/C10COOH or $C11NH_2$/$C11CH_3$) were prepared by mixing a 1 mmol dm^{-3} solution of each thiol and the total concentration of thiols was 1 mmol dm^{-3} in ethanol. The glass plates with a gold thin layer were immersed into the reaction mixtures at room temperature for 24 h to form two-component-mixed SAMs. The glass plates were sequentially washed with ethanol and Milli-Q water three times each and then dried under a stream of dried nitrogen gas.

2.2.4 Surface analyses of glass plates carrying amino groups

Infrared (IR) adsorption spectra of sample surfaces were collected by the reflection-adsorption method (FTIR-RAS) using a Spectrum One (Perkin-Elmer, USA) spectrometer equipped with a Refractor^{TM} (Harrick Sci. Co., NY, USA) and a mercury-

cadmium telluride (MCT) detector cooled by liquid nitrogen. Glass plates with a gold layer at 199 nm of thickness were used for FTIR-RAS analyses. Spectra were obtained using the *p*-polarized infrared light at an incident angle of 75° in the chamber purged with dry nitrogen gas for 128 scans at 4 cm^{-1} resolution from 4000 to 750 cm^{-1}. The areas of peaks at 2965–2966 cm^{-1} assigned to the asymmetric stretching mode of methyl groups were used to determine the surface concentrations of CH_3 groups, and the areas of peaks at 1719–1720 cm^{-1} assigned to the stretching mode of carboxyl groups were used to determine the surface concentrations of COOH groups[6].

2.2.5 Protein deposition observed by surface plasmon resonance (SPR)

The SPR apparatus employed in this study was a homemade apparatus[5,6] prepared referring to the report by Knoll[9]. The BK7 glass plate with the gold layer (49 nm in thickness) was coupled to a hemicylindrical prism with an immersion oil (n = 1.515, Cargille Laboratories, Cedar Grove, NJ). The sample surface was irradiated with a *p*-polarized He-Ne laser light (λ = 632.8 nm) through the prism. The intensity of the reflected light was monitored as a function of the incident angle. The incident angle, at which the reflectivity reached a minimum, was described as the SPR angle. Human serum diluted with VB to 10% (10% NHS) was used in this study. A flow chamber with a sample plate was placed on a prism of the SPR apparatus, and VB was circulated at a flow rate of 3.0 cm^3/min in the flow chamber assembly. Reflectance was monitored during the flow of the liquid samples at an incident angle of 0.5° less than the SPR angle. Human serum was then introduced into the flow chamber assembly and circulated at a flow rate of 3.0 cm^3/min for 90

min. To clear serum from the sample surface, VB was introduced and circulated for additional 20 min. All experiments were performed at 37 ℃.

To identify proteins deposited on the surface, solutions of specific antibodies or antisera were flowed through the apparatus after exposure of the sample surface to human serum. Each of the antisera/antibodies, rabbit anti-human C3b, sheep anti-human C1q, rabbit anti-HSA and goat anti-IgG diluted to 1% with VB was applied and circulated for 90 min and then VB was introduced for 20 min to wash out the antibody solution. The thickness of the protein layer was calculated from the shift in the SPR angle (ΔSPR) using Fresnel fits for the system BK7/Cr/Au/SAM/protein/water, where the refractive indices of SAM and protein were assumed to be 1.45. The amounts of proteins adsorbed onto the surfaces were estimated from the thickness presuming that the density of the protein layer was 1 as follows[5]:

$$\text{The amount of adsorbed protein } (\text{ng/cm}^2) = 500 \times \Delta\text{SPR}(^\circ) \tag{2.1}$$

The change of the resonance angle was estimated to determine the amount of proteins on surfaces.

2.2.6 Released amounts of the soluble form of the membrane attack complex, SC5b-9

A hand-made incubation chamber was used to examine release of SC5b-9 when different surfaces were exposed to 10% NHS. The chamber was composed of two glass plates carrying the same sample surface and a silicone gasket of 1 mm thickness with a hole of 20 mm in diameter. After 10% NHS were incubated in the chamber for 1.5 h at 37 ℃, they were collected and EDTA was immediately added to a

final concentration of 10 mmol dm^{-3} to stop further activation of the complement system. A commercial enzyme-linked immunosorbent assay (ELISA) kit (Quidel SC5b-9(TCC) EIA kit, Quidel Corp., CA, USA) was used to determine the soluble form of membrane attack complex, SC5b-9 in the collected 10% NHS. The measurement procedure was performed in accordance with supplier instructions.

2.2.7 Statistical analysis

Data from the experiments are expressed as the mean ± standard error of the mean. A one-way analysis of variance (ANOVA) was used to identify the statistical significance of the data. ANOVA was followed by post-hoc pair-wise t-tests adjusted using Holm's method and employing R language environment ver. 2.9.1[10].

2.3 Results

2.3.1 Surface analysis

Mixed SAMs, which can be easily prepared by using two or more different kinds of alkanethiols with different terminal groups, can provide well-defined surfaces with serially varied surface properties. These SAMs have been used for studying the interaction between artificial materials and biological phenomena[6,11]. Glass plates with a 1 nm layer of chromium and a 49 nm gold layer were immersed into solutions of the series of reaction solutions with different molar ratios of two thiols, leading to the formation of the layers of mixed SAMs carrying various molar ratios of NH_2/CH_3 or NH_2/COOH on the gold layer (Scheme 2.1).

Compositions of two series of mixed SAMs were determined from the absorption intensity of FTIR-RAS spectra. The molar ratios of NH_2 in the two kinds of

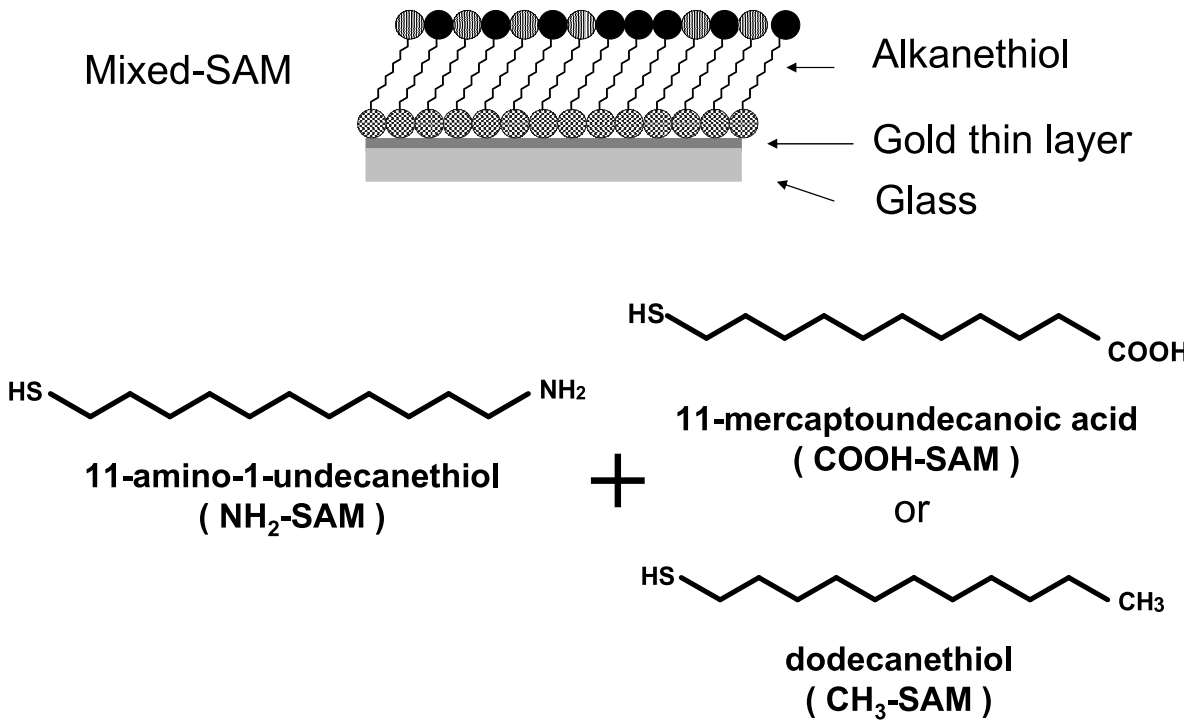

Scheme 2.1 Scheme of the sample surfaces.

Symbols correspond to NH_2 (●), either CH_3 or COOH (◍), and SH (◍) groups.

mixed-SAM surfaces are plotted against those of the reaction mixtures in Fig. 2.1. For NH_2/CH_3 mixed SAMs, the surface concentrations of NH_2 gradually increased as the concentrations of amines increased in the reaction mixtures, but the surface concentration of NH_2 never reached the levels found in the reaction mixture across the whole concentration range as previously observed[11]. In contrast, for the preparation of NH_2/COOH mixed SAMs, the surface concentrations of NH_2 sharply increased as a function of the NH_2 concentrations in the reaction mixtures and remained around 50% over a wide concentration range. This outcome might be due to salt formation between NH_2 and COOH in solutions. The hetero-dimer of alkane thiols was selectively immobilized on the gold surface[12].

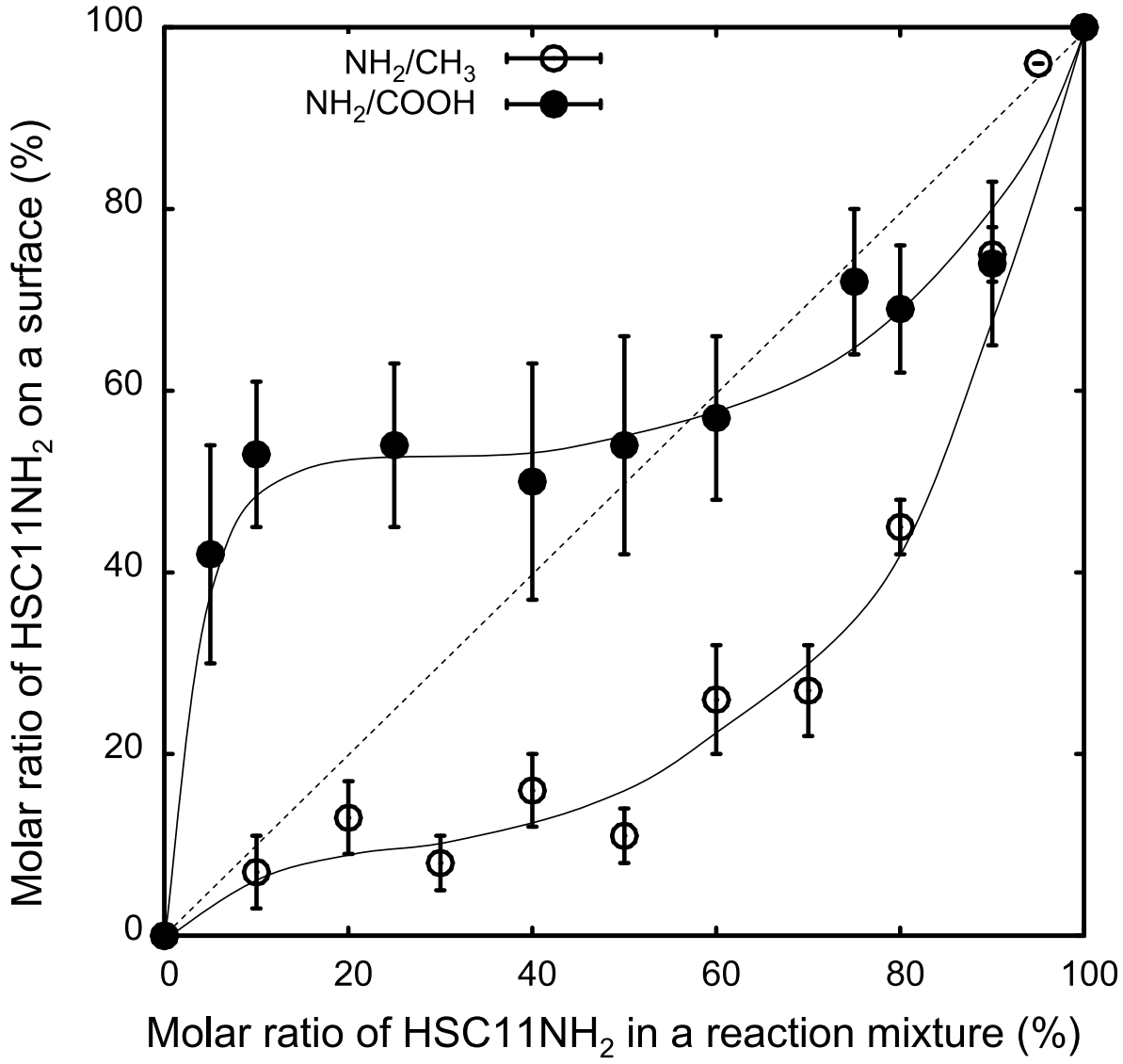

Fig. 2.1 Surface compositions of SAMs formed in mixtures of 11-amino-1-undecanethiol (NH_2) and alkanethiols with methyl (CH_3) or carboxy (COOH) end groups. Error bars represent ± SEM (n=3).

2.3.2 Interaction of serum proteins with NH_2/CH_3 mixed SAMs

A comparison of the adsorption of serum proteins onto a series of NH_2/CH_3 mixed SAMs as a function of time shows that the SPR signals sharply increased during the initial few minutes and reached plateau around 20 min after exposure to 10% NHS (Fig. 2.2A). C3b or C3bBb is expected to be immobilized on surface when the

complement system is activated by the surface. After flushing out serum from the sensor chamber with VB, the application of 1% anti-human C3b antibody solution to determine the presence of C3b or C3bBb resulted in only a modest increase in the SPR signals (Fig. 2.2B).

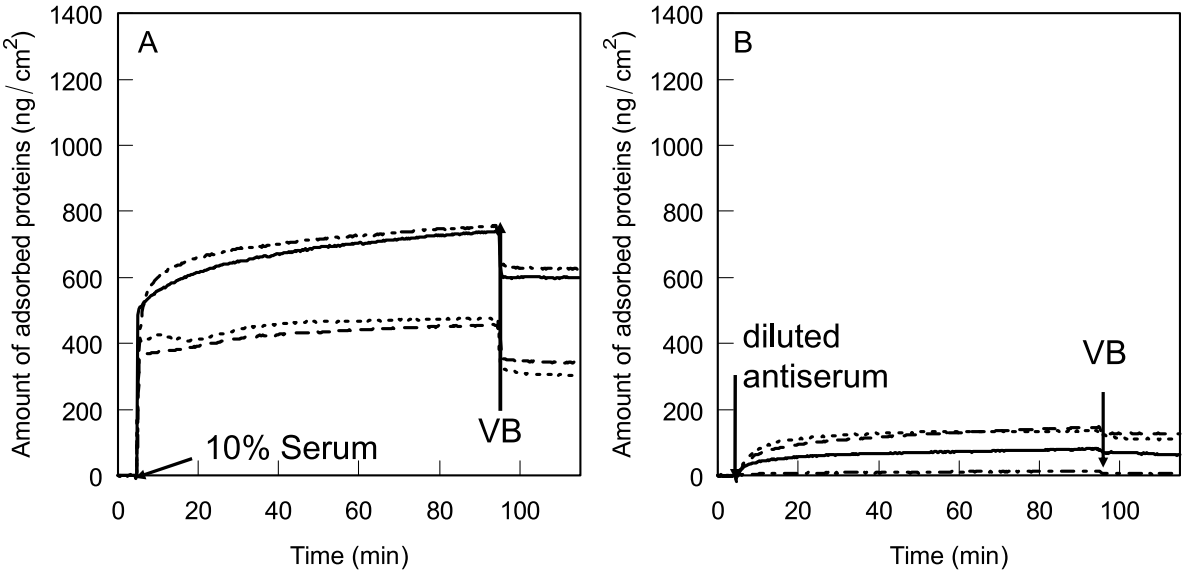

Fig. 2.2 SPR sensorgrams during exposure of 10% NHS (A) and 1% anti-C3b antiserum (B) to a series of NH_2/CH_3 mixed SAM surfaces.
(·····):NH_2/CH_3=0/100; (- - -):NH_2/CH_3=45/55; (——):NH_2/CH_3=100/0; (·-·-·):NH_2/CH_3=100/0 with 10 mmol dm^{-3} EDTA supplemented 10% NHS.

Protein adsorption from 10% NHS was examined on a series of NH_2/CH_3 mixed SAMs and the protein composition in the adsorbed protein layers was examined using specific antibodies against C3b, C1q, immunoglobulin G (IgG) and serum albumin (HSA). Although the amounts of total adsorbed serum proteins showed a small increase with increasing NH_2 density on the surfaces, over the range of 300 ng/cm^2 to 420 ng/cm^2, their differences were small. The amount of immobilized anti-HSA antibody surpassed that of any other antibodies examined, with values of $\sim$ 400–600 ng/cm^2. Although maximum immobilization of anti-HSA was observed

on a mixed SAM with NH_2/CH_3 = 35/65, no significant differences were observed between mixed SAMs with different surface NH_2/CH_3 compositions (p = 0.2767, ANOVA). Immobilized anti-IgG levels decreased with increasing surface NH_2 concentration. The amounts of immobilized anti-C3b antibody were comparable to that of anti-IgG antibody, less than 200 ng/cm^2 at all examined points. C1q was hardly detected on any NH_2/CH_3 mixed SAMs using anti-C1q antibody.

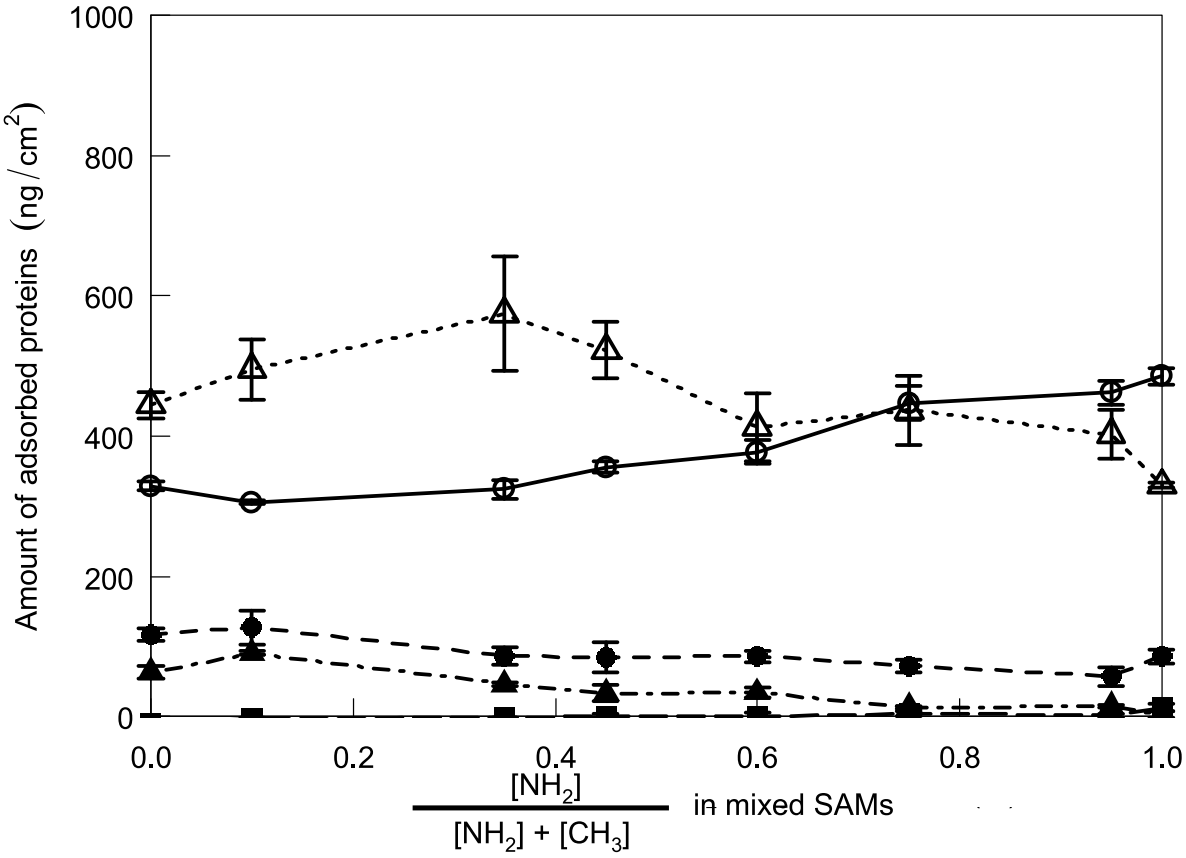

Fig. 2.3 Amounts of adsorbed proteins.

Serum proteins (—○—), and anti-C3b (- ● -), C1q (— ■ -), HSA (· · △ · ·) and IgG (· -▲-) antibodies onto the protein layer adsorbed on NH_2/CH_3 mixed SAM surfaces. Error bars represent ± SEM (n=3).

2.3.3 Interaction of proteins with NH_2/COOH mixed SAMs

Similarly as for NH_2/CH_3 mixed SAMs, time-course sensorgrams were prepared for a series of NH_2/COOH mixed SAMs to illustrate the protein adsorption from 10% NHS (Fig. 2.4A) and anti-human C3b antibody immobilization onto the formed protein layer (Fig. 2.4B). Initial sharp increases of SPR angles due to a difference of the refractive indices caused by changing VB to 10% serum (Fig. 2.4A) were followed by slow increases during 80 min. The largest increase was observed for the NH_2/COOH=55/45 SAM. After flushing out serum with VB, 1% anti-human C3b antibody solution was applied. A large increase of the SPR signal was observed for the protein layer formed on the NH_2/COOH mixed SAMs with $\sim$ 50 to 60% NH_2 density (Fig. 2.4B). Such an increase in the SPR signal was not observed on CH_3-SAM (Fig. 2.2) or with 100% NH_2-SAM. When EDTA was added to the serum, no slow increase was observed in a SPR sensorgram, and no immobilization of anti-human C3b antibody was observed on NH_2/COOH mixed SAMs modified with $\sim$ 50 to 60% NH_2 (Fig. 2.4B).

After the exposure of the surfaces to 10% serum, plentiful amounts of proteins were adsorbed on NH_2/COOH SAMs, regardless of the NH_2/COOH compositions (Fig. 2.5). Treatment with serum protein antibodies revealed that the amounts of immobilized anti-HSA antibody and anti-C3b antibody varied inversely. Amounts of anti-C3b antibody increased with increasing surface NH_2 concentration, reaching the maximum at $\sim$ 50 to 60% NH_2 density. In contrast, the amounts of anti-HSA antibody showed a minimum at $\sim$ 50 to 60% density and then increased with increasing surface NH_2 concentrations. When the complement system is activated,

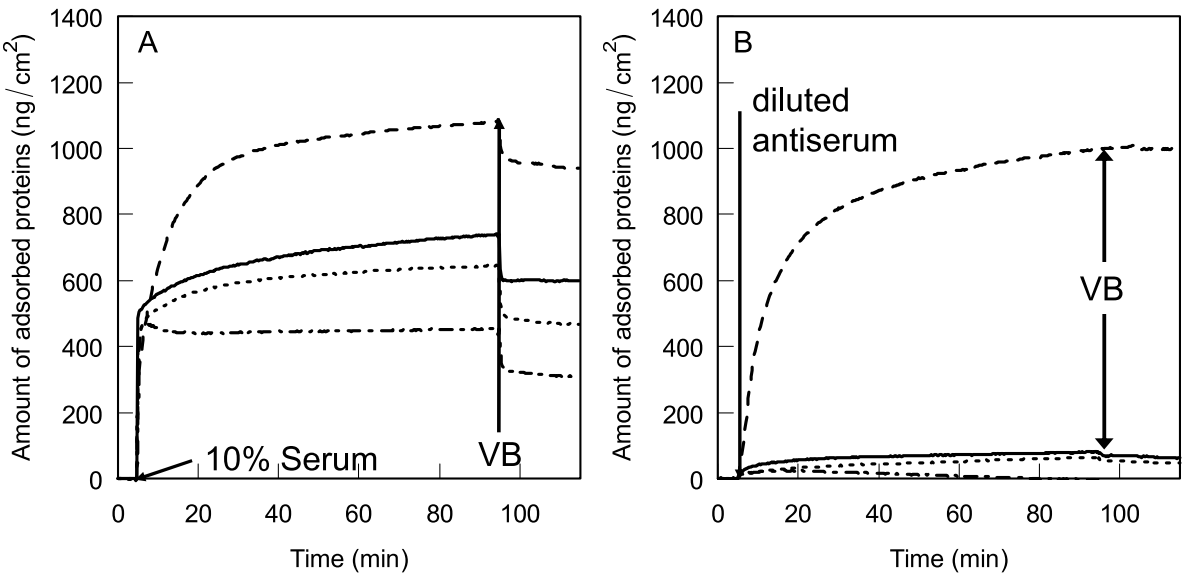

Fig. 2.4 SPR sensorgrams during exposure of 10% NHS (A) and 1% anti-C3b antiserum (B) to a series of NH_2/COOH mixed SAM surfaces.
(·····):NH_2/COOH=0/100; (- - -):NH_2/COOH=55/45; (——):NH_2 100%; and (-·-):NH_2/COOH=55/45 with 10 mmol dm^{-3} EDTA supplemented 10% NHS. NH_2 100% was the same as for Fig. 2.2. Error bars represent ± SEM (n=3).

the major component of the protein layer is C3b or C3bBb. On the other hand, when the complement system is not activated, the major component of the protein layer is albumin or IgG reflecting protein concentration in serum. Immobilized anti-C1q and anti-IgG antibodies were hardly detected on any NH_2/COOH SAMs.

These results indicate that NH_2/COOH mixed SAMs with ∼ 50 to 60% NH_2 activate the complement system through the alternative pathway, but NH_2- or COOH-SAMs are not activators.

2.3.4 Release of SC5b-9

As a consequence of activation of the complement system, a terminal complement complex, C5b-9, is generated by the assembly of C5 though C9. In the absence of a target cell membrane, for example, complement activation occurs on artificial materials, C5b-9 binds to regulatory S proteins, and is released into serum as

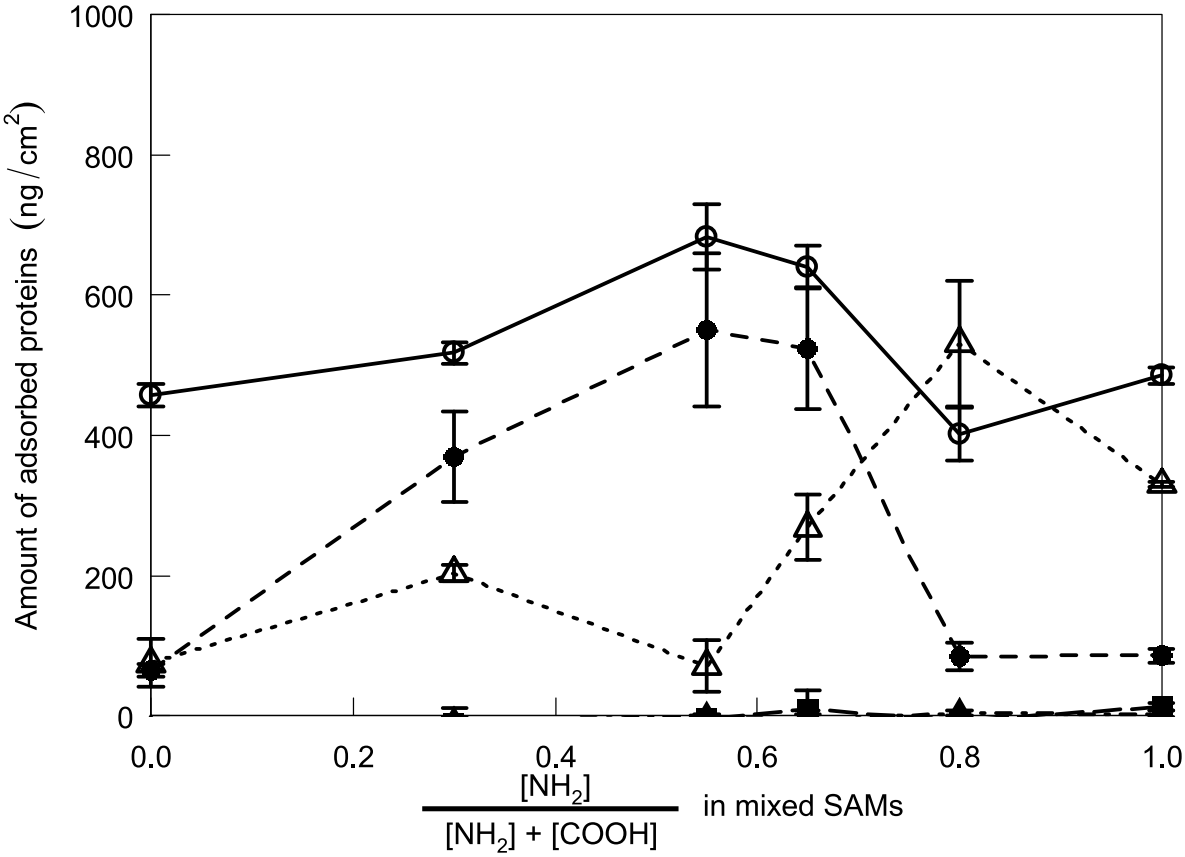

Fig. 2.5 Amounts of adsorbed proteins.

Serum proteins (—○—), and anti-C3b (- ●-), C1q (— ■-), HSA (·· △ ··) and IgG (· -▲-) antibodies onto the protein layer adsorbed on NH_2/COOH mixed SAM surfaces. Error bars represent ± SEM (n=3).

a non-lytic SC5b-9 complex. The concentrations of SC5b-9 complex released into serum exposed to SAMs were measured to evaluate the activation of the complement (Fig. 2.6). The amount of SC5b-9 from 10% NHS samples exposed to the OH-SAM surface was also included as the positive control. Although released amount of SC5b-9 on NH_2/COOH $\simeq$ 1:1 surface tended to be larger than those on COOH-SAM and NH_2-SAM, no statistical difference was observed among these three surfaces (p = 0.356 and p = 0.373, respectively). This result is partially due to large standard deviation of SC5b-9 amount on around NH_2/COOH $\simeq$ 1:1 SAM.

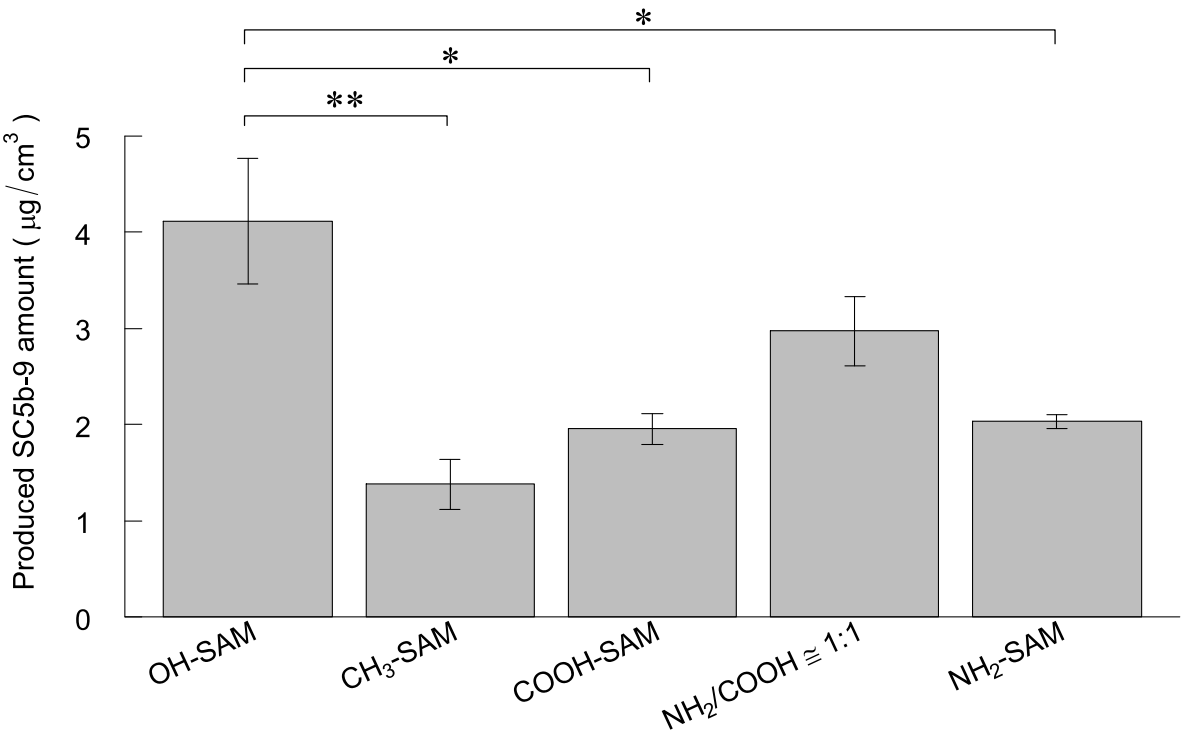

Fig. 2.6 Release of SC5b-9 in 10% diluted serum exposed to OH-, CH_3-, COOH- and NH_2-SAM, and $NH_2/COOH \simeq 1{:}1$ mixed SAM. OH-SAM is used as a control surface. Experiments were repeated at least 3 times for each surface using the same pooled serum. Error bars a represent $\pm$ SEM (n=3). Amount of SC5b-9 in naïve 10% NHS and fully activated by incubation with zymosan were 0.026 $\pm$ 0.007 $\mu g/cm^3$ (n = 2) and 20 $\pm$ 4 $\mu g/cm^3$ (n = 2), respectively. Statistical significance; *:$p < 0.05$, **:$p < 0.01$.

2.4 Discussion

Numerous studies have investigated the interaction of the complement system with material surfaces. Craddock et al.[13,14] reported that transient leukopenia during hemodialysis was induced through the complement activation on the hemodialysis membrane. Hydroxyl groups on a dialysis membrane made of regenerated cellulose[3,4] cause activation of the complement system. An activation mechanism of the complement system on surfaces carrying OH group was proposed. C3 is hydrolyzed to C3a in plasma, and a thioester group in a C3b molecule is exposed to

its surface and thus is able to react with nucleophilic hydroxyl groups on the surface. The bound C3b interacts with factor B, forming C3 convertase, and positions C3bBb onto the surface. This process amplifies the complement activation and triggers the complement loop activation, that is, the complement activation through the alternative pathway. This mechanism has long been accepted[15]. The amino group is also a nucleophilic group. Surfaces carrying amino groups are expected to be potential activators of the complement system through the alternative pathway[7]. In Chapter 1, the NH_2-SAM and a polyethyleneimine (PEI) coated surface were employed as model surfaces to study the interactions between amino groups and the serum complement pathways. Although much protein was adsorbed from serum solutions on the two types of amino surfaces, C3b deposition on the surfaces was hardly detected. Only a small amount of SC5b-9 complex, which is produced when the complement system is activated, was detected in serum after exposure of serum to the amino surfaces. These results suggest that surfaces carrying amino groups at higher densities could not effectively activate the complement system. In recent years, several groups reported that the mechanism of the activation through the alternative pathway is more complex than reported previously[16–18], and have proposed more relevant models[8,15,19,20]. Nilsson et al. claimed that the protein layer adsorbed on the material surface triggered the complement system. The behavior of the complement system in the presence of surfaces carrying amino groups is still poorly understood.

In the present work, several series of mixed SAMs, amino/methyl or amino/carboxy terminated alkanethiols, were prepared with different surface

amino group densities as model surfaces for the examination of complement activation on those surfaces.

On NH_2/CH_3 mixed SAMs, the amounts of adsorbed proteins slightly increased from 300 ng/cm^2 to 420 ng/cm^2 with increasing surface NH_2 contents. Amounts of immobilized anti-HSA antibody on the protein layer exceeded that observed for other antibodies examined. Albumin is the major component of the protein layer. Immobilized amounts of anti-C3b antibody were less than 100 ng/cm^2 at most of the examined points. When NHS was exposed to OH-SAM which is a strong activator of the complement system, immobilized amounts of anti-C3b antibody were greater than 1100 ng/cm^2, indicating that a major component of the adsorbed protein layer was C3b[5]. These facts indicated that the complement system was weakly activated. Deposition of C1q was examined to evaluate the contribution of the classical pathway. C1q was hardly detected on any NH_2/CH_3 mixed SAMs. These results indicate that the protein layer adsorbed on the material surface weakly triggered the complement system through the alternative pathway, as Nilsson et al. reported.

For the series of NH_2/COOH mixed SAMs (Fig. 2.5), the amounts of anti-C3b antibody increased with increasing surface NH_2 concentration, with a maximum at $\sim$ 50 to 60% NH_2, while for the same density of surface NH_2 groups, immobilization of anti-HSA antibody showed a minimum for SAMs with $\sim$ 50 to 60% NH_2 density and then increased with increasing surface NH_2 concentrations. Only NH_2/COOH mixed SAMs with 50–60% NH_2 can activate the complement system.

Although amino groups are considered to be potent activators of the complement

system through the alternative pathway[7], the study in Chapter 1 demonstrated that NH_2-SAM and PEI coated surfaces are not effective activators of the complement system contradicted this idea. As discussed in Chapter 1, positively charged amino groups attract various negatively charged serum proteins, such as albumin, which strongly adsorb on the surfaces through an electrostatic interaction under physiological pH conditions. Surface coverage with the adsorbed protein layer interrupts access of C3b to the surface amino groups, and thus, C3 convertase could not be formed through interaction of surface-bound C3b with Bb. As similarly observed with NH_2-SAM and PEI coated surfaces, the same mechanism prevents activation of the complement system on NH_2/CH_3 mixed SAMs with any mixed ratios. On the series of NH_2/COOH mixed SAMs, only NH_2/COOH mixed SAMs with 50–60% NH_2 can effectively activate the complement system. The surface cationic charges are neutralized by salt formation between the amino and carboxyl groups. Electrostatic interaction between surface charges and serum proteins weakens. Serum proteins cannot strongly adsorb onto the surfaces through an electrostatic interaction under physiological pH conditions. In a series of reactions, C3b formed in the liquid phase effectively approaches surface amino groups, becomes immobilized and forms C3 convertase with B, forming C3bBb, and ultimately triggers the complement activation through the alternative pathway.

2.5 Conclusion

Two series of mixed SAMs, NH_2-terminated/CH_3-terminated and NH_2-terminated/COOH-terminated, were employed to assess effects of hydrophobicity

and electrostatic charge upon the behavior of the complement system on these surfaces. NH_2-terminated/CH_3-terminated mixed SAMs were not potent activators of the complement system regardless of NH_2/CH_3 ratios in mixed SAMs and therefore the hydrophobicity is not related to the activation of the complement system onto the surface carrying the amino group. On the contrary, large amounts of C3b and/or C3bBb were deposited during exposure to 10% serum onto NH_2/COOH mixed SAMs with 50–60% NH_2 density. These results suggest that complement proteins, mainly C3, can easily access the nucleophilic NH_2 groups due to the decrease of electrostatic interaction caused by the neutralization of the electrostatic charge on that surface.

References

1. Walport M J. Complement. First of two parts. N Engl J Med 2001;344(14):1058–1066
2. Goldfarb R D, Parrillo J E. Complement. Crit Care Med 2005;33(12 Suppl):S482–S484
3. Wegmuller E, Montandon A, Nydegger U, Descoeudres C. Biocompatibility of different hemodialysis membranes: activation of complement and leukopenia. Int J Artif Organs 1986;9(2):85–92
4. Chenoweth D E. Complement activation during hemodialysis: clinical observations, proposed mechanisms, and theoretical implications. Artif Organs 1984;8(3):281–290
5. Hirata I, Morimoto Y, Murakami Y, Iwata H, Kitano E, Kitamura H, Ikada Y. Study of complement activation on well-defined surfaces using surface plasmon resonance. Colloids Surf B Biointerfaces 2000;18(3–4):285–292
6. Hirata I, Hioki Y, Toda M, Kitazawa T, Murakami Y, Kitano E, Kitamura H, Ikada Y, Iwata H. Deposition of complement protein C3b on mixed self-assembled monolayers carrying surface hydroxyl and methyl groups studied by surface plasmon resonance. J Biomed Mater Res A 2003;66(3):669–676
7. Pangburn M K. Alternative Pathway: Activation and Regulation. In: Rother K, Till G O, Hänsch G M, editors. The Complement System, Second Revised Edition. Berlin: Springer-Verlag; 1998. pp. 93–115
8. Andersson J, Ekdahl K N, Lambris J D, Nilsson B. Binding of C3 fragments on

top of adsorbed plasma proteins during complement activation on a model biomaterial surface. Biomaterials 2005;26(13):1477–1485

9. Knoll W. Polymer thin films and interfaces characterized with evanescent light. Makromol Chem 1991;192(12):2827–2856
10. R Development Core Team. R: A Language and Environment for Statistical Computing. R Foundation for Statistical Computing : Vienna, Austria; 2009. ISBN 3-900051-07-0, URL: http://www.R-project.org/
11. Arima Y, Iwata H. Effect of wettability and surface functional groups on protein adsorption and cell adhesion using well-defined mixed self-assembled monolayers. Biomaterials 2007;28(20):3074–3082
12. Ooi Y, Hobara D, Yamamoto M, Kakiuchi T. Ideal nonideality in adsorption of 2-aminoethanethiol and 2-mercaptoethane sulfonic acid to form electrostatically stabilized binary self-assembled monolayers on Au(111). Langmuir 2005;21(24):11185–11189
13. Craddock P R, Fehr J, Dalmasso A P, Brighan K L, Jacob H S. Hemodialysis leukopenia. Pulmonary vascular leukostasis resulting from complement activation by dialyzer cellophane membranes. J Clin Invest 1977;59(5):879–888
14. Craddock P R, Fehr J, Brigham K L, Kronenberg R S, Jacob H S. Complement and leukocyte-mediated pulmonary dysfunction in hemodialysis. N Engl J Med 1977;296(14):769–774
15. Nilsson B, Ekdahl K N, Mollnes T E, Lambris J D. The role of complement in biomaterial-induced inflammation. Mol Immunol 2007;44(1–3):82–94
16. Cheung A K, Parker C J, Wilcox L, Janatova J. Activation of the alternative

pathway of complement by cellulosic hemodialysis membranes. Kidney Int 1989;36(2):257–265

17. Françoise Gachon A M, Mallet J, Tridon A, Deteix P. Analysis of proteins eluted from hemodialysis membranes. J Biomater Sci Polym Ed 1991;2(4):263–276
18. Lhotta K, Wurzner R, Kronenberg F, Oppermann M, Konig P. Rapid activation of the complement system by cuprophane depends on complement component C4. Kidney Int 1998;53(4):1044–1051
19. Sellborn A, Andersson M, Hedlund J, Andersson J, Berglin M, Elwing H. Immune complement activation on polystyrene and silicon dioxide surfaces Impact of reversible IgG adsorption. Mol Immunol 2005;42(5):569–574
20. Wetterö J, Askendal A, Bengtsson T, Tengvall P. On the binding of complement to solid artificial surfaces in vitro. Biomaterials 2002;23(4):981–991

Chapter 3

Complement activation by polymers carrying hydroxyl groups

3.1 Introduction

When artificial materials come into contact with blood, the plasma proteins and cells interact with the material surface. Various biological responses are induced, such as adsorption of proteins, activation of the complement and coagulation systems, inflammatory reactions, and cell adhesion. For the development of biomaterials for use in biomedical devices that will be exposed to blood, the complete understanding and control of these interactions are essential.

The complement system, a cascade of enzyme reactions involving approximately 30 fluid-phase and cell membrane-bound proteins, plays an important role in the body's defense systems against pathogens[1]. Activation of the complement system is initiated through three pathways: the classical, lectin, and alternative pathways. The classical pathway is initiated by the formation of immune-complexes[2,3], the lectin pathway is triggered by the binding of mannose-binding lectin to carbohydrate chains on foreign microorganisms[4,5], and the alternative pathway is activated by the non-specific binding of complement protein C3 to nucleophilic groups on foreign substrates[6,7].

Complement activation by polymeric materials has been extensively studied in relation to hemodialysis membranes. For example, dialysis membranes made of cellulose or its derivatives activate the complement system[8,9]. Crosslinked dextran (Sephadex®) also activates the complement system[10]. Other studies indicate that polymeric membranes carrying surface hydroxyl groups, or nucleophilic groups, strongly activate the complement system through the alternative pathway[11–15]. In contrast to these observations, Videm et al. reported that solutions of dextran, which have a medicinal application as a blood substitute and a plasma expander, did not strongly activate the complement system at the dextran concentrations used in clinical settings[16]. These studies were conducted by different research groups under different experimental conditions, making direct comparisons difficult. These seemingly contradictory results led us to question whether the state of the polymer, either immobilized on a surface or free in solution, affects the complement activation.

In this chapter, dextran and poly(vinyl alcohol)(PVA) were used as model polymers carrying hydroxyl groups. The deposition of serum proteins and complement fragment C3b onto polymer-immobilized surfaces were examined by using a surface plasmon resonance (SPR) apparatus. Using enzyme-linked immunosorbent assay (ELISA), the release of complement fragments C3a and SC5b-9 were also compared after exposure of serum samples to either a polymer-immobilized surface and to a solution of polymer dissolved in neutral buffer.

3.2 Materials and methods

3.2.1 Preparation of serum and buffers

Blood samples, collected from eight healthy volunteer donors who had a meal at least 4 h prior to donation, were pooled and mixed together. To separate serum, aliquots (10 cm^3) of the blood were divided equally into sterile glass tubes, left on a clean bench at ambient temperature for 30 min for blood coagulation to occur, and then centrifuged at 1100 $\times$ g at 4 ℃ for 30 min. The serum supernatants were then pooled in a bottle, mixed well, and divided equally into vials in an ice bath, and stored at -80 ℃ until use.

Veronal buffer (VB), composed of 5 mmol dm^{-3} sodium barbital (Nacalai Tesque, Inc., Kyoto, Japan), 142 mmol dm^{-3} NaCl, 3.7 mmol dm^{-3} HCl, 0.15 mmol dm^{-3} $CaCl_2$, and 1.0 mmol dm^{-3} $MgCl_2$ (pH 7.4), was prepared according to the protocol for CH_{50} measurement[17]. For investigations involving the inhibition of complement activation, ethylenediamine-*N*,*N*,*N*′,*N*′-tetraacetic acid (EDTA, Dojindo Laboratories, Kumamoto, Japan) was added to VB (without $CaCl_2$ and $MgCl_2$) for a final concentration of 10 mmol dm^{-3} (EDTA-VB). To block the classical pathway, *O*,*O*′-bis(2-aminoethyl)ethyleneglycol-*N*,*N*,*N*′,*N*′-tetraacetic acid (EGTA, Sigma-Aldrich, St. Louis, MO) and $MgCl_2$ were added to VB (without $CaCl_2$ and $MgCl_2$) at final concentrations of 10 mmol dm^{-3} and 2.5 mmol dm^{-3}, respectively (EGTA-Mg^{2+}).

3.2.2 Preparation of dextran-immobilized surface

Glass plates (BK7, refractive index: 1.515, size: 25 $\times$ 25 $\times$ 1 mm, Arteglass Associates Co., Kyoto, Japan) were immersed for 5 min into a piranha solution (7:3 mix-

ture of concentrated sulfuric acid and 30% hydrogen peroxide) at room temperature, washed three times with deionized water, sequentially rinsed three times with deionized water and 2-propanol, and finally stored in 2-propanol until use. These glass plates were dried under a stream of dried nitrogen gas and then mounted on the rotating stage of a thermal evaporation coating apparatus (V-KS200, Osaka Vacuum, Ltd., Osaka, Japan). A chromium layer was deposited at 1 nm of thickness, and then a gold layer was deposited at 49 nm of thickness onto the glass plates.

The gold-coated glass plate was immersed in an 1 mmol dm^{-3} solution of 11-mercaptoundecanoic acid (Sigma-Aldrich, St. Louis, MO) in ethanol at room temperature for 24 h to form a self-assembled monolayer (SAM) carrying carboxylic acid functional groups. The plate was washed with ethanol three times and dried in a stream of nitrogen gas. The plate was then immersed in a mixture of 0.1 mol dm^{-3} trifluoroacetic anhydride (Wako Pure Chemical Industries, Ltd., Osaka, Japan) and 0.2 mol dm^{-3} triethylamine (Nacalai Tesque, Inc., Kyoto, Japan) in anhydrous *N*,*N*-dimethylformamide for 25 min to form interchain anhydrides[18] (Scheme 3.1A). The plate was washed with dichloromethane, dried in a stream of nitrogen, and then immersed in 10% dextran (MW: 200,000–300,000, MP Biomedicals, Solon, OH) solution in dimethyl sulfoxide supplemented with 2 mg/cm^3 of 4-(dimethylamino)pyridine (4-DMAP) (Nacalai Tesque) as a catalyst[19]. After incubation at 40 ℃ for 48 h, the plate was washed with Milli-Q water, and stored in Milli-Q water until use.

3.2.3 Preparation of PVA-immobilized surface

The gold-coated glass plate was immersed in a 0.5 mmol dm^{-3} solution of 11-undecanal disulfide (ProChimia Surfaces Sp. z o.o., Sopot, Poland) in ethanol at

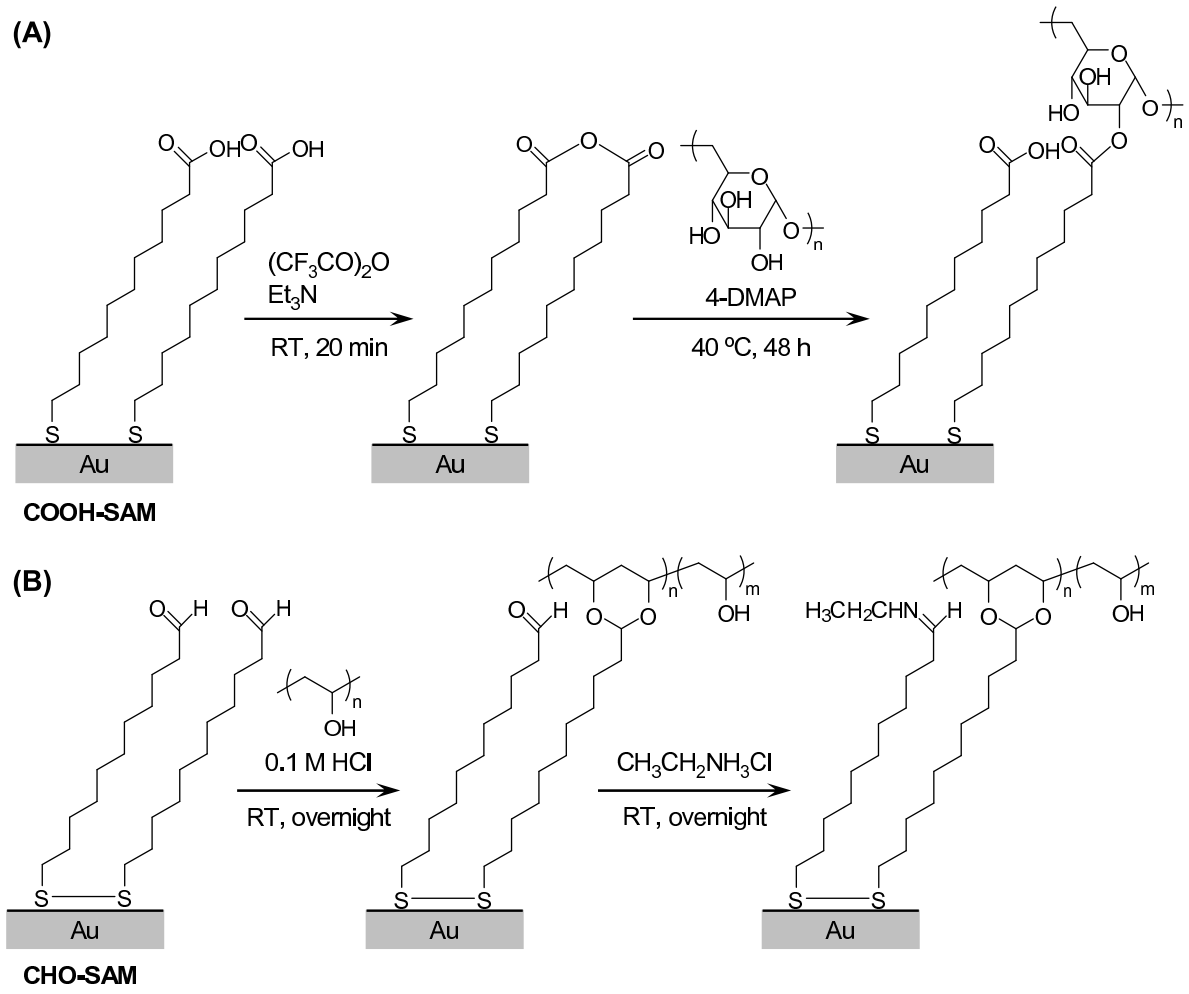

Scheme 3.1 Immobilization of dextran (A) and PVA (B) to SAMs on gold.

room temperature for 24 h to form aldehyde-terminated SAM (Scheme 3.1B). The plate was washed with ethanol three times and dried in a stream of nitrogen gas. The plate was then immersed in 1% PVA (DP = 1,700, DS = 98%, Unitika Ltd., Osaka, Japan) aqueous solution containing 0.1 mol dm^{-3} HCl and incubated at room temperature for 24 h. The plate was washed with Milli-Q water, and dried in a stream of nitrogen gas. To block unreacted aldehyde groups, the plate was immersed in a 1 mol dm^{-3} aqueous solution of ethylamine hydrochloride. The plate was washed with Milli-Q water, and stored in Milli-Q water until use.

3.2.4 Surface characterization of dextran- and PVA-immobilized surfaces

X-ray photoelectron spectroscopy (XPS) was employed to obtain atomic compositions of surfaces using an ESCA-850V instrument (Shimadzu Co., Kyoto, Japan). Magnesium was used as a target of the electrons generated by the filament with an electric current of 30 mA at 8 kV. The take-off angle of the sample surface was 90° and the operating pressure was less than 1×10^{-5} Pa. All spectra were corrected referring to the peak of Au $4f_{7/2}$ to 83.8 eV.

Infrared adsorption spectra of sample surfaces were collected by the reflection–adsorption method (FTIR–RAS) using a Spectrum One spectrometer (Perkin-Elmer Inc., Boston, MA) equipped with a Refractor^{TM} (Harrick Scientific Co., Ossining, NY) and a mercury–cadmium telluride (MCT) detector cooled by liquid nitrogen. Glass plates with a gold layer of 199 nm thickness were used for FTIR-RAS analysis. Spectra were acquired (128 scans at 4 cm^{-1} resolution from 4000 to 750 cm^{-1}) using the *p*-polarized infrared light at an incident angle of 75° in the chamber purged with dry nitrogen gas.

Static water contact angles on surfaces were determined by the sessile drop method using a contact angle meter (CA-X, Kyowa Interface Science Co. Ltd., Saitama, Japan) at room temperature. A 10 μl water droplet was placed on a substrate and the contact angle was determined three times. This procedure was repeated five times at different places on the same surface.

3.2.5 Surface plasmon resonance (SPR)

The SPR apparatus employed in this study[11] was a home-made apparatus prepared as described by Knoll[20]. The BK7 glass plate with the gold layer (49 nm in thickness) was coupled to a hemicylindrical prism with an immersion oil (n = 1.515, Cargille Laboratories, Cedar Grove, NJ). The sample surface was irradiated with a *p*-polarized He-Ne laser light (λ = 632.8 nm) through the prism. The intensity of the reflected light was monitored as a function of the incident angle. The incident angle, at which the reflectivity reached minimum, was described as the SPR angle.

The thickness of an immobilized polymer layer in air was also estimated by SPR. The glass plate with the polymer layer was set on the SPR instrument and the reflectivity was measured in air as a function of the incident angle of the laser light. Thickness of the polymer layer was determined by the SPR angle shift using Fresnel's law for the multi-layer system, BK7/Cr/Au/SAM/polymer/air[20,21]. The refractive indices for SAM, dextran, and PVA were 1.45, 1.54 (value for cellulose instead of dextran)[22], and 1.52[22], respectively.

3.2.6 Protein adsorption from human serum

Protein adsorption from undiluted human serum was examined by SPR. A flow chamber with a sample plate was placed on a prism of the SPR apparatus, and VB was circulated at a flow rate of 3.0 cm^3/min in the flow chamber assembly. Reflectance was monitored during the flow of the liquid samples at an incident angle of 0.5° less than the SPR angle. Undiluted human serum was then introduced into the flow chamber assembly for 90 min. To wash out serum from the sample

surface, VB was introduced and circulated for an additional 20 min. All experiments were performed at 37 ℃. Introduction of undiluted human serum resulted in a large increase in the reflectance (bulk effect) due to its high refractive index. To correct for changes in the reflectance, standard solutions with different refractive indices (Mill-Q water, VB, and 2 mol dm^{-3} NaCl) were employed.

To identify proteins deposited on the surface, solutions of specific antibodies were flowed through the apparatus after exposure of the sample surface to human serum. A 1% solution of antiserum/antibody diluted in VB was flowed for 90 min onto the surface of the protein layer formed on the surface and then VB was introduced for 20 min to wash out the antibody solution. Antibodies employed were polyclonal rabbit anti-human C3b antiserum (RAHu/C3b, Nordic Immunology, Tilburg, The Netherlands), polyclonal sheep anti-human C1q (PC020, The Binding Site Ltd., Birmingham, UK), and polyclonal goat anti-human IgG (109-005-088, Jackson ImmunoResearch Laboratories, Inc., West Grove, PA). The thickness of the protein layer was calculated from the shift in the SPR angle (ΔSPR) using Fresnel fits for the system BK7/Cr/Au/SAM/protein/water, where the refractive indices of SAM and protein were assumed to be 1.45. The amounts of proteins adsorbed onto the surfaces were estimated from the thickness presuming that the density of the protein layer was 1 as follows[11]:

$$\text{The amount of adsorbed protein (ng/cm}^2) = 500 \times \Delta\text{SPR}(^\circ) \tag{3.1}$$

For studies requiring conditions that block complement activation, serum was supplemented with EDTA at a final concentration of 10 mmol dm^{-3}. To examine the effects of inhibition of the classical and the lectin pathways, serum was sup-

plemented with EGTA and $MgCl_2$ (final concentrations of 10 mmol dm^{-3} and 2.5 mmol dm^{-3}, respectively).

3.2.7 Quantification of generated complement fragments

To prepare a cell, a silicone spacer (inner diameter: 20 mm, thickness: 1 mm) was placed between the two test surfaces. Serum (approximately 340 μl) was injected into the circular space in the cell and incubated for 90 min at 37 ℃. Serum was then collected and EDTA was added at a final concentration of 10 mmol dm^{-3} to halt the complement activation. The concentration of the complement fragments (C3a and SC5b-9) in the fluid phase was determined by commercially available enzyme-linked immunosorbent assay (ELISA) kits (C3a: OptEIA Human C3a ELISA, BD Biosciences Pharmingen, CA; SC5b-9: SC5b-9 plus ELISA, QUIDEL Corp., CA).

3.2.8 Quantification of generated complement fragments in polymer solution

Aliquots of dextran or PVA solutions in VB were added to human serum. The final concentration of dextran or PVA in the assay was varied (dextran: 0.002–1%, PVA: 0.001–0.1%) while the final concentration of serum was held constant at 95%. Serum samples supplemented with EDTA and zymosan (10 mg/cm^3) were used as negative and positive controls, respectively. The procedure for quantification of complement fragments was the same as described above.

3.2.9 Statistical analysis

Significant differences between two groups were examined using Student's *t*-test. A $p < 0.05$ was considered as statistically significant. All statistical calculations were

performed by the software JMP ver. 7.0.1 (SAS Institute, Cary, NC).

3.3 Results

3.3.1 Surface characterization

Using FTIR-RAS, XPS, and water contact angle measurements, the dextran and PVA immobilized onto SAMs on gold were characterized (Scheme 3.1).

Dextran was immobilized through ester bonds onto a COOH-SAM (Scheme 3.1A). FTIR-RAS spectrum for COOH-SAM showed asymmetric and symmetric C–H stretching bands of methylene groups at 2922 cm^{-1} and 2854 cm^{-1} and two C=O stretching bands at 1739 cm^{-1} and 1718 cm^{-1}, which were caused by the free and hydrogen bonded carboxylic acids, respectively[18] (Fig. 3.1A). After treatment of COOH-SAM with trifluoroacetic anhydride, two C=O stretching bands appeared at 1819 cm^{-1} and 1733 cm^{-1}, which were assigned to in-phase and out-of-phase stretching bands of the two coupled carbonyl groups, respectively[18]. The spectrum of the dextran-immobilized surface showed new bands at 3100–3600 cm^{-1}, assignable to an O–H stretching band, at 1148 cm^{-1} and 1051 cm^{-1} assignable to C–O–C stretching[23].

PVA was immobilized onto a SAM functionalized with aldehydes through acetal bonds (Scheme 3.1B). The FTIR-RAS spectrum of the CHO-SAM shows two C–H stretching bands at 2928 and 2852 cm^{-1}, which were assigned to the asymmetric and asymmetric C–H stretching of methylene groups, respectively (Fig. 3.1B). The band observed at 1729 cm^{-1} is assigned to the C=O stretching band of the carbonyl group[24,25]. The spectrum of the PVA-immobilized surface shows new bands

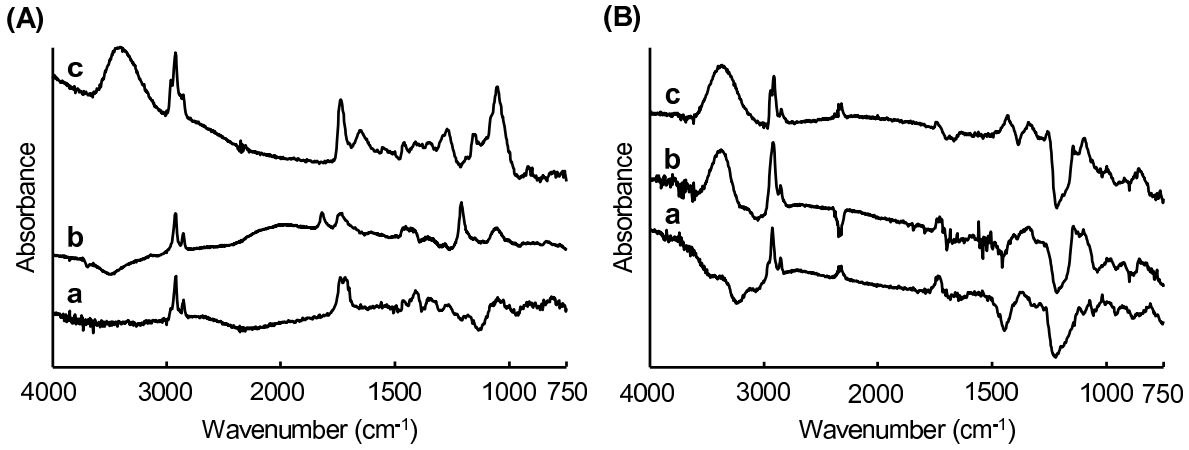

Fig. 3.1 FTIR-RAS spectra of modified gold surfaces. (A-a): COOH-SAM, (A-b): Interchain anhydride-SAM, and (A-c): Dextran-immobilized surface. (B-a): CHO-SAM, (B-b): PVA-immobilized surface and (B-c): PVA-immobilized surface followed by blocking with ethylamine hydrochloride.

at 3100–3600 cm^{-1}, assigned as an O–H stretching band, at 1145 cm^{-1} and 1098 cm^{-1} assigned respectively as the C–O stretching in the crystalline region and the C–O stretching in the amorphous region, and at 845 cm^{-1}, corresponding to CH_2 rocking[26]. For the PVA-immobilized surface after blocking with ethylamine hydrochloride, the intensity of the C=O stretching band at 1729 cm^{-1} decreased (Fig. 3.1B-c).

Dextran- and PVA-immobilized surfaces were also characterized by XPS, water contact angle, and SPR measurements (Table 3.1). Oxygen concentration increased upon immobilization of either dextran or PVA. For CHO-SAM and PVA-immobilized surfaces, N *1s* signals were observed when the free aldehyde groups were blocked by ethylamine through Schiff base formation. The water contact angle decreased after immobilization of either dextran or PVA. The relatively high water contact angles for CHO-SAM and PVA-immobilized surfaces may be attributed to introduction of hydrophobic ethylene chains after reaction with ethylamine. The

Table. 3.1 Characteristics of polymer-immobilized surfaces. Data shown are means ± SD (n = 3).

	Contact angle	Atomic compositions (%)				Thickness
	(°)	C	O	N	S	(nm)
COOH-SAM	16.8 ± 4.1	82.2 ± 1.0	13.5 ± 0.9	0	4.3 ± 0.4	–
Dextran-immobilized	5.3 ± 0.1	65.6 ± 1.5	32.4 ± 1.5	0	2.0 ± 0.1	2.4 ± 0.1
CHO-SAM	70.5 ± 1.1	77.6 ± 2.7	9.9 ± 1.7	4.0 ± 1.7	8.5 ± 1.4	–
PVA-immobilized	36.8 ± 1.4	71.2 ± 1.0	23.9 ± 1.8	2.1 ± 0.8	2.8 ± 0.9	1.7 ± 0.0

thicknesses of the dextran and PVA layers in the dry state determined by SPR measurements were 2.4 nm and 1.7 nm, respectively.

Taken together, these results indicated that dextran and PVA layers were successfully immobilized on SAMs as depicted in Scheme 3.1.

3.3.2 Complement activation on dextran or PVA immobilized surfaces observed by SPR

Complement activation on dextran or PVA immobilized surfaces was examined using an SPR apparatus (Fig. 3.2 and 3.3). When COOH-SAM or dextran-immobilized surfaces were sequentially exposed to VB and undiluted human serum, rapid increases of the SPR angle were observed. These increments are due to the large change in refractive indices when going from VB to human serum. The SPR angle then slowly increased for COOH-SAM. For the case of the dextran-immobilized surface, the angle gradually increased an additional 2.0° after several minutes of induction time. When serum was removed by flushing VB through the system, the SPR angle rapidly decreased due to the change in refractive index of the solution. The SPR angle shift (ΔSPR) after the introduction of VB into the chamber (Fig. 3.2A) is attributed to protein adsorption (see Eq. 3.1) and indicated that a larger amount of serum proteins had adsorbed onto the dextran-immobilized surface as compared

to COOH-SAM in undiluted serum. After the surfaces were washed with VB, an anti-human C3b antiserum solution was applied to the surfaces carrying adsorbed serum proteins to evaluate the amount of C3b or C3bBb which was produced by complement activation (Fig. 3.2B). The SPR angle shifts caused by binding of anti-C3b antibody on the COOH-SAM and dextran-immobilized surfaces were 0.64° and 1.78°, respectively. The large amount of anti-C3b antibody bound on the dextran-immobilized surface suggested that a major component in the layer of serum protein on the surface was C3b or C3bBb.

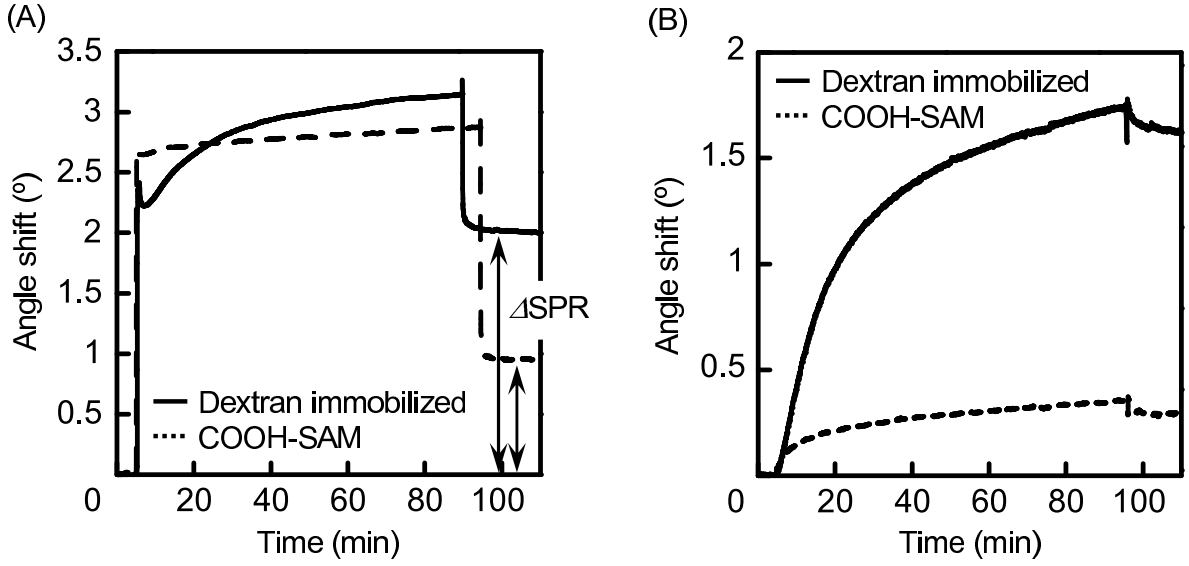

Fig. 3.2 SPR sensorgrams during exposure of COOH-SAM and dextran-immobilized surfaces to normal human serum (A) and subsequent exposure to anti-C3b antiserum (B). ΔSPR indicates an increase in SPR angle after exposure to serum and subsequent rinse with buffer and corresponds to the amount of adsorbed serum proteins according to Eq. 3.1.

Complement activation on PVA-immobilized surface and its basal substrate (CHO-SAM) was also examined by SPR (Fig. 3.3). Aldehyde groups on both surfaces were blocked with ethylamine. For ethylamine-blocked CHO-SAM, the SPR angle rapidly increased just after exposure to human serum and then was followed

by a slow increase over 90 min of incubation (Fig. 3.3A). The initial increase of the SPR angle was due to the change of refractive indices from VB to serum (Fig. 3.3A). For the case of PVA-immobilized surface, the SPR angle greatly increased to 2.0° after several minutes of induction time. The amount of adsorbed proteins remaining on the PVA-immobilized surface after washing with VB exceeded that for the CHO-SAM. The SPR angle shifts caused by binding of anti-C3b antibody on the surfaces carrying adsorbed serum proteins were 0.91° and 1.72°, respectively (Fig. 3.3B), and suggested that a large amount of complement component, C3b or C3bBb, was immobilized onto the PVA-immobilized surface.

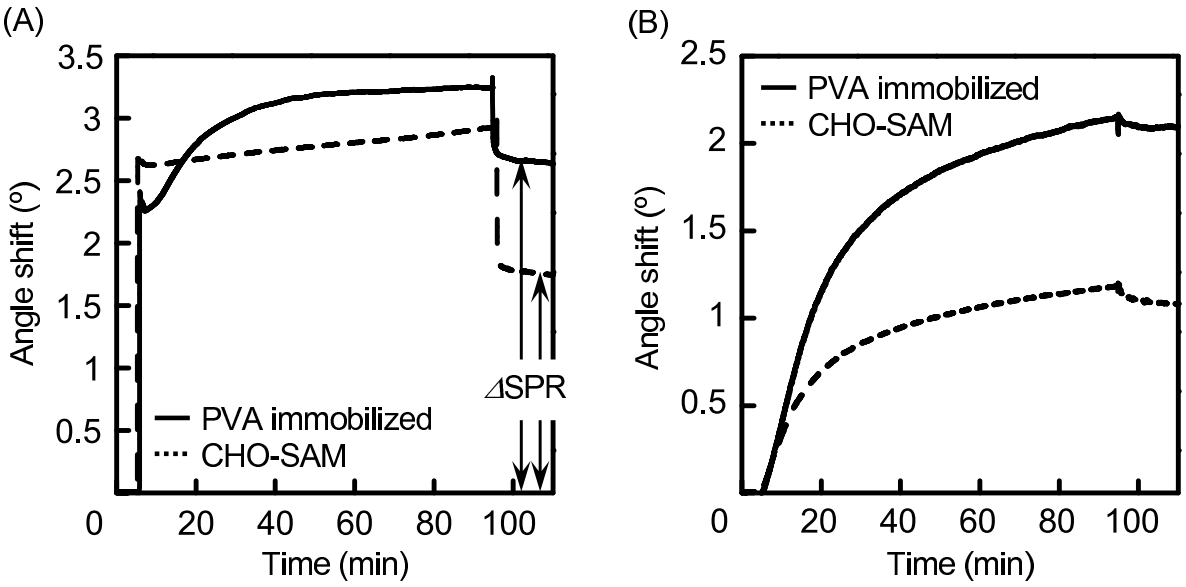

Fig. 3.3 SPR sensorgrams during exposure of CHO-SAM after blocking with ethylamine hydrochloride and PVA-immobilized surfaces to normal human serum (A) and subsequent exposure to anti-C3b antiserum (B). ⊿SPR indicates an increase in SPR angle after exposure to serum and subsequent rinse with buffer and corresponds to the amount of adsorbed serum proteins according to Eq. 3.1.

EDTA is known to inhibit all three pathways of complement activation, while EGTA-Mg^{2+} can inhibit only the classical and the lectin pathways. To distinguish which of the complement pathways are activated on dextran- and PVA-immobilized

surfaces, protein adsorption and subsequent binding of anti-C3b antibody were examined in serum supplemented with EDTA and with EGTA-Mg^{2+} (Fig. 3.4). When serum supplemented with 10 mmol dm^{-3} EDTA was employed, the amounts of adsorbed proteins greatly decreased on all the dextran- and PVA-immobilized surfaces. In particular, protein adsorption on the PVA-immobilized surface was less than $\sim$ 60 ng/cm^2, indicating that the PVA surface was practically resistant to protein adsorption when the complement activation was inhibited. Binding of anti-C3b antibody was not observed on either surface in the presence of EDTA. Thus, the deposition of C3b or C3bBb on dextran- and PVA-immobilized surfaces shown in Fig. 3.2 and Fig. 3.3 was due to complement activation by any of the three pathways. However, in the presence of 10 mmol dm^{-3} EGTA and 2 mmol dm^{-3} Mg^{2+} in serum, the large amounts of adsorbed protein and bound anti-C3b antibody observed on dextran- and PVA-immobilized surfaces did not differ significantly from the serum controls in the absence of chelating agents. Taken together, these results suggest that exposure of serum to dextran- and PVA-immobilized surfaces activated the complement system through the alternative pathway.

3.3.3 Generation of complement fragments

The release of complement fragments C3a and SC5b-9 were compared by the ELISA method after serum samples were exposed to surfaces carrying either immobilized dextran or PVA or when mixed with solutions of dextran or PVA.

The amount of SC5b-9 was markedly increased when serum was exposed to surfaces carrying either dextran or PVA (Fig. 3.5). Thus, this strong activation of the complement system by dextran- or PVA-immobilized surfaces was consistent with

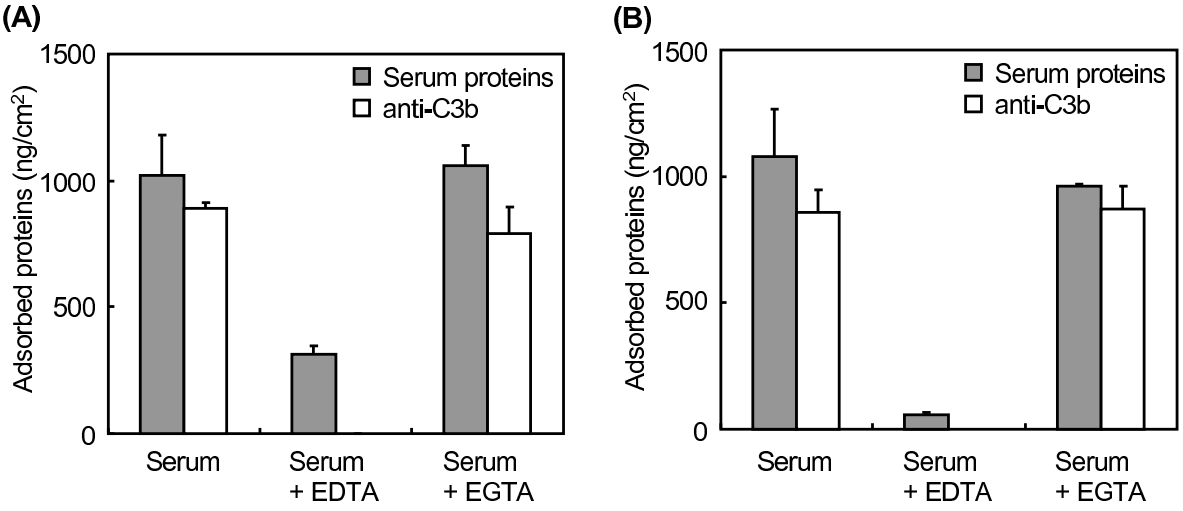

Fig. 3.4 Amounts of serum proteins adsorbed on dextran (A) or PVA (B) immobilized surface and subsequent anti-C3b antibodies bound to those surfaces with a serum protein layer. Data shown are means ± SD (n = 3). Serum, normal human serum (NHS); serum + EDTA, NHS + 10 mmol dm^{-3} EDTA; and serum + EGTA, NHS + 10 mmol dm^{-3} EGTA + 2.5 mmol dm^{-3} $MgCl_2$.

the results of the SPR measurements summarized in Fig. 3.4. The amounts of dextran and PVA on the surfaces, which were estimated from their thickness (Table 3.1), were 1.5 μg and 1.1 μg, respectively, presuming that the densities of the polymer layers were 1. In the experimental setting, 1.5 μg of dextran or 1.1 μg of PVA were exposed to 340 μl serum. When the effects of soluble dextran and PVA on complement activation were examined, polymer concentrations in serum ranged from 0.02 to 10 mg/cm^3 for dextran and from 0.01 to 1 mg/cm^3 for PVA. Even though the amount of generated SC5b-9 increased as the concentration of added polymer increased in the serum samples, these values were much lower than those observed for immobilized surfaces. Even in the presence of 2200 times more soluble dextran and 300 times more soluble PVA in the serum, the amount of released SC5b-9 did not achieve the levels observed with the immobilized-polymer surfaces. Therefore, dextran and PVA dissolved in serum cannot effectively activate the complement

system.

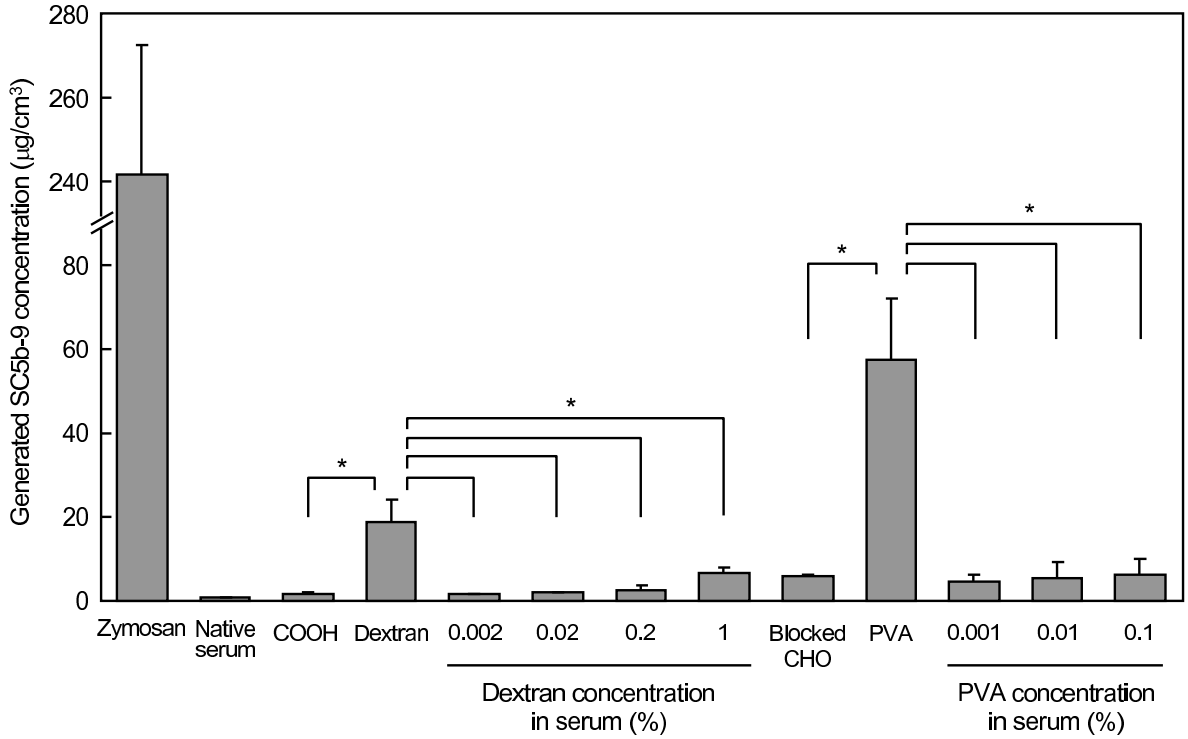

Fig. 3.5 Concentrations of SC5b-9 generated in serum exposed to four different kinds of surfaces and serum mixed with soluble dextran or PVA. Data shown are means ± SD (n = 3). An asterisk denotes a significant difference ($p < 0.05$).

The amounts of C3a released were also determined (Fig. 3.6). Effects of the polymer state on C3a release were not so clear, but followed the same general tendency as those observed in SC5b-9 release. When dextran or PVA solutions were added to serum, the levels of generated C3a were lower than those for dextran- and PVA-immobilized surfaces.

3.4 Discussion

Dextran and PVA are water soluble, nonionic polymers carrying hydroxyl groups. Since these polymers do not strongly interact with proteins[27–30], surface modification with these polymers should provide non-fouling surfaces and may be applied

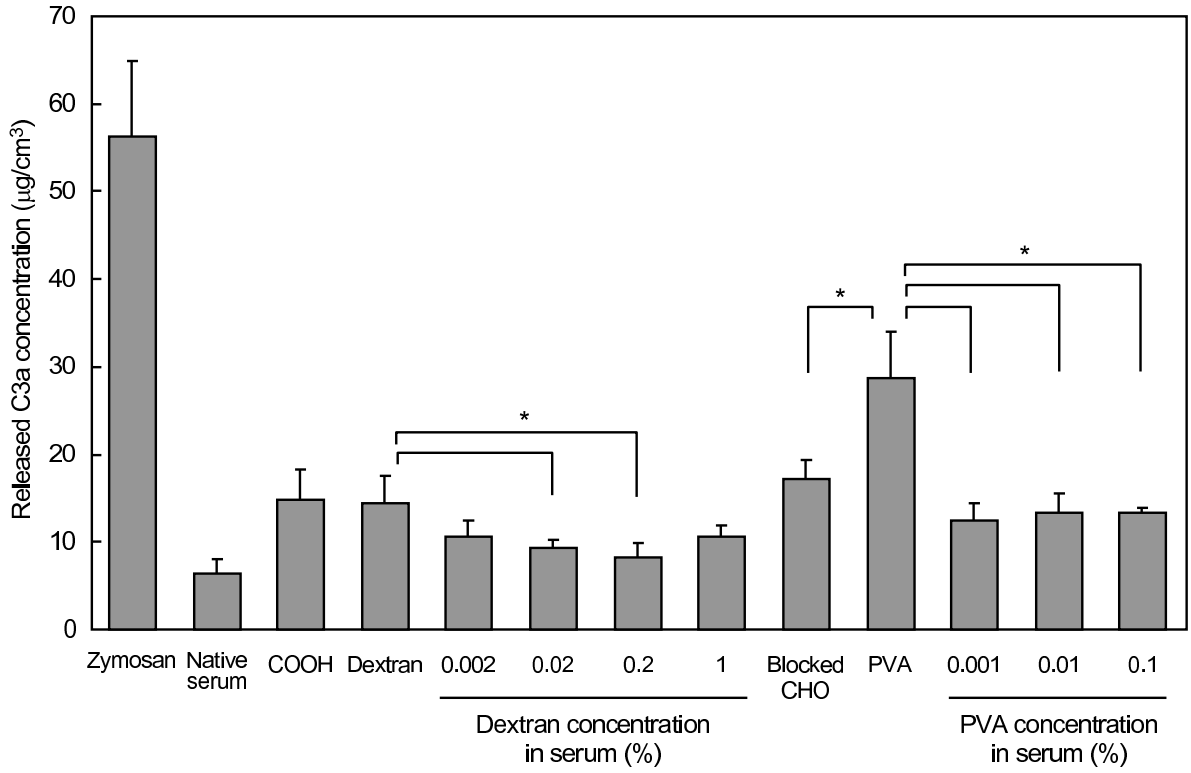

Fig. 3.6 Concentrations of C3a generated in serum exposed to four different kinds of surfaces and serum mixed with soluble dextran or PVA. Data shown are means ± SD (n = 3). An asterisk denotes a significant difference ($p < 0.05$).

to medical devices and biosensors. However, protein adsorption behavior from serum differs from that of a solution of a single protein. Protein adsorption was previously examined on SAMs of alkanethiols carrying hydroxyl groups[11,12] and hydroxyl-terminated oligo(ethylene glycol)[15]. Although those surfaces showed low protein adsorption from solutions containing a single protein, large amounts of proteins adsorbed on those surfaces and the complement system was strongly activated when the surfaces were exposed to normal human serum. Such diverse behaviors are expected to occur on dextran- and PVA-immobilized surfaces.

Crosslinked dextran (Sephadex®)[10], dextran-grafted nanoparticles[31–33], and PVA-coated polyethylene tubes[34] strongly activate the complement system, but soluble

dextrans do not, even at the concentrations found in plasma substitutes[16]. The present study was designed to investigate this discrepancy.

SPR measurements in this chapter clearly demonstrated that large amounts of serum proteins were deposited on dextran- and PVA-immobilized surfaces (Fig. 3.2 and 3.3). Binding of antibody against C3b identified the deposited proteins as C3b or C3bBb. Both non-specific protein adsorption and C3b deposition on these surfaces were greatly reduced in the presence of 10 mmol dm^{-3} EDTA, which blocks all three complement system activation pathways (Fig. 3.4). These observations indicated that the complement system was strongly activated by these surfaces.

The basal surfaces used for polymer immobilization (COOH-SAM for dextran, CHO-SAM for PVA) also activated the complement system, but to a lesser extent (Figs. 3.2 and 3.3). Complement activation on material surfaces is closely related to non-specific adsorption of serum proteins[35]. On COOH- and CHO-SAMs, the amounts of bound anti-C3b were small compared with those of adsorbed serum proteins, suggesting that serum proteins other than C3b adsorbed on the surfaces. When dextran or PVA was immobilized, non-specific protein adsorption was greatly reduced by the shielding effect of polymers. The contribution of the basal surfaces to the complement activation is minimal, and data in this chapter indicate that the complement system was mainly activated by dextran or PVA on the surface of the substrate.

Three pathways can activate the complement system: the classical, the lectin, and the alternative pathway. Complement activation via the classical pathway is triggered by non-specifically adsorbed proteins such as immunoglobulins when ar-

tificial materials are brought into contact with serum. Adsorption of immunoglobulins on a material surface leads to rapid complement activation through the classical pathway[36]. In an experiment executed in this chapter, binding of anti-IgG was not observed on dextran and PVA-immobilized surfaces after short incubation (5 min) of human serum, indicating that IgG did not adsorb on these surfaces (data not shown). The lectin pathway is initiated by binding of the complex of mannose-binding lectin and the mannose-binding lectin-associated serine proteases to exposed mannose groups on the cell surface[4,5]. Specific antibodies against dextran in normal serum initiated the complement activation[37]. Both the classical and the lectin pathways can be inhibited by addition of EGTA-Mg^{2+} in serum. For dextran- and PVA-immobilized surfaces, blocking by addition of EGTA-Mg^{2+} resulted in only small decreases in the amounts of adsorbed proteins and bound anti-C3b compared to control serum samples lacking EGTA-Mg^{2+} (Fig. 3.4). These results suggest that complement activation on dextran- and PVA-immobilized surfaces is mainly mediated by the alternative pathway and is initiated by immobilization of C3b onto hydroxyl groups of dextran and PVA.

ELISA measurement showed that complement fragment SC5b-9 generated in serum markedly increases when dextran- and PVA-immobilized surfaces contact to serum (Fig. 3.5). In contrast, C3a concentration exhibited a small increase for dextran-immobilized surface compared with dextran solution (Fig. 3.6). It was reported that generated C3a adsorbs on material surface[38]. Since immobilized dextran does not fully inhibit non-specific adsorption of serum proteins (Fig. 3.4A, serum + EDTA), adsorption of C3a on dextran-immobilized surface is considered to occur,

which results in a decrease in apparent concentration of C3a released in serum. Nevertheless, C3a release exhibited same tendency as SC5b-9 release.

Dextran- and PVA-immobilized surfaces strongly activated the complement system, but soluble polymers in serum could not. Thus, the state of the polymer greatly modulates complement activation behavior. For dextran-coated nanoparticles, it was reported that complement activation depends on dextran conformation[31,33]. However, the cause for the different behaviors in polymers immobilized on substrates and soluble polymers is not clear yet. At this point, following two mechanisms which induce the differences were speculated. Complement activation through the alternative pathway is initiated in the fluid phase with spontaneous and continuous generation of $C3b^7$. The C3b alters its conformation resulting in exposure of a highly reactive thioester group on surface of a C3b molecule[39–41]. The thioester group becomes accessible for nucleophilic attack but is readily hydrolyzed by surrounding water (half life: $\sim$ 60 μs)[42]. When the short-lived C3b is formed near surface carrying nucleophilic groups, it easily reacts with nucleophilic groups and immobilized on the surface followed by formation of a complex with factor B to give C3 convertase, or C3bBb. The C3bBb effectively convert C3 to C3b near the surface, the C3b molecules near the surface shortly immobilized on the surface and stabilized. Thus, the surface-bound C3b amplifies the complement activation. On the other hand, when a polymer solution is added to serum, spontaneously formed C3b is also stabilized by reacting with a nucleophilic group of the polymer in the serum and then form a C3bBb. The C3bBb effectively converts C3 to C3b, but the C3b hardly finds a nucleophilic group and

thus reacts with it much more slowly than that formed near the surface carrying nucleophilic groups, because a local concentration of nucleophilic groups near the formed C3b is much lower in the serum than on the surface.

Binding of pro-enzyme factor B to surface-bound C3b and subsequent cleavage of factor B by factor D yields C3bBb complex (C3 convertase), which converts C3 into C3a and C3b. In addition, it results in the formation of C3b2Bb (C5 convertase), which cleaves C5 to ultimately lead to the terminal complement complex C5b-9. While surface-bound C3b amplifies the complement activation, factor H and I inactivate C3b. These amplification / inactivation reactions are considered to be determined by accessibility of each factor to susceptible sites of surface-bound C3b. Crystal structure of C3bBb[43] and three dimensional structure of C3bBb determined by electron microscopy[44] revealed that factor B binds to C3b apart from the thioester domain, which contains thioester bond for covalent binding to surfaces. Crystal structure of complex of C3b and factor H fragment ($\sim$ 31 kDa) also revealed that factor H fragment binds large portion of C3b including the thioester domain[45]. For C3b bound to dextran and PVA on surfaces, activator (factor B) is expected to be able to interact with their binding sites, but full length factor H (155 kDa) and I (88 kDa) hardly access to their binding site in C3b due to steric hindrance since binding sites of factor H and I are surrounded by immobilized polymers and a planer substrate. On the other hand, for C3b bound to a dextran and PVA soluble chain in serum, regulators (factor H and I) maybe access to their binding site in C3b, because C3b carries a relatively small soluble dextran or PVA chain.

To elucidate these speculations, an investigation of the effect of the water content

of the PVA and dextran layers on the complement activation has been undertaken and the effect of polymer sizes and geometries, that is, soluble polymer chains, nano-gels and flat layers of dextran and PVA is intended to be examined, on the complement activation. These results will be reported in due course.

3.5 Conclusion

It was clearly showed that dextran- and poly(vinyl alcohol)-immobilized surfaces strongly activated the complement system, but soluble dextran or poly(vinyl alcohol) in serum could not, even when amounts of the soluble polymers added to serum were 4 – 2000 times greater than those on the polymer-immobilized surfaces. These results suggest that the physical states of the polymers, that is, immobilized on the surface or soluble in serum, greatly modulate complement activation.

References

1. Walport M J. Complement. First of two parts. N Engl J Med 2001;344(14):1058–1066
2. Sim R B, Reid K B. C1: molecular interactions with activating systems. Immunol Today 1991;12(9):307–311
3. Reid K B M. Classical Pathway of Activation. In: Rother K, Till G O, Hänsch G M, editors. The Complement System, Second Revised Edition. Berlin: Springer-Verlag; 1998. pp. 68–86
4. Fujita T, Matsushita M, Endo Y. The lectin-complement pathway–its role in innate immunity and evolution. Immunol Rev 2004;198(1):185–202
5. Reid K B M. Lectin Pathway of Non-self Recognition. In: Rother K, Till G O, Hänsch G M, editors. The Complement System, Second Revised Edition. Berlin: Springer-Verlag; 1998. pp. 86–92
6. Law S-K A, Dodds A W. The internal thioester and the covalent binding properties of the complement proteins C3 and C4. Protein Sci 1997;6(2):263–274
7. Pangburn M K. Alternative Pathway: Activation and Regulation. In: Rother K, Till G O, Hänsch G M, editors. The Complement System, Second Revised Edition. Berlin: Springer-Verlag; 1998. pp. 93–115
8. Chenoweth D E. Complement activation during hemodialysis: clinical observations, proposed mechanisms, and theoretical implications. Artif Organs 1984;8(3):281–290

9. Wegmuller E, Montandon A, Nydegger U, Descoeudres C. Biocompatibility of different hemodialysis membranes: activation of complement and leukopenia. Int J Artif Organs 1986;9(2):85–92
10. Carreno M-P, Labarre D, Jozefowicz M, Kazatchkine M D. The ability of sephadex to activate human complement is suppressed in specifically substituted functional sephadex derivatives. Mol Immunol 1988;25(2):165–171
11. Hirata I, Morimoto Y, Murakami Y, Iwata H, Kitano E, Kitamura H, Ikada Y. Study of complement activation on well-defined surfaces using surface plasmon resonance. Colloids Surf B Biointerfaces 2000;18(3–4):285–292
12. Hirata I, Hioki Y, Toda M, Kitazawa T, Murakami Y, Kitano E, Kitamura H, Ikada Y, Iwata H. Deposition of complement protein C3b on mixed self-assembled monolayers carrying surface hydroxyl and methyl groups studied by surface plasmon resonance. J Biomed Mater Res A 2003;66(3):669–676
13. Gorbet M B, Sefton M V. Complement inhibition reduces material-induced leukocyte activation with PEG modified polystyrene beads (Tentagel) but not polystyrene beads. J Biomed Mater Res A 2005;74(4):511–522
14. Jang H S, Ryu K E, Ahn W S, Chun H J, Dal Park H, Park K D, Kim Y H. Complement activation by sulfonated poly(ethylene glycol)-acrylate copolymers through alternative pathway. Colloids Surf B Biointerfaces 2006;50(2):141–146
15. Arima Y, Toda M, Iwata H. Complement activation on surfaces modified with ethylene glycol units. Biomaterials 2008;29(5):551–560
16. Videm V, Mollens T E. Human Complement Activation by Polygeline and Dextran 70. Scand J Immunol 1994;39(3):314–320

17. Whaley K, North J. Haemolytic assays for whole complement activity and individual components. In: Sim R B, Dodds A W, editors. Complement. Walton Street, Oxford : Oxford University Press; 1997. pp. 19–47

18. Yan L, Marzolin C, Tefort A, Whitesides G M. Formation and Reaction of Interchain Carboxylic Anhydride Groups on Self-Assembled Monolayers on Gold. Langmuir 1997;13(25):6704–6712

19. Stevens M M, Allen S, Davies M C, Roberts C J, Schacht E, Tendler S J B et al. The Development, Characterization, and Demonstration of a Versatile Immobilization Strategy for Biomolecular Force Measurements. Langmuir 2002;18(17):6659–6665

20. Knoll W. Polymer thin films and interfaces characterized with evanescent light. Makromol Chem 1991;192(12):2827–2856

21. Azzam R M A, Bashara N M. Reflection and Transmission of Polarized Light by Stratified Planar Strucures. In: Ellipsometry and Polarized Light. Amsterdam : Elsevier; 1987. pp. 269–363

22. Seferis J C. Refractive Indices of Polymers. New York: John Wiley & Sons; 1999.

23. Bautista M C, Bomati-Miguel O, del Puerto Morales M, Serna C J, Veintemillas-Verdaguer S. Surface characterisation of dextran-coated iron oxide nanoparticles prepared by laser pyrolysis and coprecipitation. J Magn Mater 2005;293(1):20–27

24. Horton R C J, Herne T M, Myles D C. Aldehyde-Terminated Self-Assembled Monolayers on Gold: Immobilization of Amines onto Gold Surfaces. J Am

Chem Soc 1997;119(52):12980–12981

25. Peelen D, Smith L M. Immobilization of Amine-Modified Oligonucleotides on Aldehyde-Terminated Alkanethiol Monolayers on Gold. Langmuir 2005;21(1):266–271
26. Peppas N A. Infrared spectroscopy of semicrystalline poly(vinyl alcohol) networks. Makromol Chem 1977;178(2):595–601
27. Österberg E, Bergström K, Holmberg K, Riggs J A, Van Alstine J M, Schuman T P, Burns N L, Harris J M. Comparison of polysaccharide and poly(ethylene glycol) coatings for reduction of protein adsorption on polystyrene surfaces. Colloids Surf A 1993;77(2):159–169
28. Fournier C, Leonard M, Le Coq-Leonard I, Dellacherie E. Coating Polystyrene Particles by Adsorption of Hydrophobically Modified Dextran. Langmuir 1995;11(7):2344–2347
29. Frazier R A, Matthijs G, Davies M C, Roberts C J, Schacht E, Tendler S J B. Characterization of protein-resistant dextran monolayers. Biomaterials 2000;21(9):957–966
30. Ikada Y, Iwata H, Horii F, Matsunaga T, Taniguchi M, Suzuki M, Taki W, Yamagata S, Yonekawa Y, Handa H. Blood compatibility of hydrophilic polymers. J Biomed Mater Res 1981;15(5):697–718
31. Passirani C, Barratt G, Devissaguet J-P, Labarre D. Interactions of nanoparticles bearing heparin or dextran covalently bound to poly(methyl methacrylate) with the complement system. Life Sci 1998;62(8):775–785
32. Chauvierre C, Labarre D, Couvreur P, Vauthier C. Novel Polysaccharide-

Decorated Poly(Isobutyl Cyanoacrylate) Nanoparticles. Pharm Res 2003;20(11):1786–1793

33. Lemarchand C, Gref R, Passirani C, Garcion E, Petri B, Muller R, Costantini D, Couvreur P. Influence of polysaccharide coating on the interactions of nanoparticles with biological systems. Biomaterials 2006;27(1):108–118
34. Black J P, Sefton M V. Complement activation by PVA as measured by ELIFA (enzyme-linked immunoflow assay) for SC5b-9. Biomaterials 2000;21(22):2287–2294
35. Nilsson B, Ekdahl K N, Mollnes T E, Lambris J D. The role of complement in biomaterial-induced inflammation. Mol Immunol 2007;44(1–3):82–94
36. Tengvall P, Askendal A, Lundström I. Complement activation by IgG immobilized on methylated silicon. J Biomed Mater Res 1996;31(3):305–312
37. Carreno M-P, Maillet F, Labarre D, Jozefowicz M, Kazatchkine M D. Specific antibodies enhance Sephadex-induced activation of the alternative complement pathway in human serum. Biomaterials 1988;9(6):514–518
38. Cheung A K, Parker C J, Wilcox L, Janatova J. Activation of the alternative pathway of complement by cellulosic hemodialysis membranes. Kidney Int 1989;36(2):257–265
39. Gros P, Milder F J, Janssen B J C. Complement driven by conformational changes. Nat Rev Immunol 2008;8(1):48–58
40. Janssen B J C, Christodoulidou A, McCarthy A, Lambris J D, Gros P. Structure of C3b reveals conformational changes that underlie complement activity. Nature 2006;444(7116):213–216

41. Abdul Ajees A, Gunasekaran K, Volanakis J E, Narayana S V L, Kotwal G J, Murthy H M K. The structure of complement C3b provides insights into complement activation and regulation. Nature 2006;444(7116):221–225

42. Sim R B, Twose T M, Paterson D S, Sim E. The covalent-binding reaction of complement component C3. Biochem J 1981;193(1):115–127

43. Rooijakkers S H M, Wu J, Ruyken M, van Domselaar R, Planken K L, Tzekou A, Ricklin D, Lambris J D, Janssen B J C, van Strijp J A G, Gros P. Structural and functional implications of the alternative complement pathway C3 convertase stabilized by a staphylococcal inhibitor. Nat Immunol 2009;10(7):721–727

44. Torreira E, Tortajada A, Montes T, de Córdoba S R, Llorca O. 3D structure of the C3bB complex provides insights into the activation and regulation of the complement alternative pathway convertase. Proc Natl Acad Sci USA 2009;106(3):882–887

45. Wu J, Wu Y-Q, Ricklin D, Janssen B J C, Lambris J D, Gros P. Structure of complement fragment C3b-factor H and implications for host protection by complement regulators. Nat Immunol 2009;10(7):728–733

Chapter 4

Effect of hydration of poly(vinyl alcohol) on complement activation

4.1 Introduction

When artificial materials come into contact with blood, the plasma proteins and cells interact with the material surface. Various biological responses are induced, such as adsorption of proteins, activation of the complement and coagulation systems, inflammatory reactions, and cell adhesion. For materials for development of biomedical devices that will be exposed to blood, the understanding and control of these interactions are essential.

It has been demonstrated that protein adsorption behavior onto artificial materials from serum differs from that from a single protein solution. Protein adsorption on SAMs of alkanethiols carrying hydroxyl groups[1,2] and hydroxyl-terminated oligo(ethylene glycol)[3] were previously examined, and dextran or poly(vinyl alcohol) (PVA) immobilized surfaces were also examined in Chapter 3. Although those surfaces showed low protein adsorption from solutions containing a single protein, large amounts of proteins adsorbed on those surfaces from normal human serum. This was mainly caused by the complement activation, a cascade of enzyme reactions involving approximately 30 soluble and membrane-bound proteins, which

plays an important role in the body's defense systems against pathogens[4]. In Chapter 3, it was found that dextran and PVA immobilized on surfaces strongly activated the complement system, but either of these polymers dissolved in serum could not. In the series of experiments, it was also found that the complement activation ability of PVA, but not dextran, immobilized on surfaces highly depended on their preparation methods.

In this chapter, the effect of water content in PVA layer on complement activation was examined. PVA-immobilized surfaces were prepared by spin-coating of a PVA solution on a self-assembled monolayer (SAM) carrying aldehyde. PVA layers with various thicknesses were prepared by changing concentrations of PVA solutions used for spin-coating. The PVA layers prepared were further annealed at 150 ℃ to increase crystallinity, associated with a decrease in water content[5–8]. Effects of these differences on activation of the complement system were examined. The amounts of serum proteins and complement fragment C3b deposited onto PVA surfaces were determined by using a surface plasmon resonance (SPR) apparatus. The amounts of complement fragments SC5b-9 released after exposure of serum to PVA surfaces were also determined using enzyme-linked immunosorbent assay (ELISA).

4.2 Materials and methods

4.2.1 Preparation of serum and buffers

Blood samples, collected from eight healthy volunteer donors who had a meal at least 4 hours prior to donation, were pooled and mixed together. To separate serum, aliquots (10 cm^3) of the blood were divided equally into sterile glass tubes, left on a

clean bench at ambient temperature for 30 min for inducing blood coagulation, and then centrifuged at 1100 × g at 4 ℃ for 30 min. The serum supernatants were then pooled in a bottle, mixed well, and divided into polypropylene vials in an ice bath, and stored at −80 ℃ until use.

Veronal buffer (VB), composed of 5 mmol dm^{-3} sodium barbital (Nacalai Tesque, Inc., Kyoto, Japan), 142 mmol dm^{-3} NaCl, 3.7 mmol dm^{-3} HCl, 0.15 mmol dm^{-3} $CaCl_2$, and 1.0 mmol dm^{-3} $MgCl_2$ (pH 7.4), was prepared according to the protocol for CH_{50} measurement[9]. For experiments under the condition that complement activation is inhibited, Ethylenediamine-*N*,*N*,*N*′,*N*′-tetraacetic acid (EDTA, Dojindo Laboratories, Kumamoto, Japan) was added to VB (without $CaCl_2$ and $MgCl_2$) to a final concentration of 10 mmol dm^{-3} (EDTA-VB). To block the classical pathway, ethylene *O*,*O*′-bis(2-aminoethyl)ethyleneglycol-*N*,*N*,*N*′,*N*′-tetraacetic acid (EGTA, Sigma-Aldrich, St. Louis, MO) and $MgCl_2$ were added to VB (without $CaCl_2$ and $MgCl_2$) to the final concentrations of 10 mmol dm^{-3} and 2.5 mmol dm^{-3}, respectively (EGTA-Mg^{2+}).

4.2.2 Preparation of PVA spin-coated surface

Glass plates (BK7, refractive index: 1.515, size: 25 × 25 × 1 mm, Arteglass Associates Co., Kyoto, Japan) were immersed for 5 min into a piranha solution (7:3 mixture of concentrated sulfuric acid and 30% hydrogen peroxide) at room temperature, washed three times with deionized water, sequentially rinsed three times with 2-propanol, and finally stored in 2-propanol until use. These glass plates were dried under a stream of dried nitrogen gas and then mounted on the rotating stage of a thermal evaporation coating apparatus (V-KS200, Osaka Vacuum, Ltd., Osaka,

Japan). A chromium layer was deposited to a thickness of 1 nm, and then a gold layer was deposited to a thickness of 49 nm onto the glass plates.

The gold-coated glass plate was immersed in a 0.5 mmol dm^{-3} solution of 11-undecanal disulfide (ProChimia Surfaces Sp. z o.o., Sopot, Poland) in ethanol at room temperature for 24 h to form aldehyde-terminated self-assembled monolayer (CHO-SAM) (Scheme 4.1A). The plate was washed with ethanol three times and dried in a stream of nitrogen gas. PVA layer was then formed on the CHO-SAM by spin-coating of 0.1 or 1% PVA (degree of polymerization = 1700, degree of saponification = 98%, Unitika Ltd., Osaka, Japan) solution in 0.1 mol dm^{-3} HCl at 3,000 rpm for 60 sec. The plate was stored in a desiccator overnight. The plate was immersed in water at 80 ℃ for 10 min to remove free PVA which had not been immobilized on the surface. The plate was rinsed with MilliQ-water three times and dried under a stream of nitrogen gas. For preparation of annealed PVA surfaces, PVA spin-coated surfaces which had been immersed in water at 80 ℃ were incubated for 2 h at 150 ℃.

4.2.3 Surface characterization of PVA spin-coated surfaces

Infrared adsorption spectra of sample surfaces were collected by the reflection-adsorption method (FTIR-RAS) using a Spectrum One (Perkin-Elmer Inc., Boston, MA) spectrometer equipped with a Refractor^{TM} (Harrick Scientific Co., Ossining, NY) and a mercury-cadmium telluride (MCT) detector cooled by liquid nitrogen. Gold-coated glass plates with a gold layer at 199 nm in thickness were used for FTIR-RAS analysis. Spectra were recorded using the *p*-polarized IR light at an incident angle of 75° in the chamber purged with dry nitrogen gas for 128 scans at 4

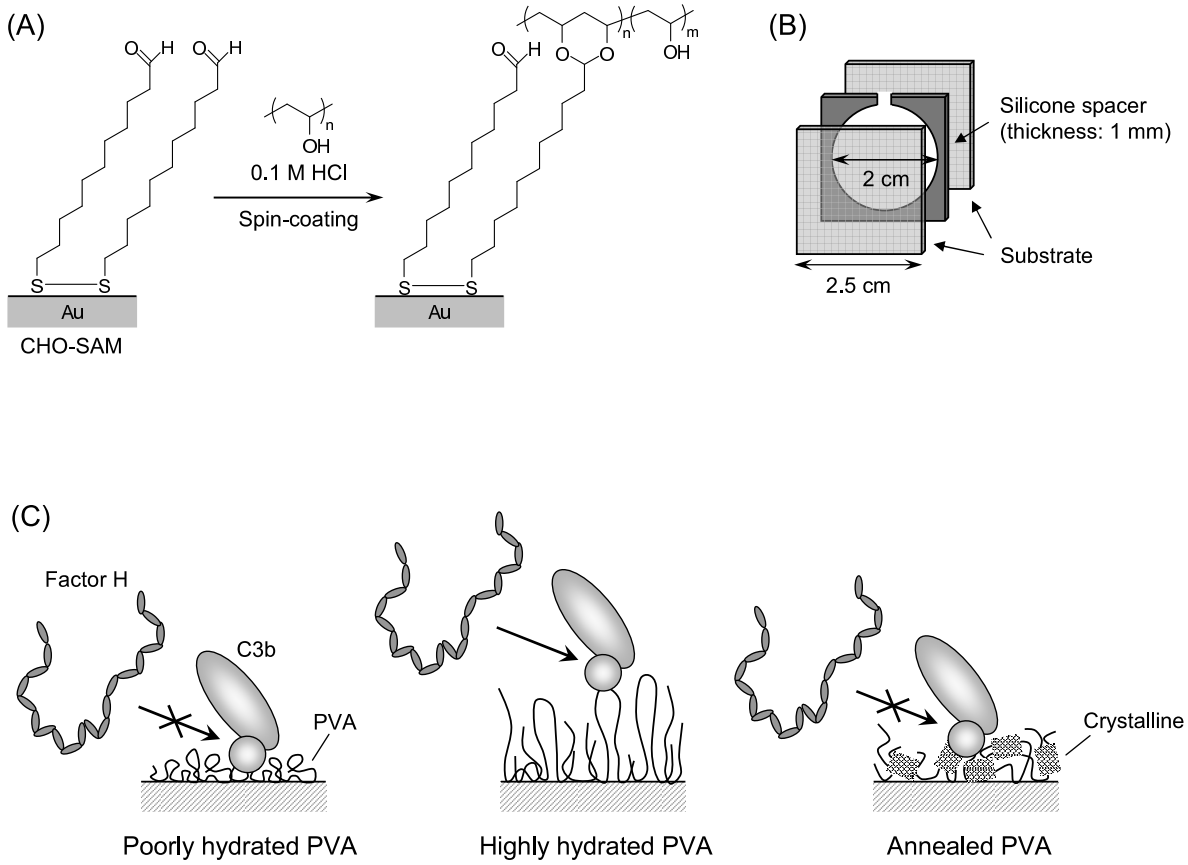

Scheme 4.1 (A) Immobilization of PVA to a SAM on gold. (B) An incubation cell used for ELISA measurement. (C) Schematic representation of interaction between PVA surfaces and complement proteins.

cm^{-1} resolution from 4000 to 750 cm^{-1}.

Static water contact angles on the surfaces were determined by the sessile drop method using a contact angle meter (CA-X, Kyowa Interface Science Co. Ltd., Saitama, Japan) at room temperature. A droplet (10 μl) of water was placed on a substrate and the contact angle was determined three times. This procedure was repeated five times at different places on the same surface.

4.2.4 Surface plasmon resonance (SPR)

The SPR apparatus employed in this study[1] was a home-made apparatus prepared referring the report by Knoll[10]. The BK7 glass plate with the gold layer (49 nm in

thickness) was coupled to a hemicylindrical prism with an immersion oil (n = 1.515, Cargille Laboratories, Cedar Grove, NJ). The sample surface was irradiated with a *p*-polarized He-Ne laser light (λ= 632.8 nm) through the prism. The intensity of the reflected light was monitored as a function of the incident angle. The incident angle, at which the reflectivity reached minimum, was regarded as the SPR angle.

The thickness of an immobilized polymer layer in air was also estimated in the dry state by SPR. The glass plate with the polymer layer was set on the SPR instrument and the reflectivity was measured in air as a function of the incident angle of the laser light. Thickness of the polymer layer was determined by the SPR angle shift using Fresnel's law for the multi-layer system, BK7/Cr/Au/SAM/PVA/air[10,11]. The refractive indices for SAM and PVA were 1.45 and 1.52[12], respectively.

4.2.5 Protein adsorption from human serum

Protein adsorption from undiluted human serum was examined by SPR. A flow chamber with a sample plate was placed on a prism of the SPR apparatus, and VB was circulated at a flow rate of 3.0 cm^3/min in the flow chamber assembly. Reflectance was monitored during the flow of the liquid samples at an incident angle of 0.5° less than the SPR angle. Undiluted human serum was then introduced into the flow chamber assembly and incubated for 90 min. To wash out serum from the sample surface, VB was introduced and circulated for additional 20 min. All experiments were performed at 37 ℃. Introduction of undiluted human serum resulted in a large increase in the reflectance (bulk effect) due to its high refractive index. To correct for changes in the reflectance, standard solutions with different refractive indices (Mill-Q water, VB, and 2 mol dm^{-3} NaCl) were employed.

To identify proteins deposited on the surface, solutions of specific antibodies were flowed through the apparatus after exposure of the sample surface to human serum. A 1% solution of anti-human C3b antiserum (RAHu/C3b, Nordic Immunology, Tilburg, The Netherlands) diluted in VB was flowed for 90 min onto the surface of the protein layer formed on the surface and then VB was introduced for 20 min to wash out the antibody solution. The thickness of the protein layer was calculated from the shift in the SPR angle (ΔSPR) using Fresnel fits for the system BK7/Cr/Au/SAM/protein/water[10,11], where the refractive indices of SAM and protein were assumed to be 1.45. The amounts of proteins adsorbed onto the surfaces were estimated from the thickness presuming that the density of the protein layer was 1 as follows[1]:

$$\text{The amount of adsorbed protein (ng/cm}^2\text{)} = 500 \times \Delta\text{SPR}(^\circ) \tag{4.1}$$

To study under the conditions that complement activation was blocked, serum was supplemented with EDTA at a final concentration of 10 mmol dm^{-3}. To study under the conditions that complement activation via the classical and the lectin pathways were blocked, serum was supplemented with EGTA and $MgCl_2$ at final concentrations of 10 and 2.5 mmol dm^{-3}, respectively.

4.2.6 Quantification of generated complement fragments

An incubation cell was prepared by placing a silicone spacer (inner diameter: 20 mm, thickness: 1 mm) between the two glass plates carrying a test surface for determination of generated complement fragments (Scheme 4.1B). Serum (approximately 340 μl) was injected into the circular space in the cell and incubated for 90

min at 37 ℃. Serum was then collected and EDTA was added to a final concentration of 10 mmol dm^{-3} to halt the complement activation. The concentration of the complement fragments (SC5b-9) in the serum was determined by a commercially available ELISA kit (SC5b-9 plus ELISA, QUIDEL Corp., CA).

4.3 Results

4.3.1 Surface characterization

A PVA solution in 0.1 mol dm^{-3} HCl was spin-coated on a CHO-SAM on gold (Scheme 4.1A). A PVA spin-coated surface was characterized by FTIR-RAS, SPR and water contact angle measurements. A FTIR-RAS spectrum for a PVA layer prepared by spin-coating of 1% PVA solution onto a CHO-SAM (Fig 4.1a) showed asymmetric and symmetric C–H stretching bands of methylene groups at 2922 cm^{-1} and 2854 cm^{-1}, respectively. Several other bands were also showed at 3100–3600 cm^{-1} assigned to O–H stretching, at 1145 cm^{-1} assigned to C–C stretching in the crystalline region, at 1098 cm^{-1} assigned to C–O stretching, and at 845 cm^{-1} assigned to CH_2 rocking[8]. When a PVA spin-coated surface was immersed in water at 80 ℃ for 10 min, the intensity of all bands decreased, indicating that PVA molecules not chemically bonded to surface CHO groups were removed (Fig 4.1b, Scheme 4.1A). When PVA was spin-coated onto a gold surface without CHO-SAM, PVA hardly remained on the surface after immersion in hot water (data not shown). These results indicate that PVA is chemically immobilized onto a CHO-SAM through acetal bonds. Annealing of PVA at 150 ℃ for 2 h slightly increased the peak at 1145 cm^{-1}, suggesting that crystallinity of PVA layer increased by annealing (Fig 4.1c). When

a 0.1% PVA solution was employed, all peak intensities decreased (Fig 4.1d), indicating smaller amount of PVA immobilized on the surface than a 1% PVA solution used. Thickness of PVA layers under dry state, which was determined by SPR measurement, is 1.3 ± 0.1 nm and 6.3 ± 0.4 nm for 0.1% and 1.0% PVA solutions used, respectively. Thickness of PVA layer increased with an increase in PVA concentration. From contact angle measurements (Table 4.1), the PVA layer prepared using 0.1% solution is more hydrophilic than that prepared using 1% PVA. Annealing made the PVA surface slightly hydrophobic.

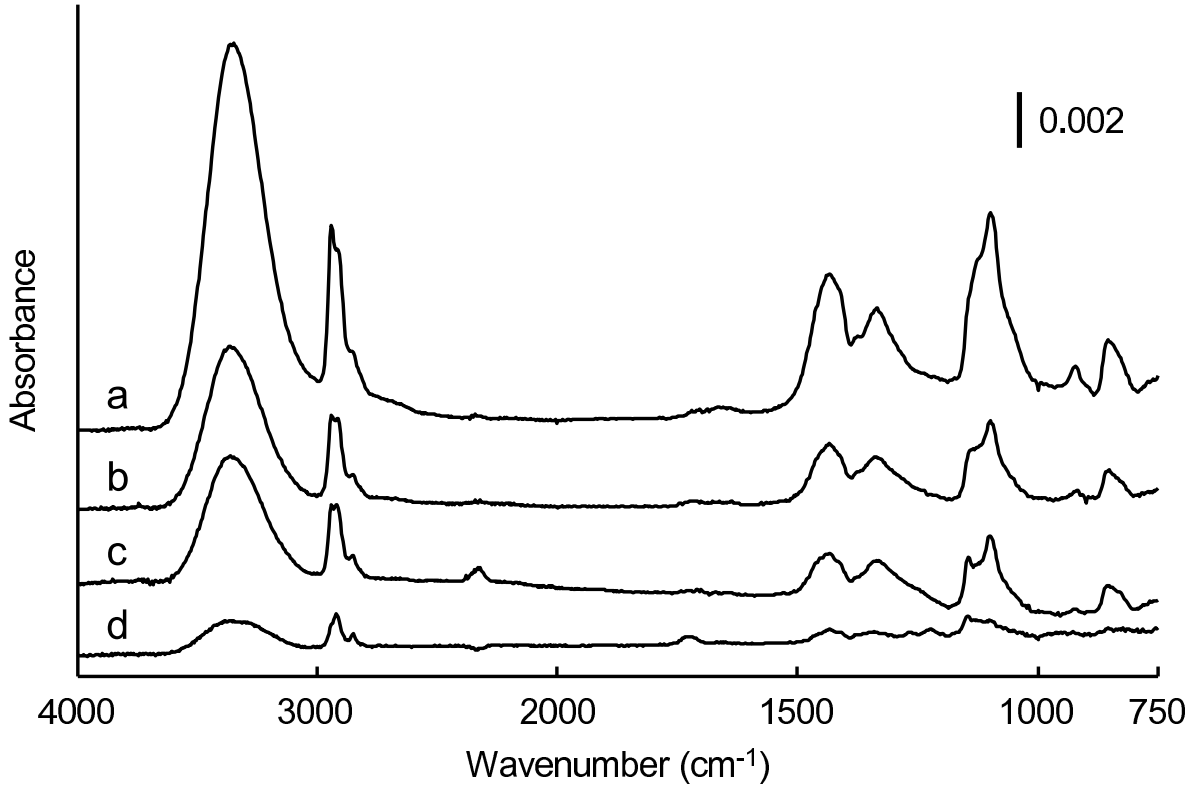

Fig. 4.1 FTIR-RAS spectra of PVA surfaces: (a) as spin-coated with 1% solution; (b) immersed in water for 10 min at 80 ℃; (c) annealed for 2h at 150 ℃; (d) spin-coated with 0.1% solution and subsequently immersed in water at 80 ℃.

Taken together, these results indicated that PVA layers were successfully formed on CHO-SAM depicted in Scheme 4.1A.

Table. 4.1 Characterization of PVA spin-coated surfaces.

PVA surfaces	Contact angle (degree)	Thickness of dry PVA (nm)[a]	Amount of PVA (ng/cm^2)[b]
0.1%[c]	36.7 $\pm$ 1.8	1.3 $\pm$ 0.1	169 $\pm$ 13
1%[c]	53.7 $\pm$ 2.0	7.4 $\pm$ 0.4	957 $\pm$ 46
1% (annealed)	62.0 $\pm$ 3.3	6.4 $\pm$ 0.1	826 $\pm$ 10

[a]determined by a surface plasmon resonance apparatus
[b]calculated from thickness supposing the density of PVA is 1.3.
[c]after immersion in water for 10 min at 80 ℃

4.3.2 Complement activation on PVA-immobilized surface

Adsorption of serum proteins and complement activation on PVA-immobilized surface was followed by an SPR apparatus. When surfaces were sequentially exposed to VB and undiluted human serum, rapid increases in the SPR angles were observed (Fig 4.2A). The initial increments are due to the large change in refractive indices between VB and human serum. The SPR angle gradually increased additional 1.3° after several minutes of an induction period on PVA surface prepared using 0.1% solution. When serum was removed by flushing VB through the system, the SPR angle rapidly decreased due to decrease in refractive index of the solution. The SPR angle shift (ΔSPR) before and after the PVA surface exposed to serum reflects protein adsorption on the surface (see Eq. 4.1). Large amounts of serum proteins adsorbed onto the PVA surfaces prepared using 0.1% PVA solution. After the surfaces were washed with VB, an anti-human C3b antiserum solution was applied to those surfaces to evaluate the amount of C3b or C3bBb which was produced by the complement activation (Fig 4.2B). The large SPR angle shift, 1.6° – 1.8°, was induced by binding of anti-C3b antibody to the protein layers on the PVA surfaces. These large

amounts of anti-C3b antibody bound on the surfaces suggest that a major component in the layer of serum proteins formed on the surface was C3b or C3bBb. On the other hand, very small amount of serum proteins adsorbed on a PVA surface which was prepared by spin-coating 1% PVA solution, washed with 80 ℃ water but without 150 ℃ annealing (Fig 4.2A, ΔSPR= $\sim$ 0.06°). Subsequent exposure to anti-C3b antibody resulted in no increase of the SPR angle. These results indicate that a PVA layer prepared with 1% solution is inert to either non-specific protein adsorption or the complement activation.

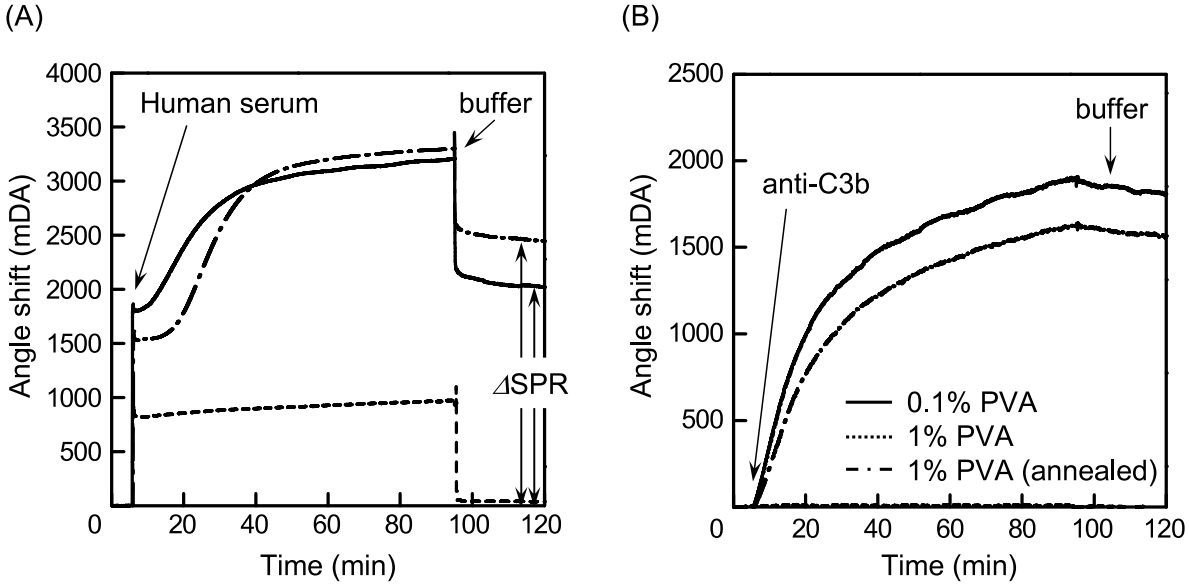

Fig. 4.2 SPR sensorgrams during exposure of PVA surfaces to normal human serum (A) and subsequent exposure to anti-C3b antiserum (B). ΔSPR indicates an increase in the SPR angle after exposure to serum and subsequent rinsing with a buffer and corresponds to the amount of adsorbed serum proteins according to eq. 4.1.

The complement system is activated through three pathways: the classical, lectin, and the alternative pathway. Sera supplemented with EDTA or EGTA-Mg^{2+} were employed to distinguish the pathways through which the complement system was activated by PVA spin-coated surfaces (Fig 4.3). EDTA is known to inhibit all three

pathways, while EGTA-Mg^{2+} inhibit only the classical and the lectin pathways. When serum supplemented with 10 mmol dm^{-3} EDTA was employed, the amounts of adsorbed proteins greatly decreased on PVA surface prepared by spin-coating 0.1% solution. PVA surface, which was spin-coated with 1% solution and subsequently annealed, also demonstrated low level of protein adsorption in the presence of EDTA. These results clearly indicate that these PVA surfaces practically resist to non-specific protein adsorption when the complement activation was inhibited. Immobilization of anti-C3b antibody was not observed on the surfaces in the presence of EDTA either, indicating that deposition of C3b or C3bBb was due to the complement activation. On the other hand, large amounts of adsorbed serum proteins and bound anti-C3b antibody were observed on these PVA surfaces in serum supplemented with 10 mmol dm^{-3} EGTA and 2 mmol dm^{-3} Mg^{2+}. These results suggest that these PVA surfaces activate the complement system through the alternative pathway. In contrast, a PVA surface, which was prepared by spin-coating 1% PVA solution, washed with 80 ℃ water but without 150 ℃ annealing, exhibited low level of serum protein adsorption and no binding of anti-C3b even when exposed to native serum, indicating the PVA surface prepared from 1% PVA solution demonstrated both non-fouling for serum proteins and non-activating for the complement system in any three kinds of sera.

4.3.3 Generation of SC5b-9

The generation of a soluble form of the membrane attack complex SC5b-9 was also examined in serum after exposure to PVA surfaces. The complex is diverted from membrane-associated C5b-9 by reacting with S protein (vitronectin), if cell

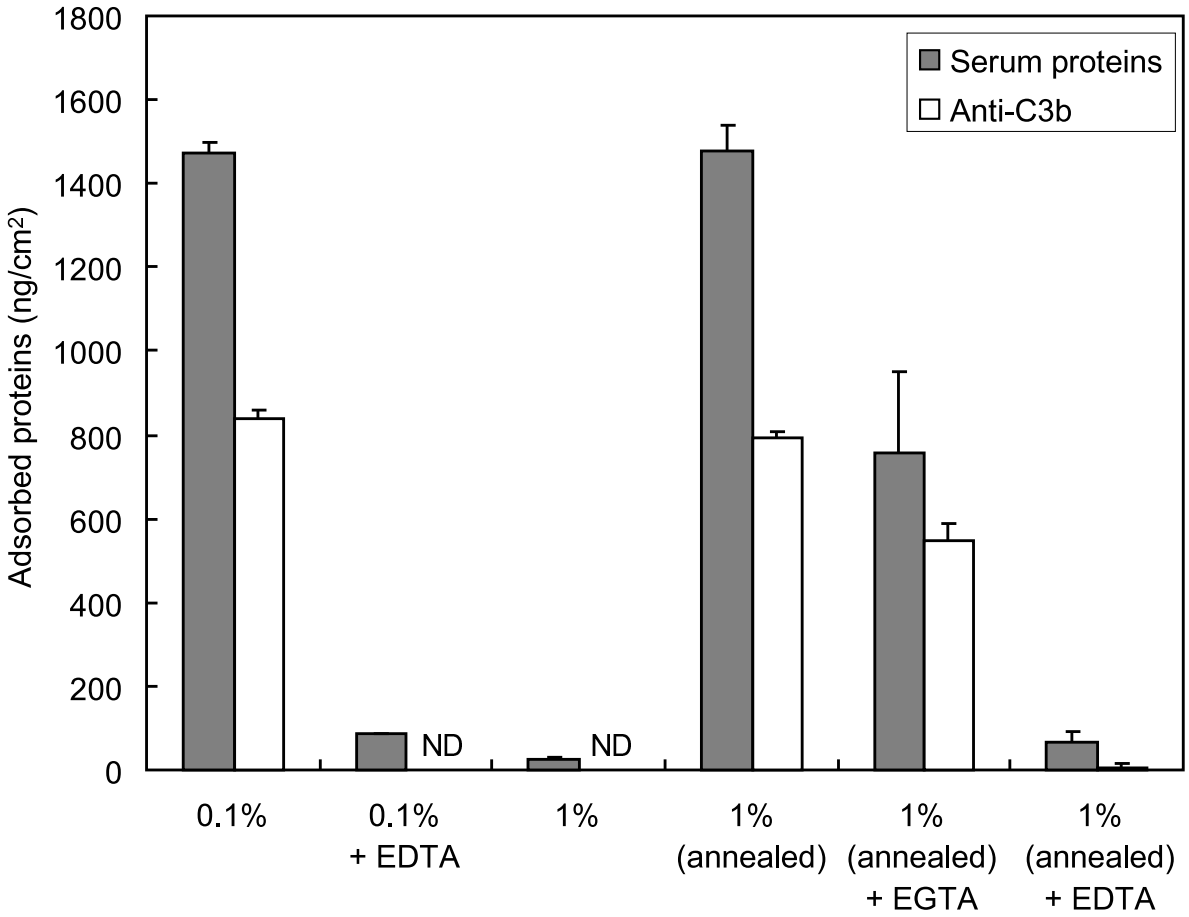

Fig. 4.3 Amounts of serum proteins adsorbed on PVA surfaces and subsequent anti-C3b antibodies bound to those surfaces with a serum protein layer. Data shown are means ± SD (n = 3). Percent: PVA concentration for spin-coating, EDTA: human serum + 10 mmol dm^{-3} EDTA, EGTA: human serum + 10 mmol dm^{-3} EGTA + 2.5 mmol dm^{-3} $MgCl_2$. ND: not detected.

membrane does not exist and its concentration effectively reflects activation of the common terminal pathway.

The SC5b-9 concentration markedly increased when serum was exposed to PVA surfaces prepared by spin-coating 0.1% PVA solution (Fig 4.4). This large amount of SC5b-9 released in serum exposed to PVA spin-coated surface well agrees with the results obtained from the SPR measurements shown in Fig 4.2. PVA surface prepared by spin-coating 1% solution showed small increase in SC5b-9 concentra-

tion in native serum, indicating that the surface is low activator for the complement system. Annealing of the PVA surface resulted in increase in amount of SC5b-9 release.

These results are consistent with the results of the SPR measurements, that is, PVA thickness and surface concentration greatly modulate the complement activation behavior.

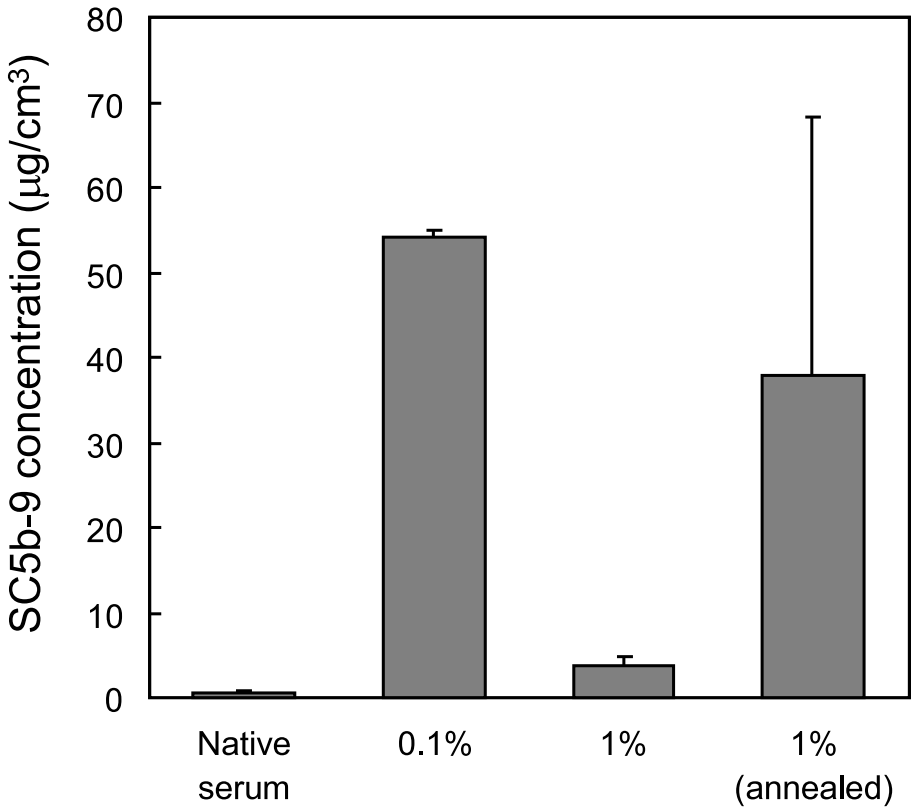

Fig. 4.4 Concentrations of SC5b-9 generated in serum exposed to PVA surfaces. Data shown are means ± SD (n = 3). SC5b-9 concentration in serum exposed to zymosan (10 mg/cm^3) was 298 ± 84 μg/cm^3 (positive control).

4.4 Discussion

PVA is a water soluble and nonionic polymer carrying hydroxyl groups and thus forms a highly hydrated layer when it is immobilized on a surface. Protein adsorption on PVA surface has been studied using solutions of a single protein such as albumin, IgG, and fibrinogen. These studies demonstrated that it does not strongly interact with any of these proteins[5–7]. Surface modification with PVA gives a non-fouling surface and thus has been applied to prepare medical devices and biosensors[5–7]. On the other hand, it has been reported that polymers carrying hydroxyl groups, such as cellulose and its derivatives, strongly activated the complement system and a large amount of C3b or C3bBb was immobilized on the their surfaces from blood or serum. Protein adsorption on SAMs of alkanethiols carrying hydroxyl groups[1,2], and hydroxyl-terminated oligo(ethylene glycol)[3] were also examined. Dextran- and poly(vinyl alcohol) (PVA)-immobilized surfaces were also examined in Chapter 3. Although those surfaces showed low protein adsorption from solutions containing a single protein, large amounts of proteins adsorbed on those surfaces and the complement system was strongly activated when the surfaces were exposed to normal human serum. In the series of experiments, however, it was also found that the complement activation ability of PVA, but not dextran, immobilized on surfaces highly depends on their preparation methods.

PVA was immobilized onto a SAM functionalized with aldehydes through acetal bonds (Scheme 4.1A) as previously described in Chapter 3. The thickness of PVA layers was controlled by PVA concentrations used for spin-coating. Ethylamine was

not employed to block unreacted aldehyde groups remaining underneath the PVA layer in the present study. If the CHO groups under the PVA layer can react with proteins in serum, a large amount of proteins immobilized in serum supplemented EDTA should be observed. No protein adsorption, however, was observed. This result indicates that no CHO group remained after PVA was immobilized or PVA chains effectively prevented the interaction of serum proteins with basal CHO-SAM surface, as described in Chapter 3.

SPR measurements in this chapter clearly demonstrated that large amounts of serum proteins deposited on PVA surfaces spin-coated with 0.1% PVA solution (Fig 4.2 and 4.3) from undiluted human serum. Subsequent binding of antibody against C3b identified the deposited proteins as C3b or C3bBb. ELISA measurement for generated SC5b-9 also revealed that the complement system was strongly activated by the surfaces. These results are consistent with those in Chapter 3, in which PVA was immobilized on CHO-SAM by immersion into a PVA solution containing 0.1 mol dm^{-3} HCl. Thickness of dry PVA layer (1.7 nm) was comparable to present study (1.3 nm, Table 4.1). These results suggest that an ultra-thin PVA layer immobilized on a substrate strongly activates the complement system.

The complement system is known to be activated through three pathways: the classical, the lectin, and the alternative pathways. For material-induced complement activation, the classical and the alternative pathways are considered to occur[13]. Complement activation via the classical pathway is triggered by non-specifically adsorbed proteins such as immunoglobulins[14] when artificial materials are brought into contact with blood or serum. For all PVA surfaces used in present study, non-

specific adsorption of serum proteins was not observed in the presence of EDTA, suggesting that immunoglobulins do not adsorbed to the PVA surfaces and thus the complement system is not activated through the classical pathway. The complement activation through the alternative pathway is initiated in the fluid phase with spontaneous and continuous generation of enzymes that cleave C3 to C3a and C3b[15]. Upon cleavage, conformation of C3b changes to make a highly reactive thioester group accessible for nucleophilic attack[16–18]. The thioester group is readily hydrolyzed by surrounding water (half life: $\sim$ 60 μs)[19]. When the short-lived C3b is formed near surface carrying nucleophilic groups, it easily reacts with nucleophilic groups and is immobilized on the surface followed by formation of a complex with factor B to give C3 convertase C3bBb. The C3 convertase is a very strong activator for the alternative pathway. PVA surfaces carry large amount of hydroxyl groups which are not covered with non-specifically adsorbed serum proteins. C3b immobilized on the PVA layer and thus a C3 convertase was formed. Thus the complement system is considered to be initiated through the alternative pathway on the PVA immobilized surface.

PVA layer prepared from 1% PVA solution, however, demonstrated resistance to non-specific protein adsorption from human serum and complement activation. This result suggests that surface structure of PVA layer greatly modulates the complement activation behavior. PVA solution was also non-activator for the complement system as reported in Chapter 3. It is considered to be related to an ability of complement proteins to interact with C3b bound to polymers. While binding of factor B to surface-bound C3b amplifies the complement activation, factor H

and I inactivate C3b. These amplification / inactivation reactions are considered to be determined by accessibility of each factor to susceptible sites of surface-bound C3b. Factor B binds to a site of C3b apart from the thioester domain, which contains thioester bond for covalent binding to surfaces[20,21], while factor H fragment (31 kDa) binds large portion of C3b including the thioester domain[22]. When C3b bound to a PVA soluble chain in serum, regulators (factor H and I) easily access to its binding site in C3b, as schematically shown in Scheme 4.1C. For PVA-immobilized surfaces, complement activation behavior is expected to be affected by the water content of PVA layer. For C3b bound to poorly hydrated PVA on surface, activator (factor B) is expected to be able to interact with their binding sites, but factor H (155 kDa) and I (88 kDa) hardly access to their binding site in C3b due to steric hindrance since binding sites of factor H and I are surrounded by PVA chains and a planer substrate. On the other hand, regulators (factor H and I) maybe access to their binding site when C3b was bound to highly hydrated PVA on surface or in solution.

Much more interesting finding in this study is effect of heat treatment of PVA layers on the complement activation. PVA layers were prepared by spin-coating of 1% PVA solution on CHO-SAM. Although the PVA layer without heat treatment is not an activator of the complement system, the surface became a strong activator after it was treated at 150 ℃. It has been reported that annealing of PVA results in an increase of crystallinity and a decrease of water content[5–8]. FTIR-RAS spectra (Fig 4.1) showed a slight increase in the peak at 1145 cm^{-1} assigned as the C–C stretching in the crystalline region[8] after annealing. It has been also reported that protein adsorption, platelet adhesion, and clot formation increased with decreasing

water content of PVA film[5] or hydrogel[6,7,23]. The density and size of the microcrystallites and the hydrated PVA chains are considered to affect protein adsorption. However, crystallinity of thin PVA layer (thickness: $\sim$ 6 nm) after annealing is uncertain while crystallinity of PVA film and hydrogel (thickness: $\sim$ 100 μm) varies from 0.1 to 0.5 by annealing[5–7]. To elucidate properties determinant for complement activation, water content of the PVA thin layer and its effect on the complement activation need to be further investigated.

4.5 Conclusion

It was clearly demonstrated that the complement activation by PVA layers highly depends on their water contents. These phenomena can be explained by accessibility of complement regulatory factors H (155 kDa) and I (88 kDa) to their binding site in C3b.

References

1. Hirata I, Morimoto Y, Murakami Y, Iwata H, Kitano E, Kitamura H, Ikada Y. Study of complement activation on well-defined surfaces using surface plasmon resonance. Colloids Surf B Biointerfaces 2000;18(3–4):285–292
2. Hirata I, Hioki Y, Toda M, Kitazawa T, Murakami Y, Kitano E, Kitamura H, Ikada Y, Iwata H. Deposition of complement protein C3b on mixed self-assembled monolayers carrying surface hydroxyl and methyl groups studied by surface plasmon resonance. J Biomed Mater Res A 2003;66(3):669–676
3. Arima Y, Toda M, Iwata H. Complement activation on surfaces modified with ethylene glycol units. Biomaterials 2008;29(5):551–560
4. Walport M J. Complement. First of two parts. N Engl J Med 2001;344(14):1058–1066
5. Ikada Y, Iwata H, Horii F, Matsunaga T, Taniguchi M, Suzuki M, Taki W, Yamagata S, Yonekawa Y, Handa H. Blood compatibility of hydrophilic polymers. J Biomed Mater Res 1981;15(5):697–718
6. Fujimoto K, Minato M, Ikada Y. Poly(vinyl alcohol) Hydrogels Prepared under Different Annealing Conditions and Their Interactions with Blood Components. ACS Symposium Series 1994;540:228–242
7. Kulik E, Ikada Y. In vitro platelet adhesion to nonionic and ionic hydrogels with different water contents. J Biomed Mater Res 1996;30(3):295–304
8. Peppas N A. Infrared spectroscopy of semicrystalline poly(vinyl alcohol) networks. Makromol Chem 1977;178(2):595–601

9. Whaley K, North J. Haemolytic assays for whole complement activity and individual components. In: Sim R B, Dodds A W, editors. Complement. Walton Street, Oxford : Oxford University Press; 1997. pp. 19–47
10. Knoll W. Polymer thin films and interfaces characterized with evanescent light. Makromol Chem 1991;192(12):2827–2856
11. Azzam R M A, Bashara N M. Reflection and Transmission of Polarized Light by Stratified Planar Strucures. In: Ellipsometry and Polarized Light. Amsterdam : Elsevier; 1987. pp. 269–363
12. Seferis J C. Refractive Indices of Polymers. New York: John Wiley & Sons; 1999.
13. Nilsson B, Ekdahl K N, Mollnes T E, Lambris J D. The role of complement in biomaterial-induced inflammation. Mol Immunol 2007;44(1–3):82–94
14. Tengvall P, Askendal A, Lundström I. Complement activation by IgG immobilized on methylated silicon. J Biomed Mater Res 1996;31(3):305–312
15. Pangburn M K. Alternative Pathway: Activation and Regulation. In: Rother K, Till G O, Hänsch G M, editors. The Complement System, Second Revised Edition. Berlin: Springer-Verlag; 1998. pp. 93–115
16. Gros P, Milder F J, Janssen B J C. Complement driven by conformational changes. Nat Rev Immunol 2008;8(1):48–58
17. Janssen B J C, Christodoulidou A, McCarthy A, Lambris J D, Gros P. Structure of C3b reveals conformational changes that underlie complement activity. Nature 2006;444(7116):213–216
18. Abdul Ajees A, Gunasekaran K, Volanakis J E, Narayana S V L, Kotwal G

J, Murthy H M K. The structure of complement C3b provides insights into complement activation and regulation. Nature 2006;444(7116):221–225

19. Sim R B, Twose T M, Paterson D S, Sim E. The covalent-binding reaction of complement component C3. Biochem J 1981;193(1):115–127
20. Rooijakkers S H M, Wu J, Ruyken M, van Domselaar R, Planken K L, Tzekou A, Ricklin D, Lambris J D, Janssen B J C, van Strijp J A G, Gros P. Structural and functional implications of the alternative complement pathway C3 convertase stabilized by a staphylococcal inhibitor. Nat Immunol 2009;10(7):721–727
21. Torreira E, Tortajada A, Montes T, de Córdoba S R, Llorca O. 3D structure of the C3bB complex provides insights into the activation and regulation of the complement alternative pathway convertase. Proc Natl Acad Sci USA 2009;106(3):882–887
22. Wu J, Wu Y-Q, Ricklin D, Janssen B J C, Lambris J D, Gros P. Structure of complement fragment C3b-factor H and implications for host protection by complement regulators. Nat Immunol 2009;10(7):728–733
23. Matsuda T. Private communication.

Chapter 5

Complement activation on degraded polyethylene glycol-covered surface

5.1 Introduction

Surface modification with polyethylene glycol (PEG) is one of the most promising strategies to prevent and/or reduce adsorption of proteins and the aftereffects of the interaction of body fluids with biomaterials[1,2]. PEG has also been used for pharmaceutical applications to shield antigenicity of proteinaceous drugs and to prolong the circulating half-life of drug-loaded nanoparticles and liposomes[3-5]. However, unanticipated body reactions such as hypersensitivity caused by PEG-modified liposomes[6-9] and rapid clearance of PEG-modified liposomes from blood[10] have been reported. Activation of the complement system has been suggested as being associated with these body reactions[11]. The complement system, which plays important roles in the body's defense system against pathogenic xenobiotics, is an enzyme cascade system that consists of approximately 30 fluid-phase and cell-membrane bound proteins[12]. It is activated through three separate pathways: the classical pathway (CP), the lectin pathway(LP), and the alternative pathway (AP) (Scheme 1 in General Introduction). Understanding the interaction of complement proteins with the PEG-modified surface may provide a basis for developing PEG-modified

materials for biomedical and pharmaceutical use.

In a previous study[13], complement activation behaviors were examined on PEG-modified surfaces; however, there were uncertainties about the experimental setup. First, diluted (10%) normal human serum (NHS) was used, and it has been reported that activation of the alternative pathway may be diminished with use of diluted serum[14,15]. In addition, the PEG-modified surfaces were not sufficiently characterized. In the current study, a PEG-modified surface on a gold surface was prepared using a self-assembled monolayer of α-mercaptoethyl-ω-methoxy-polyoxyethylene (HS-mPEG). Then, detailed surface analyses of PEG-modified surfaces were carried out using the reflection-adsorption method (FTIR-RAS) and X-ray photoelectron spectrometry (XPS) and activation of the complement system were examined using undiluted NHS to obtain more detailed insight into the mechanisms of complement system activation by the PEG-modified surfaces.

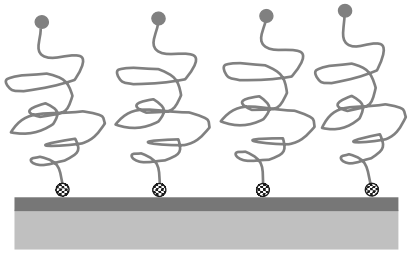

HS-mPEG

$HS\text{-}CH_2CH_2(OCH_2CH_2)_n\text{-}OCH_3$

mPEG surfaces

mPEG surfaces examined after preparation procedure	: “naive mPEG"
mPEG surfaces stored in −20 °C freezer for 12 days	: “F-mPEG"
mPEG surfaces stored in a dessicator under room light	: “R-mPEG"
mPEG surfaces irradiated with UV light for 60 min.	: "UV-mPEG"

Scheme 5.1 Schematic illustration of a surface modified with methoxy-capped PEG.

5.2 Materials and methods

5.2.1 Reagents and antibodies

HS-mPEG (SUNBRIGHT ME-050SH, Mn = 5000, NOF Corporation, Tokyo, Japan) was used as provided. Barbital sodium, calcium chloride, magnesium chloride, and *O,O'*-bis(2-aminoethyl)ethyleneglycol-*N,N,N',N'*-tetraacetic acid (EGTA) (all purchased from Nacalai Tesque, Inc., Kyoto, Japan) and ethylenediamine-*N,N,N',N'*-tetraacetic acid (EDTA; Dojindo Laboratories, Kumamoto, Japan) were of reagent grade. EDTA cheletes Ca^{2+} and Mg^{2+} cations and inhibits all three activation pathways of the complement system. EGTA with abundant Mg^{2+} cation captures Ca^{2+} cation and thus inhibits the classical and the lectin pathways of the complement system. Ethanol (reagent grade, Nacalai Tesque) was deoxygenized with nitrogen gas bubbling before use. Water was purified with a Milli-Q system (Millipore Co.). Polyclonal rabbit anti-human C3b antibody (RAHu/C3b) was purchased from Nordic Immunological Laboratories (Tilburg, The Netherlands) and its solution prepared and stored in accordance with supplier instructions.

5.2.2 Preparation of NHS and buffers

All participants enrolled in this research provided informed consent, which was approved and accepted by the ethics review board of the Institute for Frontier Medical Sciences, Kyoto University. Blood was donated from 10 healthy volunteers who had consumed a meal at least 4 h before the donation. The preparation method for the NHS has been described elsewhere[13]. Briefly, the collected blood was kept at ambient temperature for 30 min and centrifuged at 4 ℃. Supernatant was pooled and

mixed and stored at −80 ℃ until use. Veronal buffer (VB) was prepared referring to a protocol of CH_{50} measurement[16]. To prevent complement activation completely, 10 μl of 0.5 mol dm^{-3} EDTA aqueous solution (pH 7.4) was added to 490 μl of NHS (final concentration of EDTA, 10 mmol dm^{-3}). To block the classical pathway of the complement system, 10 μl of a mixture of 0.5 mol dm^{-3} EGTA and 0.1 mol dm^{-3} $MgCl_2$ aqueous solution (pH 7.4) was added to 490 μl of NHS (final concentration of EGTA, 10 mmol dm^{-3}; Mg^{2+}, 2 mmol dm^{-3}).

5.2.3 Preparation of self-assembled monolayer (SAM) of HS-mPEG

Glass plates were coated with gold as previously reported[13]. The gold-coated glass plate was immersed in a 4 mmol dm^{-3} solution of HS-mPEG in a 1:6 mixture of Milli-Q water and ethanol at room temperature for at least 24 h to form the HS-mPEG–coated surface (Scheme 5.1). Finally, the glass plate carrying a monolayer of HS-mPEG was sequentially washed with ethanol and Milli-Q water three times with each and then dried under a stream of dried nitrogen gas. The plate carrying a monolayer of HS-mPEG (naïve mPEG) was subjected to complement activation tests. The plates were stored in a desiccator under room light for a predetermined time to assess the effects of deterioration of the mPEG layer on complement activation (R-mPEG). To observe more directly the effects of UV oxidation, surfaces carrying HS-mPEG were UV irradiated at 20 cm from a 15-W germicidal lamp (Matsushita Electric Industrial Co., Ltd., Osaka, Japan) in air at room temperature for 60 min (UV-mPEG)[13](Scheme 5.1). Plates carrying 11-mercaptoundecanol (Sigma-Aldrich Co., St. Louis, MO, USA) were formed as previously reported[17,18] and used as a positive control.

5.2.4 Surface analyses of modified surfaces carrying HS-mPEG

Infrared (IR) adsorption spectra of sample surfaces were collected by the reflection-adsorption method (FTIR-RAS) using a Spectrum One (Perkin-Elmer, USA) spectrometer equipped with a Refractor^{TM} (Harrick Sci. Co., NY, USA) in a chamber purged with dry nitrogen gas and a mercury-cadmium telluride detector cooled by liquid nitrogen. Gold-coated glass plates with a gold layer of 49 nm thickness were used for FTIR-RAS analysis. Spectra were obtained using the *p*-polarized IR light at an incident angle of 75° for 128 scans at 4 cm^{-1} resolution from 4000 to 750 cm^{-1}. Surfaces were also analyzed by using XPS. The XPS spectra of the surfaces were collected by an ESCA-850V (Shimadzu Co., Kyoto, Japan), with a magnesium target and an electric current through the filament of 30 mA at 8 kV. The pressure of the analysis chamber was less than 1×10^{-5} Pa. All spectra shown in the figures were corrected by reference to the peak of Au $4f_{7/2}$ to 83.8 eV.

5.2.5 Total protein and C3b deposition observed by surface plasmon resonance (SPR)

An home-made SPR apparatus was used in this research[17]. Gold-coated glass plates with a gold layer of 49 nm thickness were used. Undiluted NHS or NHS supplemented with EDTA or EGTA was injected into a flow cell, and change in the SPR angle was monitored as a function of time for 90 min. After the NHS was washed out with VB, a solution of rabbit anti-human C3b antiserum diluted to 1% with VB was applied to detect C3b and C3b degraded products, and the change of the SPR angle was estimated to determine antibody binding on the surface.

Protein layer thickness was calculated from the SPR angle shift using Fresnel fits for the system BK7/Cr/Au/SAM/protein/water[18,19]. Both refractive indices of SAM and protein layers were assumed to be 1.45[18,19], and the density of the protein layer was assumed to be 1.0. From these values, the amounts of proteins adsorbed onto the surfaces could be estimated from the following simple relation[17]:

1.0 degree SPR angle shift (DA) $\rightarrow$ 0.5 μg of protein on 1 cm^2 of the surface (5.1)

5.2.6 Release of the soluble form of the membrane attack complex, SC5b-9, and anaphylatoxins C3a and C5a

A hand-made incubation chamber was used to examine release of SC5b-9, C3a-desArg and C5a-desArg when NHS samples were exposed to different surfaces. The chamber was composed of two glass plates carrying the same sample surfaces and a silicone gasket of 1 mm thickness with a hole of 20 mm in diameter. After NHS samples were incubated in the chamber for 1.5 h at 37 ℃, they were collected and EDTA was immediately added to a final concentration of 10 mmol dm^{-3} to stop further activation of the complement system. Commercial enzyme-linked immunosorbent assay (ELISA) kits (for C3a-desArg detection: BD OptEIA Human C3a ELISA, BD Biosciences Pharmingen, CA, USA; for C5a-desArg detection: BD OptEIA Human C5a ELISA, BD Biosciences Pharmingen, CA, USA; for the soluble form of membrane attack complex – SC5b-9: Quidel SC5b-9(TCC) EIA kit, Quidel Corp., CA, USA) were used to determine the fragments, C3a-desArg and C5a-desArg, and the complex, SC5b-9, in the collected NHS samples. The measurement procedure was performed in accordance with supplier instructions.

5.2.7 Statistical analysis

Data from the experiments are expressed as the mean ± standard deviation. A one-way analysis of variance (ANOVA) was used to identify the statistical significance of the data. ANOVA was followed by post-hoc pair-wise *t*-tests adjusted using Holm's method and employing R language environment ver. 2.9.1[20].

5.3 Results

5.3.1 Analyses of HS-mPEG surfaces

FTIR adsorption spectra and XPS spectra were obtained to study HS-mPEG SAM formation and its deterioration during storage under ambient conditions and in a −20 ℃ freezer (F-mPEG). Fig. 5.1A shows the C–O–C stretch region of the IR spectra and Fig. 5.1B shows the C *1s* region of the XPS spectra for naïve mPEG, F-mPEG, R-mPEG, and UV-mPEG. Signal intensities obtained from R-mPEG and UV-mPEG surfaces significantly decreased in the region of C–O–C stretch of the IR spectra. For XPS spectra, the intensity ratios of C *1s* over Au *4f* signals also decreased with storage under the ambient conditions or treatment by UV irradiation. These results suggest that the mPEG layers became thinner by degradation of mPEG chains or that an mPEG surface became heterogeneous by removal of some part of the mPEG surface during storage and UV irradiation. Fig. 5.1 also includes the result of an mPEG surface that was stored in a −20 ℃ freezer for 12 days (F-mPEG). The F-mPEG surfaces did not demonstrate such changes in either the FTIR adsorption spectra or XPS spectra. Therefore, the mPEG surface could be stored without damage in a −20 ℃ freezer for at least 12 days.

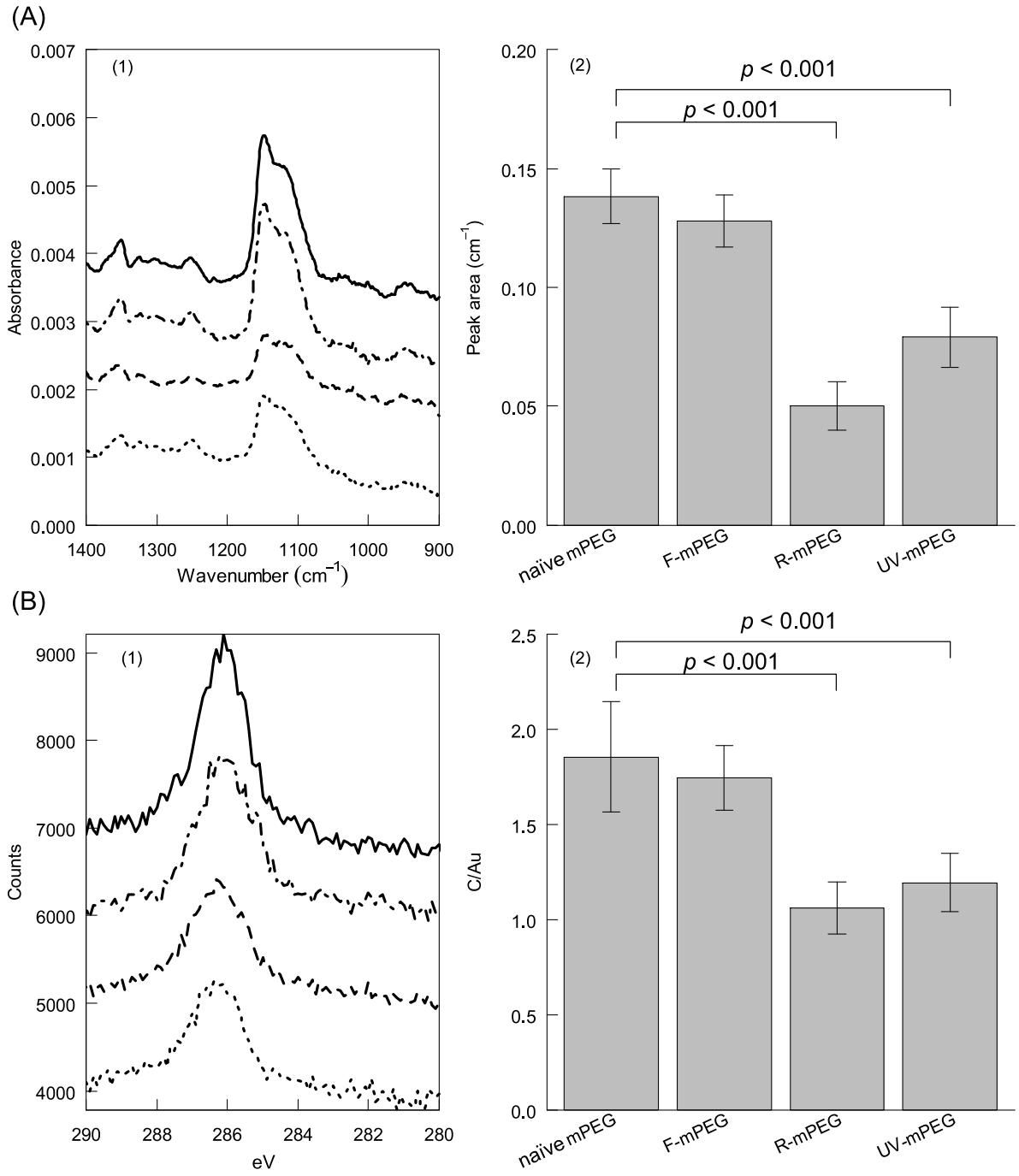

Fig. 5.1 Analyses of mPEG–carrying surfaces.

FTIR-RAS spectra and peak areas of C–O–C stretch region (A); error bars represent ± SD (n=8). XPS spectra of carbon atoms and intensity ratios of C *1s* over Au *4f* signals of mPEG carrying surfaces (B); error bars represent ± SD (n=9). (——): naïve HS-mPEG, (·-·-·): F-mPEG, (- - - -): R-mPEG, (·····): UV-mPEG surfaces.

5.3.2 Protein adsorption and C3b deposition onto mPEG-HS surfaces

When mPEG surfaces were exposed to NHS, an SPR apparatus was used to follow protein adsorption and activation of the complement system. Fig. 5.2 shows SPR sensorgrams for the naïve mPEG, F-mPEG, and R-mPEG surfaces. Initially sharp increases in SPR angle shifts were the result of a larger refractive index of NHS than VB (Fig. 5.2A). For the cases of naïve mPEG and/or F-mPEG surfaces, no additional increase in SPR angles was observed during exposure to NHS. When NHS was washed out by infusion of VB, the SPR signals rapidly decreased to the low pre-exposure levels. The SPR angle shifts indicate that small amounts (0.04 $\mu g/cm^2$) of proteins adsorbed onto the naïve mPEG and F-mPEG surfaces. On the other hand, the SPR angle shift continuously increased during exposure to NHS on the R-mPEG surface. After the surface was exposed to NHS for 90 min, NHS was washed out by infusion of VB. A large shift in SPR angle (1600 mDA) was still observed. The amount of adsorbed proteins estimated from the SPR angle shift was 0.8 $\mu g/cm^2$.

When the complement system is activated through any of the three pathways, C3b is immobilized on surfaces, as Scheme 1 in General Introduction illustrates. After NHS was washed out, a solution of anti-C3b antiserum was applied to examine the existence of C3b and C3b degraded products in the protein layers formed on the mPEG surfaces (Fig. 5.2B). The SPR angles gradually increased with time. Only 0.17 and 0.19 $\mu g/cm^2$ of anti-C3b antibody were immobilized on the naïve mPEG and F-mPEG surfaces, respectively. On the other hand, a much larger amount of anti-C3b antibody (0.95 $\mu g/cm^2$) was bound on the protein-adsorbed layer formed on the R-mPEG surface. These results indicate that the naïve mPEG surface deteri-

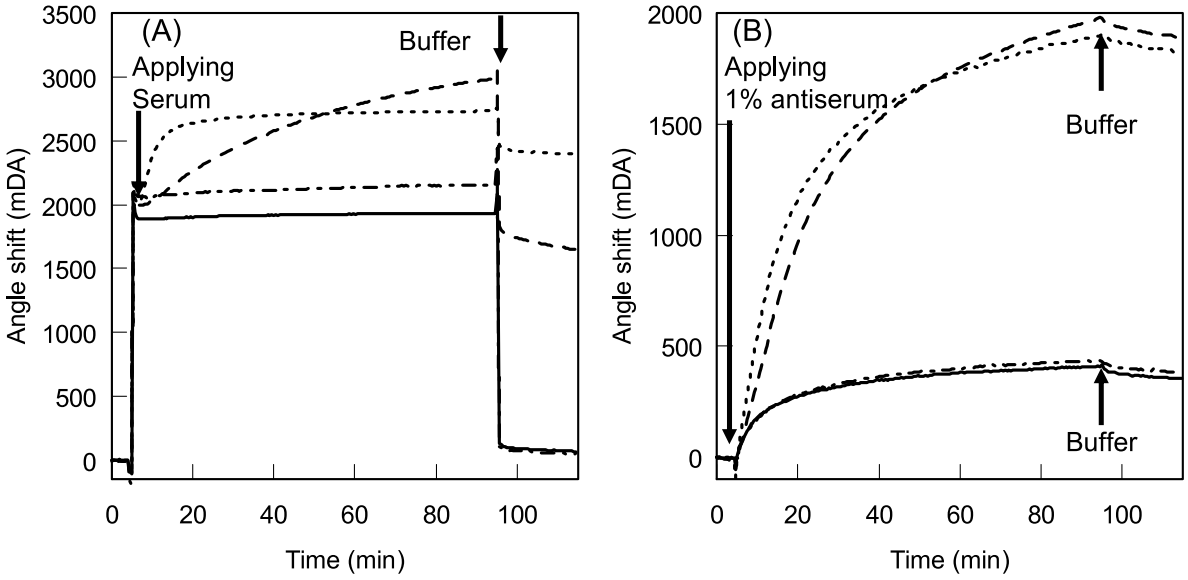

Fig. 5.2 SPR sensorgrams.
During exposure of undiluted NHS to HS-mPEG surfaces (A). Sequential exposure of 1% anti-C3b antiserum to the surfaces (B). (——): naïve HS-mPEG, (·-·-·): F-mPEG, (- - - -): R-mPEG, (·····): UV-mPEG surfaces. DA: degrees of angle.

orated during storage under ambient conditions and acquired the ability to activate the complement system.

Fig. 5.2 also includes behaviors of protein adsorption and anti-C3b antibody deposition on the UV-mPEG surface. They were the same on the UV-mPEG surfaces as on the R-mPEG. Irradiation with UV light could accelerate the deterioration of the HS-mPEG surface, and the mPEG layer gained the ability to activate the complement system.

5.3.3 Release of C3a, SC5b-9, and C5a

C3 is cleaved into C3a and C3b in the contact activation of the complement system on artificial materials. The C3 convertase, C3bBb, which forms on artificial materials, cleaves the α-chain of C3, generating C3a and C3b, and then the smaller 9-kDa anaphylatoxin C3a is released into the fluid phase and rapidly cleaved to form

C3a/C3a-desArg. Thus, the presence of C3a/C3a-desArg in the fluid phase indicates activation of the complement system. Fig. 5.3A shows the results for C3a/C3a-desArg levels in NHS samples applied to naïve mPEG, R-mPEG, and UV-mPEG. Amounts of C3a-desArg released into NHS samples on the R-mPEG and UV-mPEG surfaces were significantly greater than those on naïve mPEG surfaces.

A terminal complement complex, C5b-9, is generated by the assembly of C5 though C9 as a consequence of activation of the complement system. In the absence of a target cell membrane (that is, activation on artificial materials), it binds to regulatory proteins, like the S protein, and is released to serum as a non-lytic SC5b-9 complex. When the complement system is activated on mPEG surfaces, SC5b-9 is expect to be released into serum. Fig. 5.3B summarizes the released amounts of SC5b-9 identified when NHS samples were incubated with naïve mPEG, R-mPEG, and UV-mPEG. Although a small amount of SC5b-9 was found when naïve mPEG surfaces were examined, large amounts of SC5b-9 were observed in NHS samples exposed to the R-mPEG and UV-mPEG surfaces. Those amounts were much larger than those observed in NHS samples exposed to OH-SAM, which has been reported to be a strong complement activator[17].

The C5 convertases (C4b2a3b : the classical and the lectin pathways, C3bBb : the alternative pathway) cleaves the α-chain of C5, generating C5a and C5b, and then the smaller 11-kDa anaphylatoxin C5a is released into the fluid phase and rapidly cleaved to form C5a-desArg. Thus, the presence of C5a/C5a-desArg in the fluid phase also indicates activation of the complement system. The generated amounts of C5a-desArg were also determined, showing a tendency that was almost the same

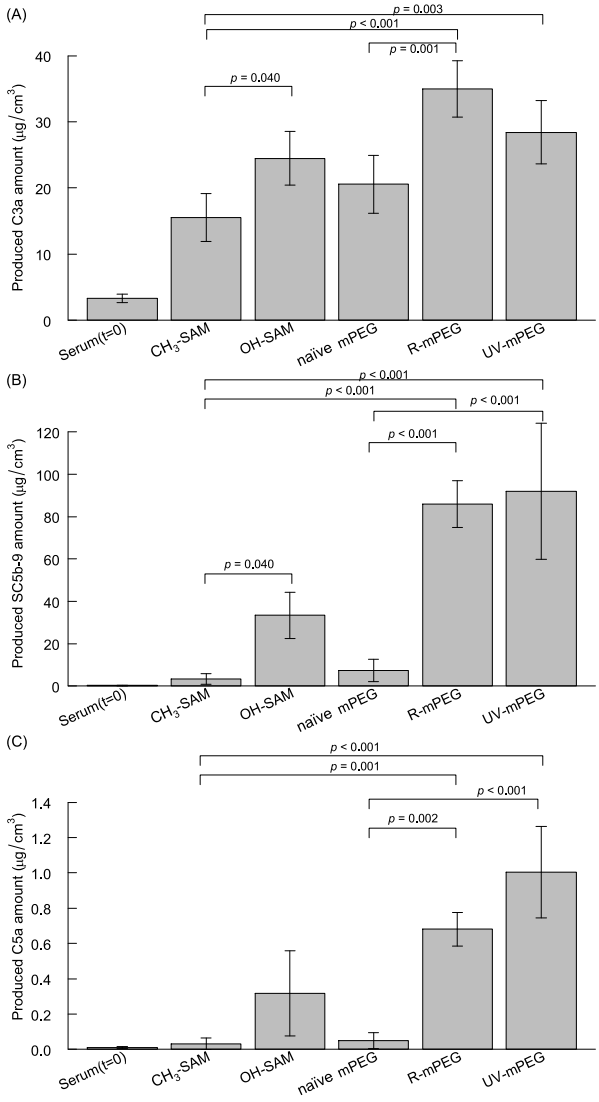

Fig. 5.3 Release of C3a-desArg, SC5b-9, and C5a into NHS.

Undiluted NHS was exposed to CH_3-, OH-SAM, and naïve mPEG, R-mPEG and UV-mPEG surfaces. CH_3- and OH-SAM were used as negative- and positive-controlled surfaces, respectively, for complement activation, and zymosan was used to fully activate complement. Experiments were repeated 3 times for each surface.

C3a-desArg (A): amounts of C3a in naïve undiluted NHS and fully activated by incubation with zymosan were 3.3 $\pm$ 0.6 $\mu g/cm^3$ (n=3) and 56.2 $\pm$ 4.5 $\mu g/cm^3$ (n=3), respectively; error bars represent $\pm$ SD.

SC5b-9 (B): amounts of SC5b-9 in naïve undiluted NHS and fully activated by incubation with zymosan were 0.3 $\pm$ 0.03 $\mu g/cm^3$ (n=3) and 310 $\pm$ 34 $\mu g/cm^3$ (n=3), respectively; error bars represent $\pm$ SD.

C5a-desArg (C): amounts of C5a in naïve undiluted NHS and fully activated by incubation with zymosan were 0.010 $\pm$ 0.007 $\mu g/cm^3$ (n=3) and 3.0 $\pm$ 0.2 $\mu g/cm^3$ (n=3), respectively; error bars represent $\pm$ SD.

as that for SC5b-9 measurements (Fig. 5.3C).

5.3.4 Activation pathway

Whereas addition of EDTA to NHS inhibited all three activation pathways, addition of EGTA-Mg^{2+} can inhibit the classical and lectin pathways, but not the alternative pathway.

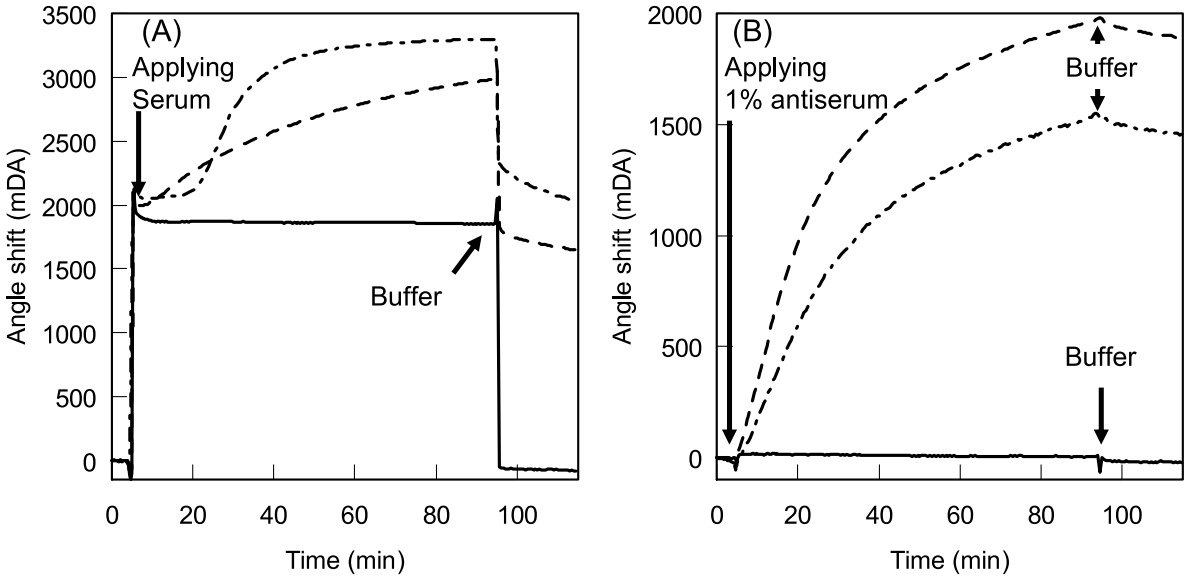

Fig. 5.4 Effect of EDTA and EGTA added to NHS on complement activation on R-mPEG surfaces.
SPR sensorgrams during exposure of NHS (A), and sequential exposure of 1% anti-C3b antiserum to the surfaces (B). (- - -): NHS (same data in Fig. 5.2), (· - · -): NHS supplemented with 10 mmol dm^{-3} EDTA, (——): NHS supplemented with 10 mmol dm^{-3} EGTA (with 2 mmol dm^{-3} Mg^{2+}). DA: degrees of angle.

Fig. 5.4 and Fig. 5.5 show effects of addition of EDTA and EGTA-Mg^{2+} on the complement activation. When an R-mPEG and UV-mPEG surface was exposed to NHS supplemented with 10 mmol dm^{-3} EDTA, the amounts of adsorbed serum proteins and anti-C3b antibody bound were greatly reduced. Practically no protein adsorbed onto the surface in the presence of EDTA. In NHS samples supplemented with 10 mmol dm^{-3} EGTA (with 2 mmol dm^{-3} Mg^{2+}), protein adsorption was re-

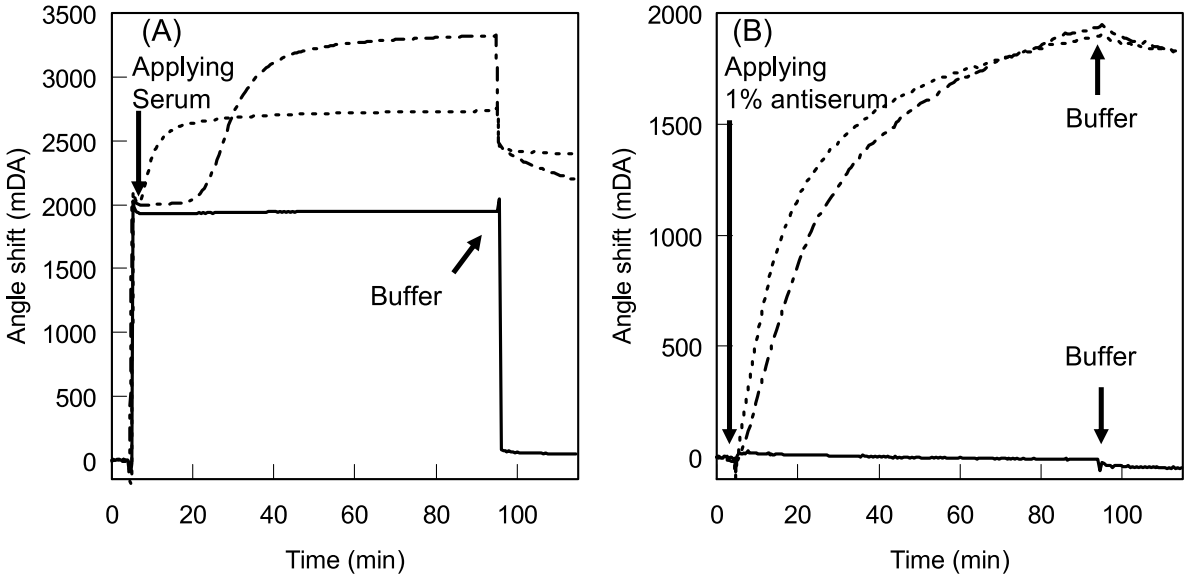

Fig. 5.5 Effect of EDTA and EGTA added to NHS on complement activation on UV-mPEG surfaces.
SPR sensorgrams during exposure of NHS (A), and sequential exposure of 1% anti-C3b antiserum to the surfaces (B). (· · · · ·): NHS (same data in Fig. 5.2), (- · - · -): NHS supplemented with 10 mmol dm^{-3} EDTA, (——): NHS supplemented with 10 mmol dm^{-3} EGTA (with 2 mmol dm^{-3} Mg^{2+}). DA: degrees of angle.

tarded but gradually increased at 20 min after exposure. Using anti-C3b antibody, A large amount of C3b/C3bBb and C3b degraded products in the protein-adsorbed layer was detected. These results indicate that the complement system was definitely activated through the alternative pathway on the R-mPEG and UV-mPEG surfaces.

5.4 Discussion

Although PEG has been widely used for preparation of biomedical devices and drug carriers to reduce interaction of artificial materials with proteins and cells, unanticipated body reactions such as hypersensitivity reactions caused by PEG-modified surfaces have been reported[6–9]. Body reactions against PEG-modified surfaces should be carefully examined. In an previous study[13], naïve mPEG, and

R-mPEG and UV-mPEG surfaces were exposed to 10% diluted NHS and then anti-C3b antiserum was applied to see immobilization of C3b on these surfaces. A large amount of anti-C3b antibody was found on R-mPEG and UV-mPEG surfaces, but not naïve mPEG. These results suggest that naïve mPEG is not an activator of the complement system, but R-mPEG and UV-mPEG surfaces are strong activators. More relevant supporting data was need to conclude it and to identify activation pathways. In this study, complement activation by the latter two surfaces was further confirmed by releases of C3a-desArg, C5a-desArg and SC5b-9 into liquid phase NHS. Even with blocking of the classical and lectin pathways by the addition of EGTA-Mg^{2+} to NHS, R-mPEG and UV-mPEG surfaces can activate the complement system. It was concluded from all of these data that R- and UV-mPEG surfaces activate the complement system through the alternative pathway.

In an previous study[13], a surface carrying tri(ethylene glycol)-terminated alkanethiol (HS-TEGOH) was examined as an activator of the complement system. When the classical pathway was blocked with EGTA-Mg^{2+}, deposition of proteins, including C3b, on it was delayed from 0 min and 40 min by addition of EGTA-Mg^{2+} to 10% NHS. Several groups have reported that a protein layer containing IgG formed on artificial materials starts the activation of the complement system through the classical pathway and then an amplification loop of the alternative pathway follows[21-24]. Complement activation should be carefully examined under more physiologically relevant conditions. It was expected that amounts of proteins (including IgG and IgM) deposited on naïve mPEG surface increase with increasing serum concentration and thus it becomes an activator. No proteins adsorption,

however, was detected on naïve mPEG surface when it was exposed to undiluted NHS. It indicates that naïve mPEG neither activates complement system through the classical nor the alternative pathway even in undiluted NHS.

Kiwada's group reported that PEG-modified liposomes activate the complement system, resulting in opsonization of liposomes[25-27]. When the spleen of a recipient was removed, no opsonization was observed. From this fact, they inferred that anti-PEG IgM[25,26] secreted from the spleen[27] activated the complement system on PEG liposomes through the classical pathway. Serum donors in this chapter had not been exposed to PEG-modified substances; thus, it is difficult to predict whether they carried anti-PEG IgM or IgG antibodies.

R-mPEG and UV-mPEG surfaces showed a 64% and 43% decrease in C–O–C peak area of IR spectra and a 43% and 36% decrease in C/Au ratios of XPS spectra, respectively. These decreases might arise from (1) the heterogeneous removal of whole HS-mPEG chains from gold surfaces or (2) removal of low molecular weight substances produced by degradation of PEG chains on the specimens. Protein adsorption was examined onto a bear Au surface, a large amount of proteins, 0.49 $\mu g/cm^2$ and 0.89 $\mu g/cm^2$, was found on it when it was exposed to NHS and 1% γ-grobulin/VB solution, respectively. In the former situation, proteins should be adsorbed onto the bare area of the surface with surface exposure to NHS supplemented with EDTA. As Fig. 5.4 shows, however, no protein adsorption was observed. This finding indicates that the latter situation is more likely. It has been reported that PEG chains are degraded through mechanical shocks, heating, and irradiation with light[28,29]. Mkhatresh et al.[28] proposed a degradation mechanism of

PEG chains under light irradiation as follows:

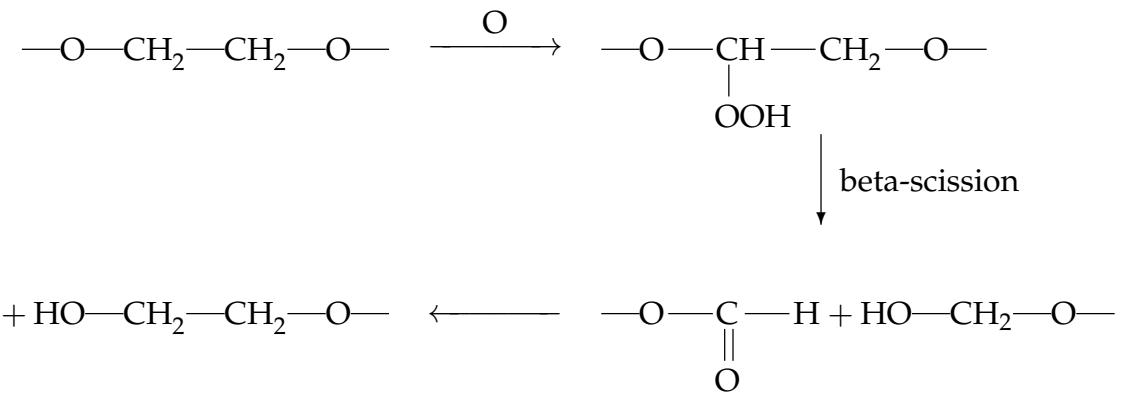

The resulting fragments of PEG chains carry OH groups at the chain ends. The nucleophilic OH groups have been reported to strongly activate the complement system through the alternative pathway. As mentioned previously, complement activation on the mPEG surfaces robustly correlates with decreased PEG chain length on the surfaces. These facts indicate that the PEG layer easily deteriorated, resulting in formation of a surface carrying nucleophilic OH groups, and thus gained the ability to activate the complement system through the alternative pathway after storage in a dessicator under ambient light for several days or after UV irradiation.

5.5 Conclusion

A PEG-modified surface strongly activates the complement system through the alternative pathway after its storage under ambient conditions for several days. After storage of the PEG-modified surface under ambient conditions for several days, FTIR-RAS and XPS both revealed deterioration of the PEG layer, resulting in formation of a surface carrying OH groups, and thus gained the ability to activate the complement system. PEG-modified artificial materials, proteins, and liposomes should be carefully stored.

References

1. Harris J M. Poly(ethylene Glycol) Chemistry: Biotechnical and Biomedical Applications. New York: Plenum Press; 1992.
2. Kingshott P, Griesser H J. Surfaces that resist bioadhesion. Curr Opin Solid State Mater Sci 1999;4(4):403-412
3. Nucci M L, Shorr R, Abuchowski A. The therapeutic value of poly(ethylene glycol)-modified proteins. Adv Drug Deliv Rev 1991;6(2):133-151
4. Harris J M, Chess R B. Effect of pegylation on pharmaceuticals. Nat Rev Drug Discov 2003;2(3):214-221
5. Duncan R. The dawning era of polymer therapeutics. Nat Rev Drug Discov 2003;2(5):347-360
6. Uziely B, Jeffers S, Isacson R, Kutsch K, Wei-Tsao D, Yehoshua Z, Libson E, Muggia F M, Gabizon A. Liposomal doxorubicin: Antitumor activity and unique toxicities during two complementary phase I studies. J Clin Oncol 1995;13(7):1777-1785
7. de Marie S. Liposomal and lipid-based formulations of amphotericin B. Leukemia 1996;10(SUPPL. 2):93-96
8. Alberts D S, Garcia D J. Safety aspects of pegylated liposomal doxorubicin in patients with cancer. Drugs 1997;54(SUPPL. 4):30-35
9. Skubitz K M, Skubitz A P N. Mechanism of transient dyspnea induced by pegylated-liposomal doxorubicin (Doxil^{TM}). AntiCancer Drugs 1998;9(1):45-50

10. Laverman P, Brouwers A H, Dams E T M, Oyen W J G, Storm G, Van Rooijen N, Corstens F H M, Boerman O C. Preclinical and clinical evidence for disappearance of long-circulating characteristics of polyethylene glycol liposomes at low lipid dose. J Pharmacol Exp Ther 2000;293(3):996-1001
11. Moghimi S M, Szebeni J. Stealth liposomes and long circulating nanoparticles: critical issues in pharmacokinetics, opsonization and protein-binding properties. Prog Lipid Res 2003;42(6):463-78
12. Walport M J. Complement. First of two parts. N Engl J Med 2001;344(14):1058-1066
13. Arima Y, Toda M, Iwata H. Complement activation on surfaces modified with ethylene glycol units. Biomaterials 2008;29(5):551-560
14. Andersson J, Ekdahl K N, Lambris J D, Nilsson B. Binding of C3 fragments on top of adsorbed plasma proteins during complement activation on a model biomaterial surface. Biomaterials 2005;26(13):1477-1485
15. Tengvall P, Askendal A, Lundström I. Complement activation by 3-mercapto-1,2-propanediol immobilized on gold surfaces. Biomaterials 1996;17(10):1001-1007
16. Whaley K, North J. Haemolytic assays for whole complement activity and individual components. In: Sim R B, Dodds A W, editors. Complement. Walton Street, Oxford : Oxford University Press; 1997. pp. 19-47
17. Hirata I, Morimoto Y, Murakami Y, Iwata H, Kitano E, Kitamura H et al. Study of complement activation on well-defined surfaces using surface plasmon resonance. Colloids Surf B Biointerfaces 2000;18(3-4):285-292

18. Azzam R M A, Bashara N M. Reflection and Transmission of Polarized Light by Stratified Planar Strucures. In: Ellipsometry and Polarized Light. Amsterdam : Elsevier; 1987. 269-363
19. Knoll W. Polymer thin films and interfaces characterized with evanescent light. Makromol Chem 1991;192(12):2827-2856
20. R Development Core Team. R: A Language and Environment for Statistical Computing. Vienna, Austria : R Foundation for Statistical Computing, 2009. ISBN 3-900051-07-0, URL: http://www.R-project.org/
21. Pangburn M K. Alternative Pathway: Activation and Regulation. In: Rother K, Till G O, Hänsch G M, editors. The Complement System, Second Revised Edition. Berlin: Springer-Verlag; 1998. pp. 93-115
22. Lhotta K, Wurzner R, Kronenberg F, Oppermann M, Konig P. Rapid activation of the complement system by cuprophane depends on complement component C4. Kidney Int 1998;53(4):1044-1051
23. Nilsson U R. Deposition of C3b/iC3b leads to the concealment of antigens, immunoglobulins and bound C1q in complement-activating immune complexes. Mol Immunol 2001;38(2-3):151-160
24. Tengvall P, Askendal A, Lundström I. Studies on protein adsorption and activation of complement on hydrated aluminium surfaces in vitro. Biomaterials 1998;19(10):935-940
25. Ishida T, Ichihara M, Wang XY, Yamamoto K, Kimura J, Majima E et al. Injection of PEGylated liposomes in rats elicits PEG-specific IgM, which is responsible for rapid elimination of a second dose of PEGylated liposomes. J

Control Release 2006;112(1):15-25

26. Wang XY, Ishida T, Kiwada H. Anti-PEG IgM elicited by injection of liposomes is involved in the enhanced blood clearance of a subsequent dose of PEGylated liposomes. J Control Release 2007;119(2):236-244
27. Ishida T, Ichihara M, Wang XY, Kiwada H. Spleen plays an important role in the induction of accelerated blood clearance of PEGylated liposomes. J Control Release 2006;115(3):243-250
28. Mkhatresh O A, Heatley F. A ^{13}C NMR Study of the Products and Mechanism of the Thermal Oxidative Degradation of Poly(ethylene oxide). Macromol Chem Phys 2002;203(16):2273-2280
29. Morlat S, Gardette J-L. Phototransformation of water-soluble polymers. I: photo- and thermooxidation of poly(ethylene oxide) in solid state. Polymer 2001;42(14):6071-6079

Summary

Chapter 1

The complement system is strongly activated by surfaces carrying nucleophilic groups, such as OH groups, and triggered by deposition of complement protein fragment, C3b. Surfaces carrying amino groups, the other representative nucleophilic group, are expected to be potential activators of the complement system through the alternative pathway. Few studies thus far have examined the potential of artificial materials carrying amino groups in activating the complement system. In this study, an NH_2-SAM and a PEI-coated surface were employed as model surfaces to study interactions between amino groups and serum complement pathway. SAMs of 11-mercaptoundecanol (OH-SAM) and 1-dodecanethiol (CH_3-SAM) were used as control surfaces, respectively. Although much protein was adsorbed from serum solutions on the two types of amino surfaces, amounts of C3b deposition were much less than those observed on OH-SAM. Amounts of C3a released on the amino surfaces were the same levels as that of CH_3-SAM, but significantly smaller than that on OH-SAM. These facts suggest that the nucleophilic amino groups on NH_2-SAM and PEI-coated surfaces do not directly activate the alternative pathway, but the protein-adsorbed layers formed on amino surfaces activate it, but to an extent much smaller than that on OH-SAM. In addition, no deposition of C1q molecules on the amino surfaces was found, suggesting that these surfaces fail to

activate the classical pathway. However, more careful studies are needed to conclude it, because it is known that C1q is only transiently detected at typical classical activation interfaces.

Chapter 2

Some studies have demonstrated that amino groups, acting as nucleophiles, are activators of the complement system, but others not. To clarify these contradictory results, complement activation on two series of NH_2/CH_3 and $NH_2/COOH$ mixed SAMs were examined. NH_2/CH_3-mixed SAMs were not potent activators of the complement system regardless of the ratio of NH_2/CH_3 in mixed SAMs. Numerous serum proteins, such as albumin, were adsorbed onto those SAMs and formed a protein layer which inhibited access of C3b to amino groups. In contrast, much C3b and/or C3bBb were deposited on $NH_2/COOH$-mixed SAMs with $\sim$ 50–60% NH_2 density on the surface and SC5b-9 was found in serum exposed to this SAM, indicating activation of the complement system. These results suggest that C3b can easily access nucleophilic NH_2 groups due to the decrease of electrostatic interaction between negatively charged proteins and the NH_2 SAM surface.

Chapter 3

Hydrogels of polymers carrying surface hydroxyl groups strongly activate the complement system through the alternative pathway, although it has also been reported that solutions of polymers do not. To address these curious, inconsistent results, the effect of polymer states, either immobilized on a surface or dissolved in serum, on the complement activation was examined using a SPR apparatus and ELISA. It was

clearly showed that dextran- and PVA-immobilized surfaces strongly activated the complement system, but that soluble polymers could not, even when the amounts of the soluble polymers added to serum were 4–2000 times higher than those on the polymer-immobilized surfaces.

Chapter 4

Polymers carrying hydroxyl group have potential ability to activate the complement system when contact with blood. However, there are still unclearness in effects of their surface structure on complement activation. In this study, complement activation by PVA layers formed on surface was examined. The complement system was strongly activated by PVA surface with a dry thickness of 1.7 nm, while it was poorly activated by PVA surface with a dry thickness of 6.3 nm. Annealing of the latter for 2 h at 150 ℃ convert the surface into complement activating surface. These results suggest that complement activation highly depends on hydration states of PVA layers.

Chapter 5

Surface modification with polyethylene glycol (PEG) has been employed in the development of biomaterials to reduce unfavorable reactions. Unanticipated body reactions, however, have been reported, with activation of the complement system suggested as having involvement in these responses. In this study, a PEG-modified surface on a gold surface using a monolayer of α-mercaptoethyl-ω-methoxy-polyoxyethylene (HS-mPEG) was prepared. Neither protein adsorption nor activation of the complement system was observed on the PEG-modified

surface just after preparation. After storage of the PEG-modified surface in a desiccator under ambient light for several days or following UV irradiation, reflection-adsorption (FTIR-RAS) and X-ray photo spectrometry both revealed deterioration of the PEG layer, which became a strong activator of the complement system through the alternative pathway.

List of Publications

Chapter 1: Toda M, Kitazawa T, Hirata I, Hirano Y, Iwata H. Complement activation on surfaces carrying amino groups. Biomaterials, 2008; 29(4):407–417

Chapter 2: Toda M, Iwata H. Effects of hydrophobicity and electrostatic charge on the complement activation by amino group. ACS Appl Mater Interfaces, submitted.

Chapter 3: Arima Y, Kawagoe M, Toda M, Iwata H. Complement Activation by Polymers Carrying Hydroxyl Groups. ACS Appl Mater Interfaces 2009;1(10):2400–2407

Chapter 4: Arima Y, Kawagoe M, Toda M, Iwata H. Effect of hydration of poly(vinyl alcohol) on complement activation. ACS Appl Mater Interfaces, submitted.

Chapter 5: Toda M, Arima Y, Iwata H. Complement activation on degraded polyethylene glycol-covered surface. Acta Biomaterialia, accepted.

Related Publications

1. Hirata I, Hioki Y, Toda M, Kitazawa T, Murakami Y, Kitano E, Kitamura H, Ikada Y, Iwata H. Deposition of complement protein C3b on mixed self-assembled monolayers carrying surface hydroxyl and methyl groups studied by surface plasmon resonance. J Biomed Mater Res A 2003;66(3):669–676
2. Arima Y, Toda M, Iwata H. Complement Activation on Surfaces Modified with Ethylene Glycol Units. Biomaterials 2008; 29(5):551–560

Other Collaborative Publications

1. Ohyama T, Nishide T, Iwata H, Sato H, Toda M, Taki W. Vascular endothelial growth factor immobilized on platinum microcoils for the treatment of intracranial aneurysms: experimental rat model study. Neurol Med Chir (Tokyo) 2004;44(6):279–285
2. Ohyama T, Nishide T, Iwata H, Sato H, Toda M, Toma N, Taki W. Immobilization of basic fibroblast growth factor on a platinum microcoil to enhance tissue organization in intracranial aneurysms. J Neurosurg 2005;102(1):109–115
3. Kato K, Toda M, Iwata H. Antibody arrays for quantitative immunophenotyping. Biomaterials 2007;28(6):1289–1297
4. Kuraishi K, Iwata H, Nakano S, Kubota S, Tonami H, Toda M, Toma N, Matsushima S, Hamada K, Ogawa S, Taki W. Development of nano-fiber covered stents using electrospinning. –In vitro and acute phase in vivo experiments–. J Biomed Mater Res B Appl Biomater. 2009;88(1):230–9.
5. Hamada K, Matsushima S, Toma N, Totani T, Toda M, Ogawa S, Asakura F, Sakaida H, Iwata H, Taki W. Simple Immersion of Filter Devices into an Urokinase Solution Prevents Fibrin Net Formation during Carotid Artery Stenting. J Biomed Mater Res B Appl Biomater, submitted.
6. Sano H, Toda M, Uchiyama N, Mohri M, Sugihara T, Hamada J, and Iwata H. Coils coated with the cyclic peptide SEK-1005 accelerate intra-aneurysmal organization. Neurosurgery, submitted

International Conferences

1. Toda M. Complement Activation through Alternative Pathway at Well-defined Amine-terminated Surfaces. 3rd Taiwan-Japan Joint Symposium on Biomaterials; 2001 Dec 22; National Taiwan University, Taipei, Republic of China.
2. Toda M, Kitazawa T, Hirata I, Hirano Y, Iwata H. Interaction of Serum Complement with Surfaces Carrying Amino Groups studied with Surface Plasmon Resonance. 7th World Biomaterial Congress; May 17–21 2004;Sydney Convention & Exhibition Centre, Darling Harbour, Sydney, Australia.
3. Toda M, Kitazawa T, Hirata I, Hirano Y, Iwata H. Interaction of Serum Complement with Surfaces Carrying Amino Groups studied with Surface Plasmon Resonance. Molecule-Based Information Transmission and Reception-Application of Membrane Protein Biofunction – (MB-ITR2005); Mar 3–7 2005; Okazaki city, Aichi pref, Japan.
4. Toda M, Iwata H. Activation of the complement system on NH_2/CH_3 and NH_2/COOH mixed self-assembled monolayers. 8th World Biomaterial Congress; May 28–June 1,2008; The Netherlands.

Acknowledgement

The present research was carried out from 1999 to 2009 under the continuous guidance of Dr. Hiroo Iwata, Professor of the Institute for Frontier Medical Sciences, Kyoto University. The author is deeply indebted to Professor Iwata for his constant guidance, encouragement, valuable discussion, and detailed criticism on the manuscript throughout the present work. The completion of the present research has been an exiting project and one which would not have been possible without his guidance.

The author is very grateful to Dr. Koichi Kato, Associate Professor of the Institute for Frontier Medical Sciences, Kyoto University, for his constant guidance, helpful suggestions, and intimate advice.

The author would like to thank Dr. Isao Hirata, Assistant Professor, and Dr. Masayuki Okazaki, Professor of Department of Biomaterials Science, Graduate School of Biomedical Sciences, Hiroshima University, for their instruction of surface characterization techniques and protein adsorption experiments using SPR apparatus.

The author also expresses his great thanks to Dr. Yusuke Arima, Institute for Frontier Medical Sciences, Kyoto University, Dr. Yoshiaki Hirano, Professor of Department of Chemistry and materials Engineering, Faculty of Chemistry, Materials and Bioengineering, Kansai University, Mr. Takayuki Kitazawa, Takeda Phamaceu-

tical Co.,Ltd., and Ms. Masako Kawagoe, Kuraray Co.,Ltd., for their kind cooperation and useful suggestions.

The author wishes to express his thanks to following people for their kind help, assistance, and encouragement: Dr. Masaya Yamamoto and Dr. Yasuhiko Tabata, and Ms. Kyoko Bamba, Department of Biomaterials, Institute for Frontier Medical Sciences, Kyoto University; Dr. Satoshi Arakawa, Dr. Takeshi Bamba, Dr. Chitose Kami, Mr. Takehisa Abe, Dr. Takeshi Fukuda, Dr. Seiichi Kiso, Mr. Katsumoto Terada, Mr. Hiroyuki Tonoi, Mr. Mitsuaki Mada, Dr. Tsuneaki Sakata, and the other coodinators and ex-coodinators and Dr. Masanao Shimizu, Mr. Shinji Tohyama, Mr. Tadashi Tamura, Mr. Satoru Inoue, Ms. Mayuko Ohshima, and the other staff of Kinki Bio-industry Development Organization; Mr. Takehiro Yashima, Mr. Hideki Nakamura, Mr. Masayuki Ohira, Ms. Natsuko Akeyama, and the other staff of the Kansai Bureau of Economy, Trade and Industry, Japan; Dr. Yoshiko Nakahara, Dr. Noriko Yoshikawa, Ms. Junko Hirai and the other staff of Foundation for Biomedical Research and Innovation; Mr. Takashi Miki, Planning and Coodination Bureau, City of Kobe; Dr. Motoki Kyo, Toyobo Co., Ltd.; Dr. Hideki Sato, Gunze Ltd.; Dr. Naoki Toma, Dr. Takashiro Ohyama, Dr. Keita Kuraishi, Dr. Kazuhide Hamada, Dr. Waro Taki, Department of Neurosurgery, Mie University; Dr. Shigeyuki Nakano, Hyogo Prefectural Institute of Technology; Dr. Shinichirou Kubota, Industrial Technology Center of Okayama Prefecture; Dr. Hiroki Sano, Department of Neurosurgery, Kanazawa University; Dr. Yoshiko Abe, Sekisui Medical Co., Ltd.; Ms. Kumiko Terakawa, Dr. Keiko Kawano, Dr. Kiyotaka Wasa, Dr. Atsuhito Okonogi, Dr. Hidetoshi Kotera, and the other staff of Nanometrics Lab-

oratory, Department of Micro Engineering, Graduate School of Engineering, Kyoto University; Mr. Akira Kojima, Ms. Yumiko Uchida, Ms. Hiroko Ohara and the other staff of Kyoto City Collaboration of Regional Entities for the Advancement of Technoogical Excellence, Advanced Scientific Technology and Management Research Institute of Kyoto; Dr. Yasukiyo Ueda, Mr. Toshiaki Kabuto, and the other staff of Graduate School of Engineering, Kobe University; Dr. Shuichiro Kuwajima, Dr. Naoki Miyano, and the other lecturer and staff of Nano-Medicine Merger Education Unit, Kyoto University; Dr. Hiromi Takiguchi, Graduate School of Engineering, the University of Tokyo; Dr. Yuji Teramura, Radioisotope Research Center of Kyoto University.

The author wishes to express his thanks to Mr. Yoichi Ogata, Mr. Ryusuke Nakai, Mr. Yuichi Koyamatsu, and Dr. Chiaki Yoshikawa for their kind encouragement.

General acknowledgments are due to Ms. Yoshiko Suzuki, Dr. Yoshikimi Uyama, Dr. Satoshi Fujita, Dr. Hiroyuki Tonami, Dr. Tadashi Nakaji, and other members of Professor Iwata's laboratory, and of the Institute for Frontier Medical Sciences, Kyoto University, for their kind help.

Finally, the author likes to take the opportunity to extend hearty thanks to his mother, Ms. Tsunayo Toda, and his brother, Mr. Noriaki Toda, for their cordial support and continuous encouragement.

January, 2010

Kyoto

Mitsuaki Toda